

**A Precision Search for Exotic Scalar and Tensor Couplings
in the Beta Decay of Polarized ^{37}K**

by

Melissa Anholm

A Thesis submitted to the Faculty of Graduate Studies of
The University of Manitoba
in partial fulfillment of the requirements of the degree of

DOCTOR OF PHILOSOPHY

Department of Physics and Astronomy
University of Manitoba
Winnipeg

Abstract

Abstract Goes Here

Acknowledgements

People to acknowledge here include: John Behr, Gerald Gwinner, Dan Melconian.
Also: Spencer Behling, Ben Fenker. Also-also: Alexandre Gorelov, James McNeil.
But additionally: Danny Ashery.

Contents

Abstract	ii
Acknowledgements	iii
Contents	vii
List of Figures	viii
List of Tables	x
Shit To Do	xix
1 Background and Motivation	1
1.1 Exotic Couplings	1
1.2 Fierz Interference – The Physical Signature	1
1.3 Present Limits	2
1.4 A Toy Experiment	2
2 Theoretical Overview	3
2.1 The Basics of Beta Decay	3
2.2 Mathematical Formalism	4
2.3 Our Decay	5
3 Atomic Physics Overview	7
3.1 Magneto-Optical Traps	7
3.1.1 Doppler Cooling	7
3.1.2 Zeeman Splitting	7
3.1.3 Atom Trapping with a MOT	7
3.2 Optical Pumping	7
3.3 Shake-off Electron Spectrum	7

4 The Experimental Setup	9
4.1 Double MOT System Overview and Duty Cycle	9
4.2 The AC-MOT and Polarization Setup	11
4.3 Microchannel Plates and Electric Field	15
4.4 Measurement Geometry and Detectors	15
5 Calibrations and Data Selection	19
5.1 Cloud Measurements via Photoionization	19
5.2 Beta Detector Cuts	21
5.3 The eMCP	23
5.4 The rMCP	24
6 The Experimental Signature	25
6.1 General Stuff	25
6.2 TBD	26
6.3 The Superratio and Asymmetry	26
6.4 Signature of a Fierz Term in This Experiment	27
6.5 Comparative Merits of the Superratio and Supersum for Measurement	27
7 Analysis	29
8 Estimating Systematic Effects	33
8.1 Low-energy Scintillator Threshold	33
8.2 BB1 Radius, Energy Threshold, Agreement	33
8.3 Background Modeling – Decay from Surfaces within the Chamber .	34
8.4 Quantifying the Effects Backscatter with Geant4	35
8.5 Lineshape Reconstruction	35
8.5.1 Motivation	36
8.5.2 What is it and how does it work?	36
8.5.3 The Math-Specifics	36
8.5.4 The Results – Things That Got Evaluated This Way	36
8.5.5 The low-energy tail uncertainty, and what it does	36
9 Results	37
9.1 Measured Limits on b_{Fierz} , C_S , C_T	37
9.2 Discussion of Corrections and Uncertainties	37
9.3 Relation to Other Measurements and New Overall Limits	37
Bibliography	39
Appendices	42

A Notable Differences in Data Selection between this and the Previous Result	42
A.1 Polarization Cycle Selection	42
A.2 Leading Edge / Trailing Edge and Walk Correction	42
A.3 TOF Cut + Background Modelling	43
B A PDF	44
B.1 JTW	44
B.2 Holstein	46
C Notation	51
C.1 Comparison Guide	51
C.2 Some old handwritten notes.	51
D Holstein/JTW Comparison Confusion	61
E Multipole Comparisons	66
F Notation	69
F.1 Things.2	69
F.2 Things.3	69
F.3 Beta End-point Energy	70
F.4 Beta End-point Energy.2	71
G SuperRatio	72
H Super Corrections	75
I Misc. Nuclear Physics	78
I.1 Scalars	78
I.2 Vectors	78
I.3 Axial Vectors	78
I.4 Pseudoscalars	79
I.5 Tensors	79
I.6 Comments on Parity Conservation	79
I.7 Q-Values	79
I.8 Helicity	80
I.9 Conserved Vector Current Hypothesis	80
J How To Lifetime	82
J.1 Intro	82
J.2 Now What?	84
J.3 After Picking Something...	84

K An R_{slow} Thesis Proposal	86
K.1 An Old Rslow Abstract	86
K.2 Motivation	87
K.3 The Principle of the Measurement	87
K.4 The Decay Process	88
K.5 Current Status	89
L Fucking Duh	91
L.1 Lifetimes and Half-Lifes	91

List of Figures

2.1	A level diagram for the decay of ^{37}K	6
4.1	The TRINAT experimental set-up utilizes a two MOT system in order to reduce background in the detection chamber.	10
4.2	The duty cycle used for transferring, cooling, trapping, and optically pumping ^{37}K during the June 2014 experiment.	11
4.3	An alternating-current magneto-optical trap with a duty cycle optimized for producing polarized atoms	14
4.3a	Components of a magneto-optical trap, including current-carrying magnetic field coils and counterpropagating circularly polarized laser beams.	14
4.3b	One cycle of trapping with the AC-MOT, followed by optical pumping to spin-polarize the atoms. After atoms are transferred into the science chamber, this cycle is repeated 500 times before the next transfer. The magnetic dipole field is created by running parallel (rather than anti-parallel as is needed for the MOT) currents through the two coils.	14
4.4	The TRINAT detection chamber.	16
4.4a	A decay event within the TRINAT science chamber. After a decay, the daughter will be unaffected by forces from the MOT. Positively charged recoils and negatively charged shake-off electrons are pulled towards detectors in opposite directions. Although the β^+ is charged, it is also highly relativistic and escapes the electric field with minimal perturbation.	16

4.4b	Inside the TRINAT science chamber. This photo is taken from the vantage point of one of the microchannel plates, looking into the chamber towards the second microchannel plate. The current-carrying copper Helmholtz coils and two beta telescopes are visible at the top and bottom. The metallic piece near the center is one of the electrostatic ‘hoops’ used to generate an electric field within the chamber. The hoop’s central circular hole allows access to the microchannel plate, and the two elongated holes on the sides allow the MOT’s trapping lasers to pass unimpeded at an angle of 45 degrees ‘out of the page’	16
5.1	Trap Position along TOF Axis	21
5.2	Trap Position from Camera	22
5.3	rMCP Calibration	24
6.1	Here’s why it’s better to extract b_{Fierz} from an asymmetry, in this case.	28
7.1	SOE TOF, model and data. In the end, I cut the data to use only events with a TOF between A and B. Max. possible background is like a factor of two too big.	32
8.1	Simulated Beta TOA vs emission angle w.r.t. detector orientation . .	35
9.1	Some results. I’ll want to show at least one of these things. Probably show a separate one for each runset, actually.	38
C.1	”Notes 0”	55
C.2	”Notes 1”	56
C.3	”Notes 2”	57
C.4	”Notes 3”	58
C.5	”Notes 4”	59
C.6	”Notes 5”	60

List of Tables

5.1	Cloud Position and Size	23
C.1	Notation Guide	52
C.2	Angular Momentum Notation	52
C.3	Notation Guide	53
C.4	Selected Integrals from Holstein's Eq. (51)	54

Shit To Do

■ Need to figure out how the exotic couplings actually work, mathematically.

What the fuck does “($V - A$)” even *mean*? IIRC John wants a brief mention of γ_5 ’s and γ_μ ’s, and probably a brief mention of what mumble-mumble group is mumble-mumble represented or something.

1

Figure: I need that simulated picture of the different beta energy spectra, with different values of b_{Fierz}

1

■ Do I really even *want* to include a toy experiment? And would I want to do it here?? What even is the point? I think in the past I decided it was easier to build up a description of something starting this way. But why?? Possibly as I continue to add content, it will become obvious again why I originally wanted to do this.

2

■ Is this even true? The pointlike thing? ...No. No it’s not.

3

■ JB says: The title of Holstein’s review addresses this “pointlike” issue, and he describes the “impulse approximation” in Section V. The interaction is not pointlike, because all constants are a form factor expansion in q^2 – finite size terms contribute to the Coulomb correction.

3

■ Do it! Do the master equation!

4

Figure: This thing is going to need a nuclear level diagram for 37K. Also, 37K is a really nice isotope for this, because 98% + 2%, also because it’s a mirror decay, also because it’s an alkali. Also-also, its big A_β value means we have a big thing to multiply any b_{Fierz} value there might be when we construct the superratio asymmetry to eliminate systematics.

5

■ Might be worth mentioning about the shake-off electrons too, and how many of them there are. But then nobody will trust any of the numbers I measured (how did I do that measurement, anyway?), and will want me to just use Dan's that he measured forever ago with a different set of detectors. (where are those numbers recorded anyway?) I think I have to mention how many come off and how often at least briefly, because I use the Levinger spectrum for my background modeling.	5
Figure: SOE Spectrum goes here.	8
■ mumble mumble 7ish days of beamtime, mumble mumble 2014.	9
■ Probably describe the laser transfer method slightly.	9
■ Mumble mumble UHV. Mumble mumble tail end of the Boltzmann distribution.	10
■ In order to eliminate systematic effects, the polarization direction is flipped every 16 seconds.	11
■ Probably document things about the waveform and frequency used for the beamtime, since I don't think it's in my MSc.	11
Figure: This is going to need another edge-on G4 picture of the chamber to label all the atomic components.	12
Figure: I need <i>at least</i> one atomic level diagram. But possibly as many as 3 level diagrams. Have to show energies for MOT, energies for OP, and energies for photoionization.	12
■ JB says: "I would say you don't need an atomic level diagram. You could just describe in words the semiclassical picture of atoms absorbing photons until they are nearly fully polarized, then they stop absorbing. The optical pumping + photoionization is then an <i>in situ</i> probe of the polarization. ... You would need to add in words that quantum mechanical corrections to this picture are in the optical Bloch equation approach in B. Fenker et al. The depolarized states still have high nuclear polarization (1/2 for $F = 2, M_F = 1$, 5/6 for $F = 1, M_F = 1$) and determining the ratio of those two populations provides most of the info we need – we model with the O.B.E, measure the optical pumping light polarization, and float an average transverse magnetic field. This is adequate to determine the depolarized fraction to 10% accuracy, which is all that is needed." . . .	12

■ Is my photoionization description adequate? ... in light of John's feedback: no.	12
■ JB says: "Since you worked hard on the logic triggers, a photoion spectrum with duty cycle would be appropriate if you want."	12
■ Need to describe how polarization works.	12
■ JB says: all polarization details could be deferred to [1]. (be sure to list all authors including [me]).)	12
■ Note that because the atoms within a MOT can be treated as following a thermal distribution, some fraction of the fastest atoms continuously escape from the trap's potential well. Even with the most carefully-tuned apparatus, the AC-MOT cannot quite match a similar standard MOT in terms of retaining atoms. The TRINAT AC-MOT has a 'trapping half-life' of around 6 seconds, and although that may not be particularly impressive by the standards of other MOTs, it is more than adequate for our purposes. ^{37}K itself has a radioactive half-life of only 1.6 seconds (cite someone), so our dominant loss mechanism is radioactive decay rather than thermal escape.	13
■ Anyway, here's some figures. Or possibly one figure. Whatever. Also, here's a reference to a figure. See Fig. 4.3 (works – currently “3.4”), or also its subfigures, eg Fig. 4.3b (works – currently “3.4b”) and Fig. 4.3a (works – currently “3.4a”). Maybe I have to subref them? Like, eg, Subfig. 4.3b (works – currently “3.4b”) and Subfig. 4.3a (works – currently “3.4a”). What if we try to subref everything? Consider, eg, Fig. ?? (doesn't work). Yeah, ok, so fortunately the note cites like the text. This gives an example of shit to do and not to do. Also, can't do a linebreak within a note. . .	13
■ that's this section. I should really describe the AC-MOT.	14
Figure: Back-to-back MCPs in an electric field to tag events from the trap, and to measure the trap position and polarization. Hoops to produce the electric field.	15
■ This section is disorganized and repeats itself.	15
■ ... (shown in Figure 4.4)	15
■ Mirrors are $275\ \mu\text{m}$ thick, not the $254\ \mu\text{m}$ shown in picture.	16
■ There's gotta be a better way to describe it	17
■ what's the open area of the detector? how big is each pixel?	17

■ Probably worth mentioning that we test this stuff offline on stable ^{41}K . . .	19
■ As a check: the camera measurements for photons from de-excitation. It's aimed 35 degrees from vertical, with its horizontal axis the same as one of the other axes. I think it's the TOF axis. I can check this when my computer comes back. Also, there's an unknown additional delay between some of our DAQ channels that can't be explained by accounting for cable lengths, so we really like having the check there.	19
■ Trap position – Measured using the same dataset that was used to quantify the polarization. The trap drifts slightly over the course of our data collection. Describe the rMCP calibration needed to extract this info. . .	20
■ Polarization measurement was conducted on a different set of data, collected in between the measurements used for A_β and b_{Fierz} , and at a higher electric field, because we were unable to run both our MCP detectors simultaneously.	20
■ Also, we noticed the trap drifting after one of the runs, because one of the batteries on one of the thingies adjusting the laser frequency (I think) was failing.	20
■ JB: "If we rejected the data with the MOT moving (indeed a battery determining the voltage controlled oscillator frequency offset between absorption in stable ^{41}K cell and the ^{37}K resonance) then that's all you need to say."	20
■ describe how you'd turn this into a physical description of the cloud, with like a temperature and a sail velocity and shit. with equations.	21
■ This is a stupid section name. Also, I really do need to describe how the cuts were made here somewhere, because it's non-trivial in many cases, and possibly different than what Ben did in some cases. But it won't make sense to describe what I did different if I don't describe the thing as a whole, at least a bit. The point is, this is a set of cuts/systematics that isn't really that straightforward to understand.	21
■ Energy calibration for the scintillator+PMT setup changed dramatically at one point. Describe how calibration was done. Like, one sentence or something. Something about the endpoint energy, and something about the compton edge for 511s, IIRC.	22

■ JB: “You can describe anything you did differently or improved, but you can and should otherwise defer all details of the scintillator calibration and DSSD calibration to Ben’s paper and his thesis and Spencer’s. E.g. Section 8.2 “statistical agreement between BB1 X and Y detectors’ energies only makes a small effect on results” does not need the technical details beyond that statement.”	22
■ JB: “If you have some way of documenting the coding you used, that would be great.” ... yeah, it would, wouldn’t it?	22
■ JB: eMCP. You need to describe the timing information obtained. You also need a statement of whether or not you used the position information in your cuts.	23
Figure: Needs an SOE timing spectrum. At least one of them. Experimental and simulated. Also, I have to describe how I did the simulating, and how I check that it’s OK despite the fact that the simulated spectrum looks nothing like the experimental spectrum.	23
■ Possibly this can be combined with the “Background and Motivation” or “Theory” chapters? Why do I even *have* two of those chapters, if not for this? Anyway, surely I don’t need *three* of them.	25
■ JB: You need to at some point say that the supersum is the beta energy spectrum. There are experiments trying to do this method better, but they are very difficult. UCNA published a combined energy spectrum and Abeta[Ebeta] analysis on the neutron in March 2020 [2].	26
■ I can’t help but also notice the follow-up article from September 2020 [3]. Ugh.	26
Figure: Show individual beta energy spectra. ...with a variety of different cuts, perhaps?	26
Figure: Show simulated spectra separated by scattering category.	26
Figure: Show SimpleMC spectra, show the supersum, show the superratio, show the superratio asymmetry. Maybe do some simple fits to show how much better the superratio asymmetry is than <i>not</i> the superratio asymmetry.	26
■ How do I even <i>do</i> these estimations?	33
■ It’s actually not nearly as big as I’d originally expected. It’s huge in the lineshape thing, but pretty tiny in everything else.	33

■ As per JB's comment in section 5.2: "statistical agreement between BB1 X and Y detectors' energies only makes a small effect on results" does not need the technical details beyond that statement."	33
Figure: Surely this requires at *least* one image of the pixelated BB1 data. Maybe some of a few waveforms and energy distributions too.Feels like cheating to include some of that stuff, since Ben was the one who actually used it mostly.	33
■ Remember: There's noise applied to simulated BB1s, matching some spectrum.	33
Figure: Show the "average asymmetry" (all energies) as a function of TOF, with real data, best model normalization, and extrema of model normalizations. Show our cut. Turns out, it's a lot of work for a really tiny correction. Oh well.	34
■ Oh god. Have I even <i>tried</i> to quantify the combined systematic that comes out of the TOF cut? Do I need to, or is it double-counting? Ugh, it would be such a headache to do this. Maybe I can at least do it at the end – because I might never get my code back to the way it was.	35
■ This section should reference Clifford. [4].	35
■ The citation format I'm using is really stupid. You must force yourself to ignore this right now, Melissa!	41
■ We have already specialized to β^+ decay.	44
■ Also, $\xi = G_v^2 \cos \theta_C f_1(E)$	46
■ In fact, we might want to add the other different-er terms in to this thing now, before we get ahead of ourselves.	48
■ So clearly I'm going to need terms for $\Delta F_1(E_\beta, u, v, s)$, $\Delta F_4(E_\beta, u, v, s)$, $\Delta F_7(E_\beta, u, v, s)$, $\Delta F_{10}(E_\beta, u, v, s)$, $\Delta F_{13}(E_\beta, u, v, s)$, and $\Delta F_{18}(E_\beta, u, v, s)$. We really only have expressions for some of them in Holstein's Eq. (C4). That's annoying.	48
■ There was something wrong with this assumption. Something circular. I forgot. Blah.	48
■ Or will I?	49
■ Somewhere, just list out the goddamn values of things that I inherited from Ian Towner's personal communication that one time, over multiple generations of grad students.	49
■ Seriously, I need to check what the taylor series is even expanding in. . . .	49

■ Note: It's not the case that $ \vec{J} == J$. It's actually super fucking infuriating notation.	49
■ Also, pretty sure one of those never gets used. Which one was it? idk. . . .	50
■ Must find a better way to smush this table with display style math font type-setting. At present, it's somehow both too smooshed and not smooshed enough.	51
■ In fact,	

$$\xi = G_v^2 \cos \theta_C f_1(E) \quad (0.1)$$

■	66
■ According to insight that Alexandre thought was very obvious, because it was, JTWW-style notation only happened in the first place because the lab frame matters. it's measured w.r.t. polarization or alignment or something. The integration over the two leptons is really an integration over the lab frame + one lepton.	69
■ Is that \uparrow even true?? Because I'm really not sure it is. Via Kofoedhansen, $(E_0 - E_e) = E_\nu$. So there.	71
■ A thing that's worth noting is that (I think!) recoil-order corrections have been implicitly excluded at some point here. ...Is this even true??	71
■ JB: You're describing a consequence of CVC, and are not stating the actual hypothesis.	80
■ JB: I think you don't have time to explain the CBC hypothesis. You'll just have to assume it. I personally found that the technical derivation was the only way to see what was going on.	80
■ JB: A good sketch of CVC is done in Commins' notes and his book with Bucksbaum [?]. Ian towner did it in his notes. I reproduce this in my own course notes for Phys 505 (p.21-28 of the thing John attached to that email). First you show in Dirac notation that the E&M current for pointlike particles is conserved—this just needs one use of the Dirac Equation and conservation of electric charge. Then look what happens for finite nucleons. Then construct the analogous weak interaction current for the nucleon, including three possible current terms that transform like Lorentz vectors, and note the consequences if that current is still conserved.	80

█	Figure out how to cite somebody's unpublished/semi-unpublished notes. . .	80
█	JB: Jelley [5] describes the qualitative background on his text page 110 (attached). Feynman and Gell-Mann proposed that the isovector weak vector current and the isovector E&M vector current are members of an isotriplet of currents all of which are conserved. [This idea eventually went straight into the SM electroweak interaction, with the addition of nonabelian and massive operators for the weak part, though figuring out how to make a consistent theory with the massive bosons took the combination of Yang-Mills gauge theories and then Weinberg and Salam's approaches.]	80
█	JB: What you say is one consequence, that meson exchange currents don't change the vector part of the weak interaction— this is consistent with conservation of electric charge and its analog in the weak interaction. This particular consequence is a very powerful tool in electromagnetic effects in nuclei, e.g. if you take the isovector combination of magnetic moments (^{37}Ar - ^{37}K e.g.) you get something without meson exchange corrections and therefore precisely sensitive to other higher-order physics effects. Arima and Towner separately studied this for significant parts of their careers. The axial vector interaction is changed by meson exchange currents. The recent calculation of Gysbeg et al. accounting for most of the Gamow-Teller strength is including meson exchange currents in what they call 2-body currents, natural higher-order corrections in their chiral EFT expansion of the strong interaction between nucleons when you consider electroweak interactions.	80
█	JB: But there are lots of other things that also don't change the Fermi interaction... so picking out meson exchange currents for discussion is maybe not fully motivated. Lots of people state one consequence or another of CVC to motivate what they are doing, without explaining.	81
█	Paraphrased JB: Don't try to derive CVC in this thesis. Just cite the hypothesis and say that our Abeta stuff provides a test of it.	81

████ JB: Something else beyond the thesis scope, sorry: a nonzero b_{Fierz} does not necessarily break CVC, as the vector part of the SM weak interaction could still be conserved whether or not there are other quark-lepton currents with different Lorentz structure. You could make a nonzero b_{Fierz} from a 2nd-class scalar in the nucleon-electron weak current which would break CVC, but that could not be distinguished from a quark-electron extra scalar current.	81
████ John and Dan say this paper is widely accepted to be wrong about some of the things. (Some assumption was wrong, I guess?) So then presumably what I've written here can't be trusted either.	82
████ JB: The paper that fixes the known mistakes in Severijns et al. [6] is L. Hayen and N. Severijns, 2019 [7]. It's conveniently located on the arXiv, and I should definitely go read it. The known mistake was using the ratio of integrals of the lepton momentum f_A/f_V more than once—there is a more subtle radiative correction for the Gamow-Teller piece. A paper using the formalism is D. Combs et al [8] (which is <i>also</i> conveniently located on the arXiv) with ^{19}Ne and ^{37}K results— their extraction is so close to Ben and Dan's that we conclude we are doing the formalism well. i.e. we used the f_A/f_V ratio correctly.	82
████ JB: “You don’t need anything about the atomic hyperfine structure in this thesis.”	

...

Me: yeah, that's fair. I probably should cut this whole section actually. . . 91

Chapter 1

Background and Motivation

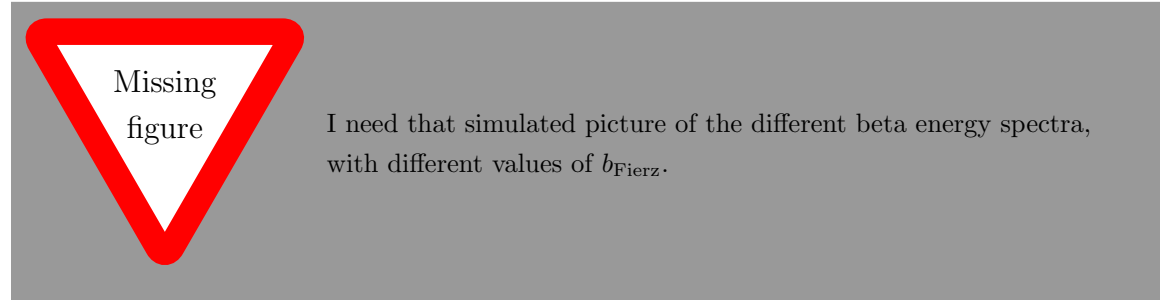
1.1 Exotic Couplings

In particular, we're interested in so-called scalar and tensor couplings within the nuclear weak force. Standard model beta decay involves only vector and axial-vector couplings, combined with a “($V - A$)” handedness (left-handed).

Need to figure out how the exotic couplings actually work, mathematically. What the fuck does “($V - A$)” even *mean*? IIRC John wants a brief mention of γ_5 's and γ_μ 's, and probably a brief mention of what mumble-mumble group is mumble-mumble represented or something.

1.2 Fierz Interference – The Physical Signature

The physical effects resulting from the presence of scalar or tensor couplings include a small perturbation to the energy spectrum of betas produced by radioactive decay.



1.3 Present Limits

A bit about other people's physics.

1.4 A Toy Experiment

A quick overview of how an experiment like this one would be set up to extract the physics of interest, to keep the reader from getting too lost in the rest of the thesis.

Do I really even *want* to include a toy experiment? And would I want to do it here?? What even is the point? I think in the past I decided it was easier to build up a description of something starting this way. But why?? Possibly as I continue to add content, it will become obvious again why I originally wanted to do this.

Chapter 2

Theoretical Overview

2.1 The Basics of Beta Decay

Standard Model beta decay is well understood. The Fermi description of beta decay can be found in any nuclear physics textbook, but you have to dig slightly harder to understand Gamow-Teller or mixed decays, all of which are relevant here.

via Krane [9] Under the Allowed Approximation, we require that a beta decay may not carry away any orbital angular momentum, because we treat the nucleus as pointlike and work in the CM frame. An Allowed decay can, however, change the total nuclear angular momentum, because the outgoing leptons have spin= 1/2 and therefore carry angular momentum. Therefore, in an allowed decay, the total nuclear angular momentum must always change by either 0 or 1.

Is this even true? The pointlike thing? ...No. No it's not.

JB says: The title of Holstein's review addresses this "pointlike" issue, and he describes the "impulse approximation" in Section V. The interaction is not pointlike, because all constants are a form factor expansion in q^2 – finite size terms contribute to the Coulomb correction.

From a 2006 paper by Severijns et al [10], the selection rules for an allowed transition are:

$$\Delta I = I_f - I_i = \{0, \pm 1\} \quad (2.1)$$

$$\hat{\Pi}_i \hat{\Pi}_f = +1 \quad (2.2)$$

Then, you can separate the allowed transitions into singlet (anti-parallel lepton spins, $S = 0$ – a Fermi transition) and triplet states (parallel lepton spins, $S = 1$ – a

Gamow-Teller transition).

Fermi decays are so-called “vector” interactions, and happen when the spin of the two leptons involved are antiparallel, so there can be no change in angular momentum (at least in the case of the Allowed approximation).

Gamow-Teller decays involve two leptons with parallel spins, so the decay must change the projection of the nuclear angular momentum, M_I , by exactly one unit (in the case of the Allowed approximation). They transition may or may not simultaneously change the total nuclear spin, I , by one unit. These are “axial-vector” interactions. (Note that $I = 0 \rightarrow I = 0$ interactions are never Gamow-Teller decays.

Probably everything in this section is yoinked from [11], pg 212.

2.2 Mathematical Formalism

In order to proceed with a measurement, we must find a master equation to describe the probability of beta decay events with any given distribution of energy and momenta among the daughter particles, as a function of the strength of the specific couplings of interest to us. To do this, two sets of formalisms are combined – the older formalism from Jackson, Treiman, and Wylde (JTW) [12], [13], which describes the effects of all types of Standard Model and exotic couplings of interest to us here, but which truncates its expression at first order in the (small) parameter of recoil energy, and a newer formalism from Holstein [14], which includes terms up to several orders higher in recoil energy, but which does not include any description of the exotic couplings of particular interest to us. We note that because any exotic couplings present in nature have already been determined to be either small or nonexistent, it is sufficient to describe these parameters with expressions truncated at first order, despite the fact that it is still necessary to describe the larger Standard Model couplings with higher-order terms.

The procedure for combining the two formalisms is described in detail in Appendix B, so we will simply provide the combined master equation here:

In the mean time, here's what happens when we integrate JTW over neutrino

Do it! Do the master equation!

direction:

$$\begin{aligned} d^3\Gamma = & \frac{2}{(2\pi)^4} F_{\mp}(Z, E_\beta) p_\beta E_\beta (E_0 - E_\beta)^2 dE_\beta d^3\hat{\Omega}_\beta \xi \\ & \times \left[1 + b_{\text{Fierz}} \frac{m_e c^2}{E_\beta} + A_\beta \left(\frac{\vec{J}}{J} \cdot \frac{\vec{p}_\beta}{E_\beta} \right) \right], \end{aligned} \quad (2.3)$$

where

$$\xi = G_v^2 \cos \theta_C f_1(E). \quad (2.4)$$

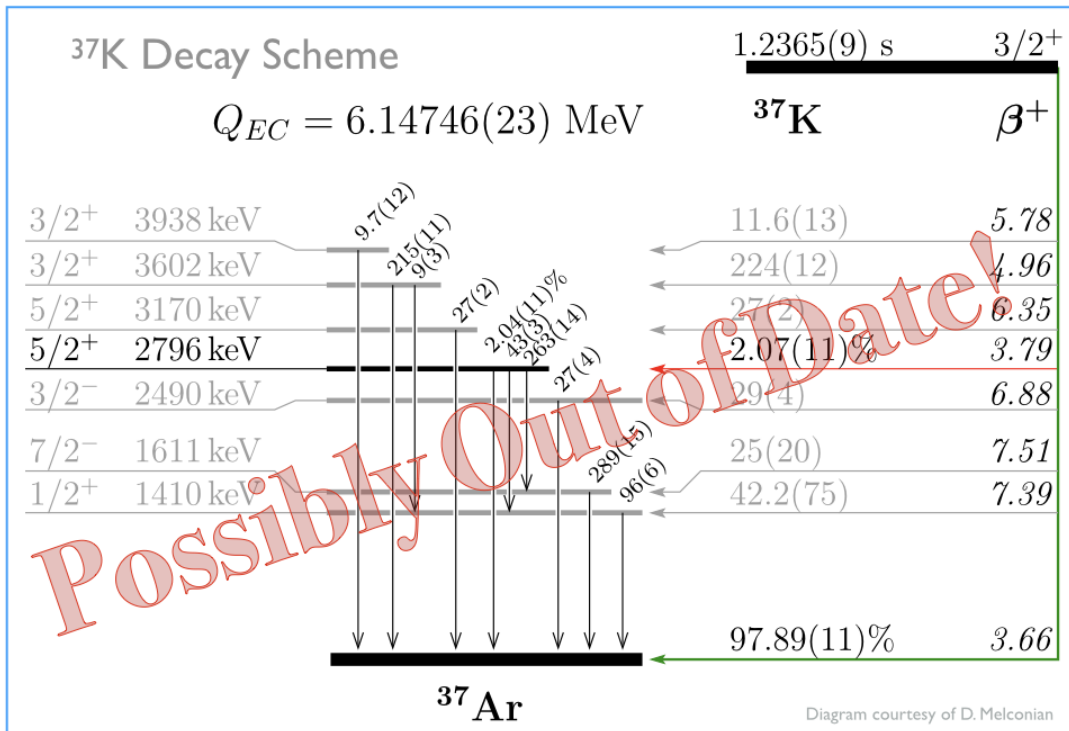
2.3 Our Decay

Talk about how great ^{37}K is for what we're doing with it. Also, drop all the math-numbers to support those assertions.

Missing figure

This thing is going to need a nuclear level diagram for ^{37}K . Also, ^{37}K is a really nice isotope for this, because $98\% + 2\%$, also because it's a mirror decay, also because it's an alkali. Also-also, its big A_β value means we have a big thing to multiply any b_{Fierz} value there might be when we construct the superratio asymmetry to eliminate systematics.

Might be worth mentioning about the shake-off electrons too, and how many of them there are. But then nobody will trust any of the numbers I measured (how did I do that measurement, anyway?), and will want me to just use Dan's that he measured forever ago with a different set of detectors. (where are those numbers recorded anyway?) I think I have to mention how many come off and how often at least briefly, because I use the Levinger spectrum for my background modeling.



2

Figure 2.1: A level diagram for the decay of ^{37}K .

Chapter 3

Atomic Physics Overview

3.1 Magneto-Optical Traps

3.1.1 Doppler Cooling

3.1.2 Zeeman Splitting

Needs a level diagram.

3.1.3 Atom Trapping with a MOT

3.2 Optical Pumping

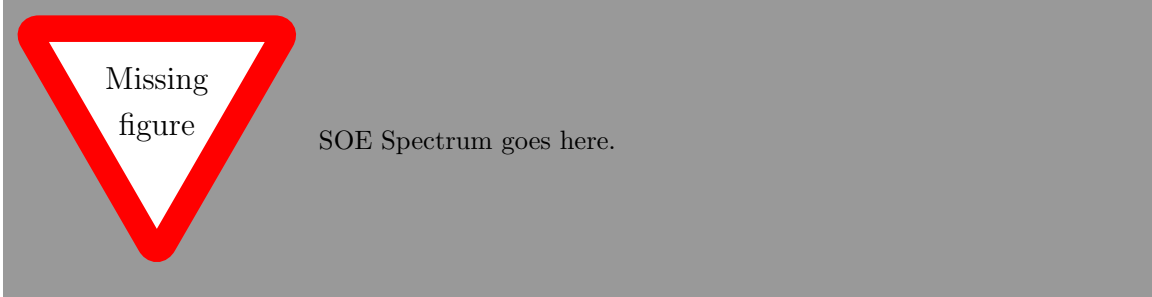
Needs a level diagram.

3.3 Shake-off Electron Spectrum

Shake-off electrons: where do they come from, and where do they go? [15].

John made some nice plots of these from the eMCP data. I did *not* use it to make a cut on eMCP hit position in the end, despite the fact that it makes the spectrum more clean, because a lot of good events don't have full hit position information, and you lose an awful lot of statistics by making the cut. I used this for modeling the background spectrum, but in the end it wasn't as elegant a result as I might have

hoped. Also, it's still an open question exactly which fraction of SOEs come from which atomic shell, but it doesn't change the resulting spectrum very much.



Chapter 4

The Experimental Setup

4.1 Double MOT System Overview and Duty Cycle

The experimental subject matter of this thesis was conducted at TRIUMF using the apparatus of the TRIUMF Neutral Atom Trap (TRINAT) collaboration. The TRINAT laboratory offers an experimental set-up which is uniquely suited to precision tests of Standard Model beta decay physics, by virtue of its ability to produce highly localized samples of isotopically pure cold atoms within an open detector geometry.

mumble mumble 7ish days of beamtime, mumble mumble 2014.

The TRINAT lab accepts radioactive ions delivered by the ISAC beamline at TRIUMF. These ions are collected on the surface of a hot zirconium foil where they are electrically neutralized, and subsequently escape from the foil into the first of two experimental chambers (the “collection chamber”). Further details on the neutralization process are presented in a previous publication [16]. Within the collection chamber, atoms of one specific isotope – for the purposes of this thesis, ^{37}K – are continuously collected into a magneto-optical trap (MOT). Approximately once per second, the atoms in the collection MOT are transferred to a second experimental chamber (the “detection chamber”) and loaded into a second MOT (see Fig. 4.1). Because the transfer and trapping mechanisms rely on tuning to specific atomic resonances, this setup allows for the selection of only a single isotope within the detection MOT, and a significantly reduced background relative to the initial beamline output. The transfer methodology is discussed in some detail within another publication [17].

Probably describe the laser transfer method slightly.

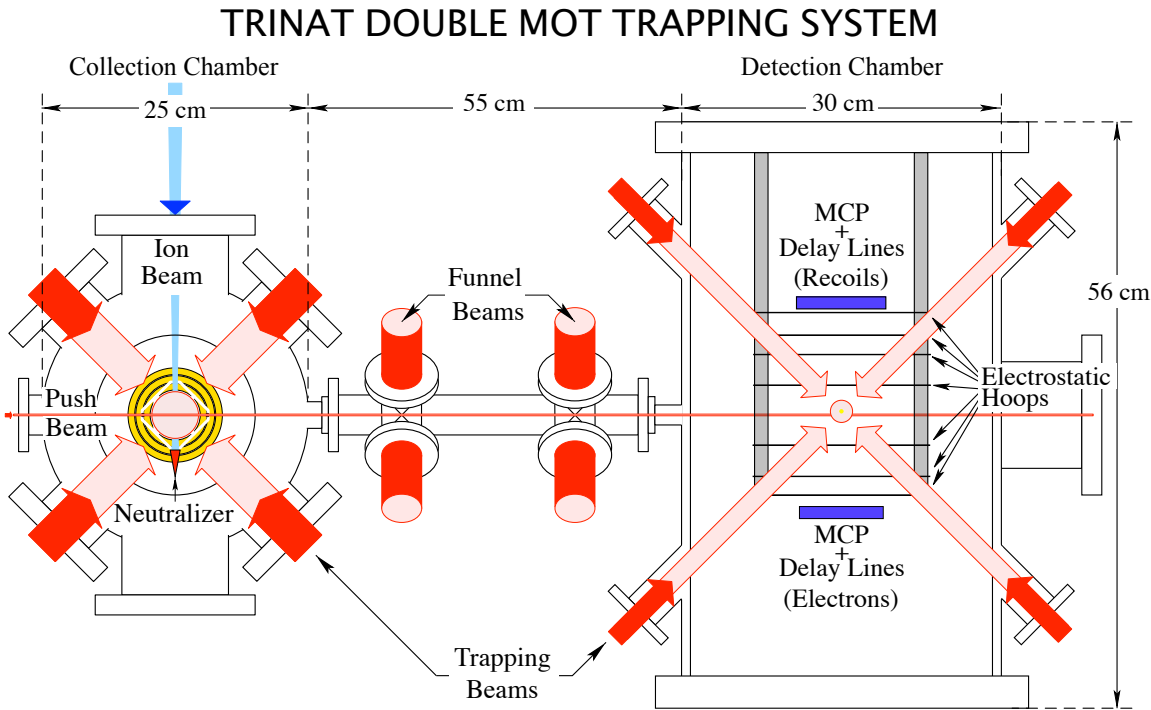


Figure 4.1: The TRINAT experimental set-up utilizes a two MOT system in order to reduce background in the detection chamber.

Once the newly transferred atoms have arrived at the second trap, the MOT cycles 500 times between a state where it is ‘on’ and actively confining atoms to a region of approximately 2 mm^3 , to a state where it is ‘off’ and instead the atoms are spin-polarized by optical pumping while the atom cloud expands ballistically before being re-trapped. Immediately following these 500 optical pumping cycles, another set of atoms is transferred in from the collection chamber to the detection chamber, joining the atoms that remain in the trap. See Fig. 4.2. This details of the trapping and optical pumping cycles are described further in Section 4.2, and the optical pumping technique and its results are the subject of a recent publication [1].

Mumble mumble UHV. Mumble mumble tail end of the Boltzmann distribution.

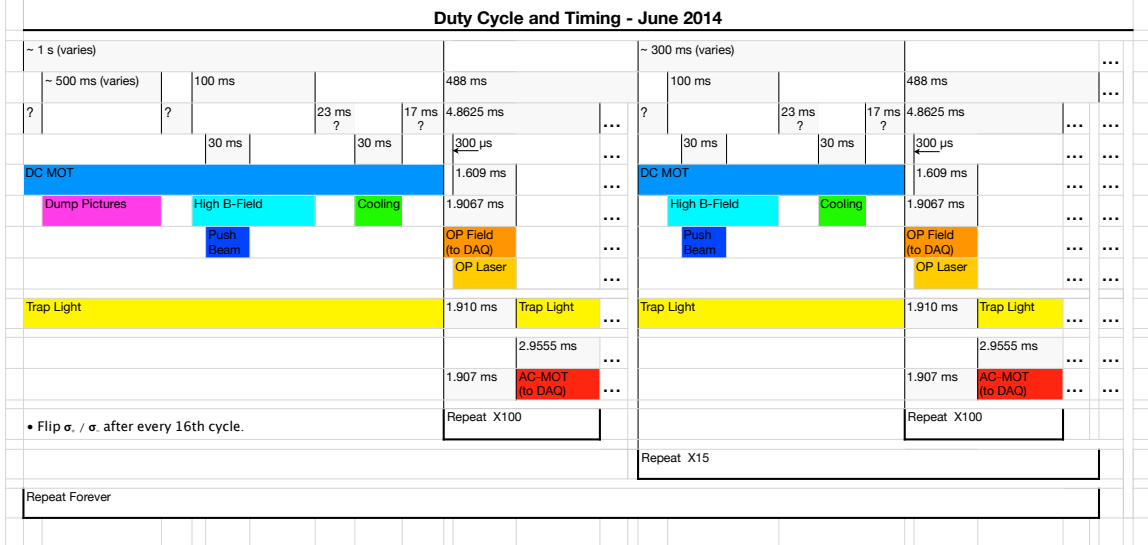


Figure 4.2: The duty cycle used for transferring, cooling, trapping, and optically pumping ^{37}K during the June 2014 experiment.

4.2 The AC-MOT and Polarization Setup

In order to facilitate a measurement of A_β , we went to great efforts to polarize the atom cloud, and quantify that polarization. This resulted in a duty cycle in which the atoms were intermittently trapped in the AC-MOT, then optically pumped to polarize them. While knowledge of the polarization is less critical in a measurement of b_{Fierz} , we still use only the polarized portion of the duty cycle in order to minimize other systematic errors, such as the scintillator energy calibration and overall trap position.

In order to eliminate systematic effects, the polarization direction is flipped every 16 seconds.

Probably document things about the waveform and frequency used for the beamtime, since I don't think it's in my MSc.

The Magneto-Optical Trap is a well-known technique from atomic physics, used to confine and cool neutral atoms [18]. The technique is used predominantly with alkalis due to their simple orbital electron structure, and is quite robust, so is appropriate for use with ^{37}K . Once set up, the trapping force is specific to the isotope for which the trap has been tuned, which makes it ideal for use in radioactive decay experiments, since the daughters are unaffected by the trapping forces keeping the parent confined.

There are two primary components necessary for any MOT: a laser, and a magnetic

field. The laser, which must be circularly polarized in the appropriate directions and tuned slightly to the red of an atomic resonance, is split into three perpendicular retroreflected beams, doppler cooling the atoms and (with the appropriate magnetic field) confining them in all three dimensions (see Figure 4.3a). The TRINAT science chamber includes 6 ‘viewports’ specifically designed to be used for the trapping laser.

Missing figure

This is going to need another edge-on G4 picture of the chamber to label all the atomic components.

Missing figure

I need *at least* one atomic level diagram. But possibly as many as 3 level diagrams. Have to show energies for MOT, energies for OP, and energies for photoionization.

JB says: “I would say you don’t need an atomic level diagram. You could just describe in words the semiclassical picture of atoms absorbing photons until they are nearly fully polarized, then they stop absorbing. The optical pumping + photoionization is then an *in situ* probe of the polarization. ... You would need to add in words that quantum mechanical corrections to this picture are in the optical Bloch equation approach in B. Fenker et al. The depolarized states still have high nuclear polarization ($1/2$ for $F = 2, M_F = 1, 5/6$ for $F = 1, M_F = 1$) and determining the ratio of those two populations provides most of the info we need – we model with the O.B.E, measure the optical pumping light polarization, and float an average transverse magnetic field. This is adequate to determine the depolarized fraction to 10% accuracy, which is all that is needed.”

Is my photoionization description adequate? ... in light of John’s feedback: no.

JB says: “Since you worked hard on the logic triggers, a photoion spectrum with duty cycle would be appropriate if you want.”

Need to describe how polarization works.

JB says: all polarization details could be deferred to [1]. (be sure to list all authors including [me]).)

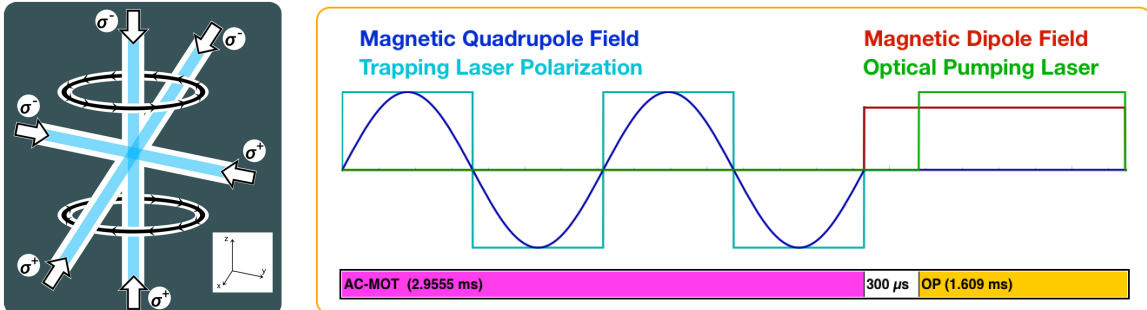
A MOT also requires a quadrupolar magnetic field, which we generate with two current-carrying anti-Helmholtz coils located within the vacuum chamber itself. The coils themselves are hollow, and are cooled continuously by pumping temperature-controlled water through them.

One feature which makes our MOT unusual has been developed as a result of our need to rapidly cycle the MOT on and off – that is, it is an “AC-MOT”. Rather than running the trap with one particular magnetic field and one set of laser polarizations to match, we run a sinusoidal AC current in the magnetic field coils, and so the sign and magnitude of the magnetic field alternate smoothly between two extrema, and the trapping laser polarizations are rapidly swapped to remain in sync with the field [19][20]. See Figure 4.3b.

Note that because the atoms within a MOT can be treated as following a thermal distribution, some fraction of the fastest atoms continuously escape from the trap’s potential well. Even with the most carefully-tuned apparatus, the AC-MOT cannot quite match a similar standard MOT in terms of retaining atoms. The TRINAT AC-MOT has a ‘trapping half-life’ of around 6 seconds, and although that may not be particularly impressive by the standards of other MOTs, it is more than adequate for our purposes. ^{37}K itself has a radioactive half-life of only 1.6 seconds (cite someone), so our dominant loss mechanism is radioactive decay rather than thermal escape.

Anyway, here’s some figures. Or possibly one figure. Whatever. Also, here’s a reference to a figure. See Fig. 4.3 (works – currently “3.4”), or also its subfigures, eg Fig. 4.3b (works – currently “3.4b”) and Fig. 4.3a (works – currently “3.4a”). Maybe I have to subref them? Like, eg, Subfig. 4.3b (works – currently “3.4b”) and Subfig. 4.3a (works – currently “3.4a”). What if we try to subref everything? Consider, eg, Fig. ?? (doesn’t work). Yeah, ok, so fortunately the note cites like the text. This gives an example of shit to do and not to do. Also, can’t do a linebreak within a note.

We spin-polarize ^{37}K atoms within the trapping region by optical pumping [1]. A circularly polarized laser is tuned to match the relevant atomic resonances, and is directed through the trapping region along the vertical axis in both directions. When a photon is absorbed by an atom, the atom transitions to an excited state and its total angular momentum (electron spin + orbital + nuclear spin) along the vertical axis is incremented by one unit. When the atom is de-excited a photon is emitted isotropically, so it follows that if there are available states of higher and lower angular momentum, the *average* change in the angular momentum projection is zero. If the



(4.3a) Components of a magneto-optical trap, including current-carrying magnetic field coils and counterpropagating circularly polarized laser beams.

(4.3b) One cycle of trapping with the AC-MOT, followed by optical pumping to spin-polarize the atoms. After atoms are transferred into the science chamber, this cycle is repeated 500 times before the next transfer. The magnetic dipole field is created by running parallel (rather than anti-parallel as is needed for the MOT) currents through the two coils.

Figure 4.3: An alternating-current magneto-optical trap with a duty cycle optimized for producing polarized atoms

atom is not yet spin-polarized, it can absorb and re-emit another photon, following a biased random walk towards complete polarization.

In order to optimally polarize a sample of atoms by this method, it is necessary to have precise control over the magnetic field. This is because absent other forces, a spin will undergo Larmor precession about the magnetic field lines. In particular, the magnetic field must be aligned along the polarization axis (otherwise the tendency will be to actually depolarize the atoms), and it must be uniform in magnitude over the region of interest (otherwise its divergencelessness will result in the field also having a non-uniform direction, which results in a spatially-dependent depolarization mechanism). Note that this type of magnetic field is not compatible with the MOT, which requires a linear magnetic field gradient in all directions (characteristic of a quadrupolar field shape), and has necessitated our use of the AC-MOT as described in Section 4.2.

that's this section. I should really describe the AC-MOT.

4.3 Microchannel Plates and Electric Field

MCPs. Hoops. Only one thing works at a time! Blarg. Upon decay, atoms literally aren't trapped anymore by the trap. No trapping forces, no slowing forces, because it's all isotope-specific.

Missing figure

Back-to-back MCPs in an electric field to tag events from the trap, and to measure the trap position and polarization. Hoops to produce the electric field.

4.4 Measurement Geometry and Detectors

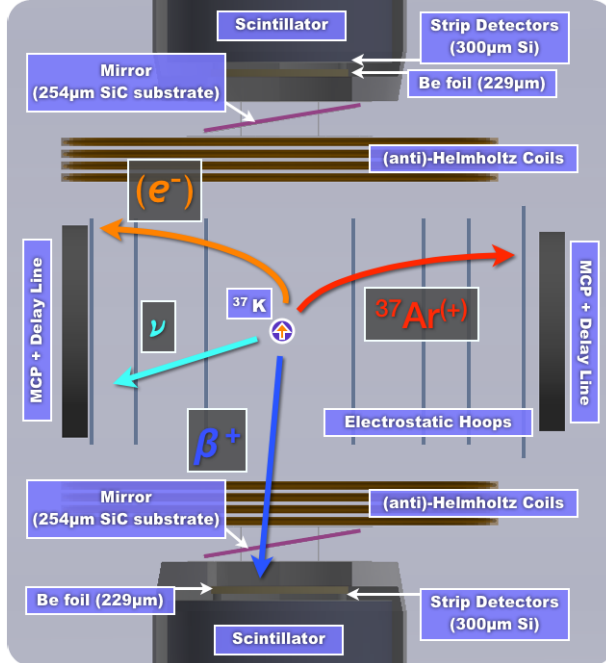
This section is disorganized and repeats itself.

Needs several diagrams. Many laser ports to make the MOT functional, and for optical pumping. Fancy mirror geometry to combine optical pumping and trapping light along the vertical axis. Water-cooled (anti-)Helmholz coils within the chamber for the AC-MOT, fast switching to produce an optical pumping field.

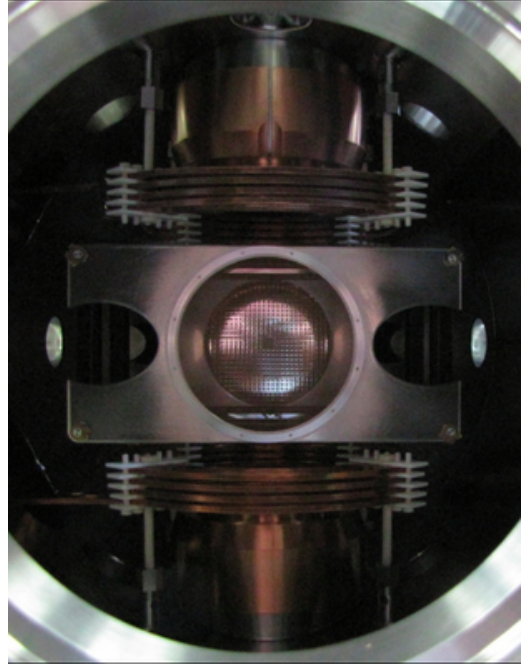
Detectors are positioned about the second MOT for data collection. The detection chamber operates at ultra-high vacuum (UHV) and provides not only the apparatus necessary to intermittently confine and then spin-polarize atoms, but also the variety of detectors and implements required to quantify their position, temperature, and polarization. The detection chamber further boasts an array of electrostatic hoops to collect both positively and negatively charged low energy particles into two microchannel plates (MCPs), and a further set of two beta detectors positioned along the polarization axis, each of which consists of a 40x40 pixel double-sided silicon strip detector (DSSD) and a scintillator and photomultiplier tube (PMT).

....(shown in Figure 4.4) ...

The beta detectors, located above and below the atom cloud along the axis of polarization (see Figure 4.4a), are each the combination of a plastic scintillator and a set of silicon strip detectors. Using all of the available information, these detectors are able to reconstruct the energy of an incident beta, as well as its hit position, and



(4.4a) A decay event within the TRINAT science chamber. After a decay, the daughter will be unaffected by forces from the MOT. Positively charged recoils and negatively charged shake-off electrons are pulled towards detectors in opposite directions. Although the β^+ is charged, it is also highly relativistic and escapes the electric field with minimal perturbation.



(4.4b) Inside the TRINAT science chamber. This photo is taken from the vantage point of one of the microchannel plates, looking into the chamber towards the second microchannel plate. The current-carrying copper Helmholtz coils and two beta telescopes are visible at the top and bottom. The metallic piece near the center is one of the electrostatic ‘hoops’ used to generate an electric field within the chamber. The hoop’s central circular hole allows access to the microchannel plate, and the two elongated holes on the sides allow the MOT’s trapping lasers to pass unimpeded at an angle of 45 degrees ‘out of the page’.

Figure 4.4: The TRINAT detection chamber.

Mirrors are 275 μm thick, not the 254 μm shown in picture.

provide a timestamp for the hit’s arrival. Together the upper and lower beta detectors subtend approximately 1.4% of the total solid angle as measured with respect to the cloud position.

The two sets of beta detectors were positioned directly along the axis of polar-

ization. Each beta detector consists of a plastic scintillator and photo-multiplier tube (PMT) placed directly behind a 40×40 -pixel double-sided silicon strip detector (DSSD). The scintillator is used to measure the overall energy of the incoming particles, as well as to assign a timestamp to these events, while the DSSD is used both to localize the hit position to one (or in some cases, two) individual pixel(s), and also to discriminate between different types of incoming particles. In particular, though the scintillator will measure the energy of an incoming beta or an incoming gamma with similar efficiency, the beta will lose a portion of its kinetic energy as it passes through the DSSD into the scintillator. By contrast, an incident gamma will deposit only a very small amount of energy in the DSSD layer, making it possible to reject events with insufficient energy deposited in the DSSD as likely gamma ray events. Given that the decay of interest to us emits positrons, we expect a persistent background 511 keV gamma rays that are not of interest to us, so it is extremely important that we are able to clean these background events from our spectrum.

It must be noted that the path between the cloud of trapped atoms and either beta detector is blocked by two objects: a $275 \mu\text{m}$ silicon carbide mirror (necessary for both trapping and optical pumping), and a $229 \mu\text{m}$ beryllium foil (separating the UHV vacuum within the chamber from the outside world). In order to minimize beta scattering and energy attenuation, these objects have had their materials selected to use the lightest nuclei with the desired material properties, and have been manufactured to be as thin as possible without compromising the experiment. As the $^{37}\text{K} \rightarrow ^{37}\text{Ar} + \beta^+ + \nu_e$ decay process releases $Q = 5.125 \text{ MeV}$ of kinetic energy [21], the great majority of betas are energetic enough to punch through both obstacles without significant energy loss before being collected by the beta detectors.

On opposing sides of the chamber, and perpendicular to the axis of polarization, two stacks of $\sim 80 \text{ mm}$ diameter microchannel plates (MCPs) have been placed (see Figure 4.4) as detectors, providing a time stamp when a particle is incident on their surfaces. Behind each stack of MCPs there is a set of delay lines, which provide position sensitivity for these detectors.

In order to make best use of these MCPs, we create an electric field in order to draw positively charged particles into one MCP, while drawing negatively charged electrons into the other MCP. Seven electrostatic hoops have been placed within the chamber (see Figure 4.4), and are connected to a series of high voltage power supplies. See Sections 5.1 and K.4 for a discussion of what sort of charged particles we expect

There's gotta be a better way to describe it

what's the open area of the detector? how big is each pixel?

to observe in these detectors and how they are created.

Scientific data has been collected at field strengths of 395 V/cm, 415 V/cm, and 535 V/cm. It should be noted that these field strengths are too low to significantly perturb any but the least energetic of the (positively charged) betas from the decay process, and these low energy betas would already have been unable to reach the upper and lower beta detectors due to interactions with materials in the SiC mirror and Be foil vacuum seal.

Chapter 5

Calibrations and Data Selection

5.1 Cloud Measurements via Photoionization

In order to measure properties of the trapped ^{37}K cloud, a 10 kHz pulsed laser at 355 nm is directed towards the cloud. These photons have sufficient energy to photoionize neutral ^{37}K from its excited atomic state, which is populated by the trapping laser when the MOT is active, releasing 0.77 eV of kinetic energy, but do not interact with ground state ^{37}K atoms. The laser is of sufficiently low intensity that the great majority of excited state atoms are *not* photoionized, so the technique is only very minimally destructive.

Probably worth mentioning that we test this stuff offline on stable ^{41}K .

Because an electric field has been applied within this region (see Section ??) the $^{37}\text{K}^+$ ions are immediately pulled into the detector on one side of the chamber, while the freed e^- is pulled towards the detector on the opposite side of the chamber. Because $^{37}\text{K}^+$ is quite heavy relative to its initial energy, it can be treated as moving in a straight line directly to the detector, where its hit position on the microchannel plate is taken as a 2D projection of its position within the cloud. Similarly, given a sufficient understanding of the electric field, the time difference between the laser pulse and the microchannel plate hit allows for a calculation of the ion's initial position along the third axis.

As a check: the camera measurements for photons from de-excitation. It's aimed 35 degrees from vertical, with its horizontal axis the same as one of the other axes. I think it's the TOF axis. I can check this when my computer comes back. Also, there's an unknown additional delay between some of our DAQ channels that can't be explained by accounting for cable lengths, so we really like having the check there.

With this procedure, it is possible to produce a precise map of the cloud's position and size, both of which are necessary for the precision measurements of angular correlation parameters that are of interest to us here. However, it also allows us to extract a third measurement: the cloud's polarization.

The key to the polarization measurement is that only atoms in the excited atomic state can be photoionized via the 355 nm laser. While the MOT runs, atoms are constantly being pushed around and excited by the trapping lasers, so this period of time provides a lot of information for characterizing the trap size and position. When the MOT is shut off, the atoms quickly return to their ground states and are no longer photoionized until the optical pumping laser is turned on. As described in Section ??, and in greater detail in [1], the optical pumping process involves repeatedly exciting atoms from their ground states until the atoms finally cannot absorb any further angular momentum and remain in their fully-polarized (ground) state until they are perturbed. Therefore, there is a sharp spike in excited-state atoms (and therefore photoions) when the optical pumping begins, and none once the cloud has been completely polarized. The number of photoion events that occur once the sample has been maximally polarized, in comparison with the size and shape of the initial spike of photoions, provides a very precise characterization of the cloud's final polarization [1].

Trap position – Measured using the same dataset that was used to quantify the polarization.

The trap drifts slightly over the course of our data collection. Describe the rMCP calibration needed to extract this info.

Polarization measurement was conducted on a different set of data, collected in between the measurements used for A_β and b_{Fierz} , and at a higher electric field, because we were unable to run both our MCP detectors simultaneously.

Anyway, here is a nice table describing the atom cloud, for each of 3 runsets, and I'll immediately reference it right now, as Table 5.1:

Also, we noticed the trap drifting after one of the runs, because one of the batteries on one of the thingies adjusting the laser frequency (I think) was failing.

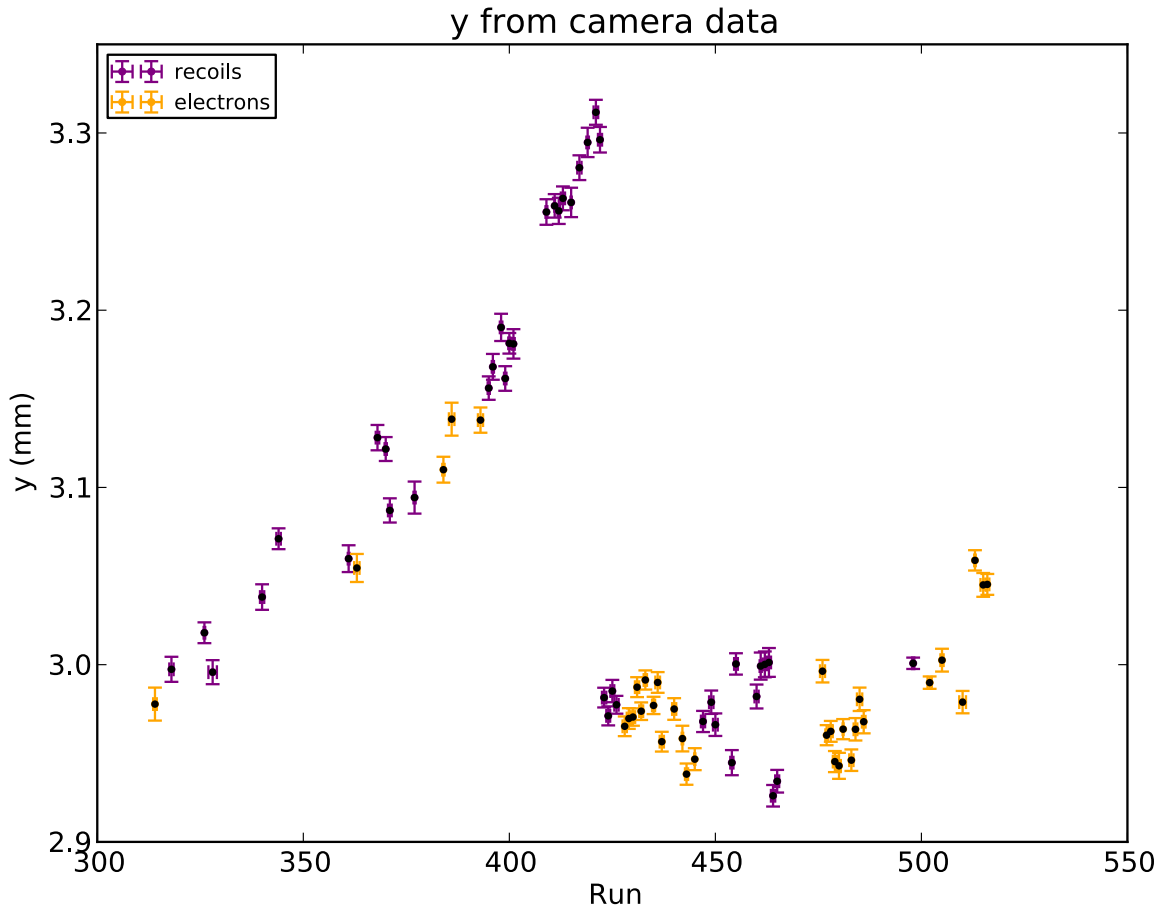


Figure 5.1: Trap Position along the “Time-of-Flight” Axis. Electron runs and recoil runs plotted by run number. (I should probably re-plot this. Maybe combine info with Fig. (5.2).)

JB: “If we rejected the data with the MOT moving (indeed a battery determining the voltage controlled oscillator frequency offset between absorption in stable ^{41}K cell and the ^{37}K resonance) then that’s all you need to say.”

describe how you’d turn this into a physical description of the cloud, with like a temperature and a sail velocity and shit. with equations.

5.2 Beta Detector Cuts

Setup is as described in Section 4.4.

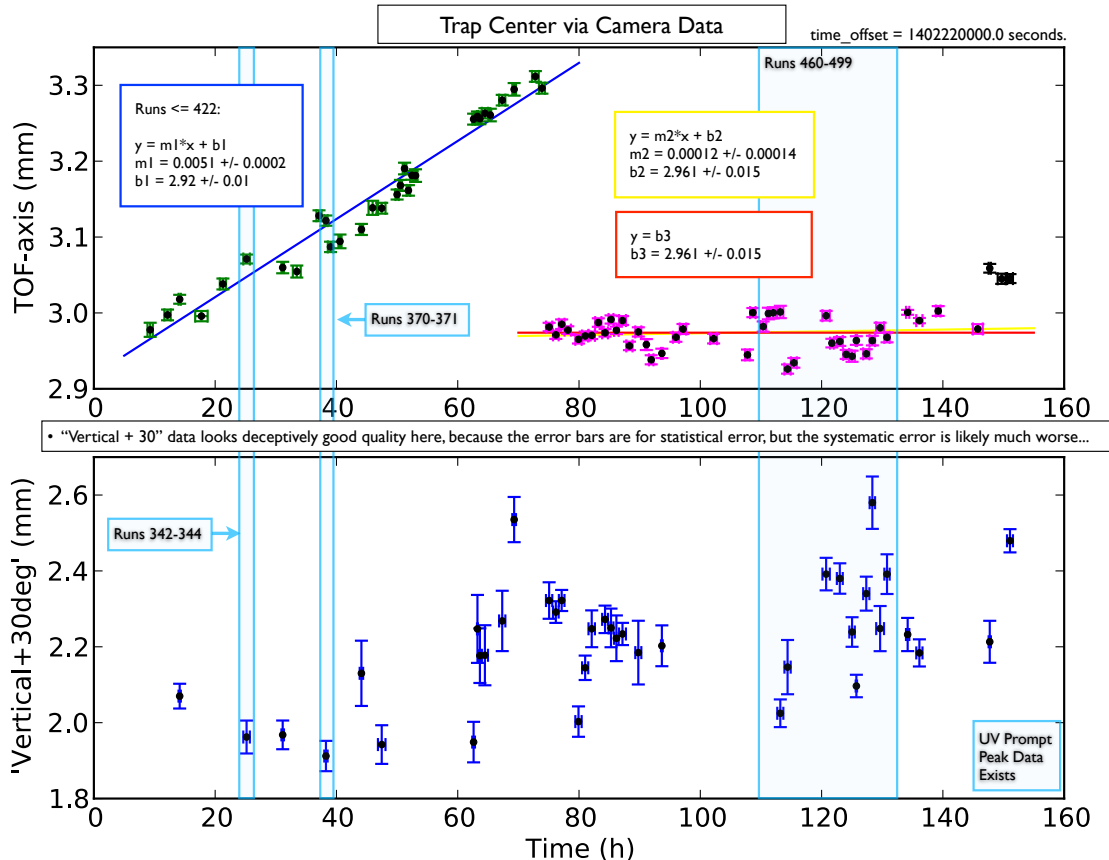


Figure 5.2: Trap Position along the “Time-of-Flight” Axis and the “Vertical+30” Axis. All runs plotted by time of run. (Need to re-plot this.)

This is a stupid section name. Also, I really do need to describe how the cuts were made here somewhere, because it's non-trivial in many cases, and possibly different than what Ben did in some cases. But it won't make sense to describe what I did different if I don't describe the thing as a whole, at least a bit. The point is, this is a set of cuts/systematics that isn't really that straightforward to understand.

Energy calibration for the scintillator+PMT setup changed dramatically at one point. Describe how calibration was done. Like, one sentence or something. Something about the endpoint energy, and something about the compton edge for 511s, IIRC.

JB: “You can describe anything you did differently or improved, but you can and should otherwise defer all details of the scintillator calibration and DSSD calibration to Ben’s paper and his thesis and Spencer’s. E.g. Section 8.2 “statistical agreement between BB1 X and Y detectors’ energies only makes a small effect on results” does not need the technical details beyond that statement.”

		Initial Position	Final Position	Initial Size	Final Size
Runset B	x	1.77 ± 0.03	2.06 ± 0.08	0.601 ± 0.013	1.504 ± 0.047
	y	-3.51 ± 0.04	-3.33 ± 0.05	1.009 ± 0.013	1.551 ± 0.018
	z	-0.661 ± 0.005	-0.551 ± 0.021	0.891 ± 0.004	1.707 ± 0.015
Runset C	x	2.22 ± 0.05	2.33 ± 0.11	1.18 ± 0.04	1.538 ± 0.087
	y	-3.68 ± 0.04	-3.31 ± 0.06	0.965 ± 0.012	1.460 ± 0.030
	z	-0.437 ± 0.09	-0.346 ± 0.037	0.927 ± 0.007	1.797 ± 0.026
Runset D	x	2.274 ± 0.012	2.46 ± 0.06	0.386 ± 0.016	1.382 ± 0.046
	y	-4.54 ± 0.04	-4.28 ± 0.04	0.986 ± 0.08	1.502 ± 0.013
	z	-0.587 ± 0.04	-0.481 ± 0.018	0.969 ± 0.003	1.861 ± 0.013

Table 5.1: Cloud Positions and Sizes – Measured immediately before and immediately following the optical pumping phase of the trapping cycle. All entries are expressed in units of mm, and the “size” parameters describe the gaussian width.

JB: “If you have some way of documenting the coding you used, that would be great.” ... yeah, it would, wouldn’t it?

5.3 The eMCP

I can describe the eMCP calibration here, even though it mostly wasn’t implemented by me. It is tangentially relevant to data selection and background estimation by providing an experimental energy spectrum for shake-off electrons. It’s actually a pretty neat algorithm that I basically wasn’t involved with.

JB: eMCP. You need to describe the timing information obtained. You also need a statement of whether or not you used the position information in your cuts.

Missing figure

Needs an SOE timing spectrum. At least one of them. Experimental and simulated. Also, I have to describe how I did the simulating, and how I check that it’s OK despite the fact that the simulated spectrum looks nothing like the experimental spectrum.

5.4 The rMCP

I did this, and they're absolutely needed to make any sense of the trap position data. These calibrations are done during AC-MOT time, and we're actually interested

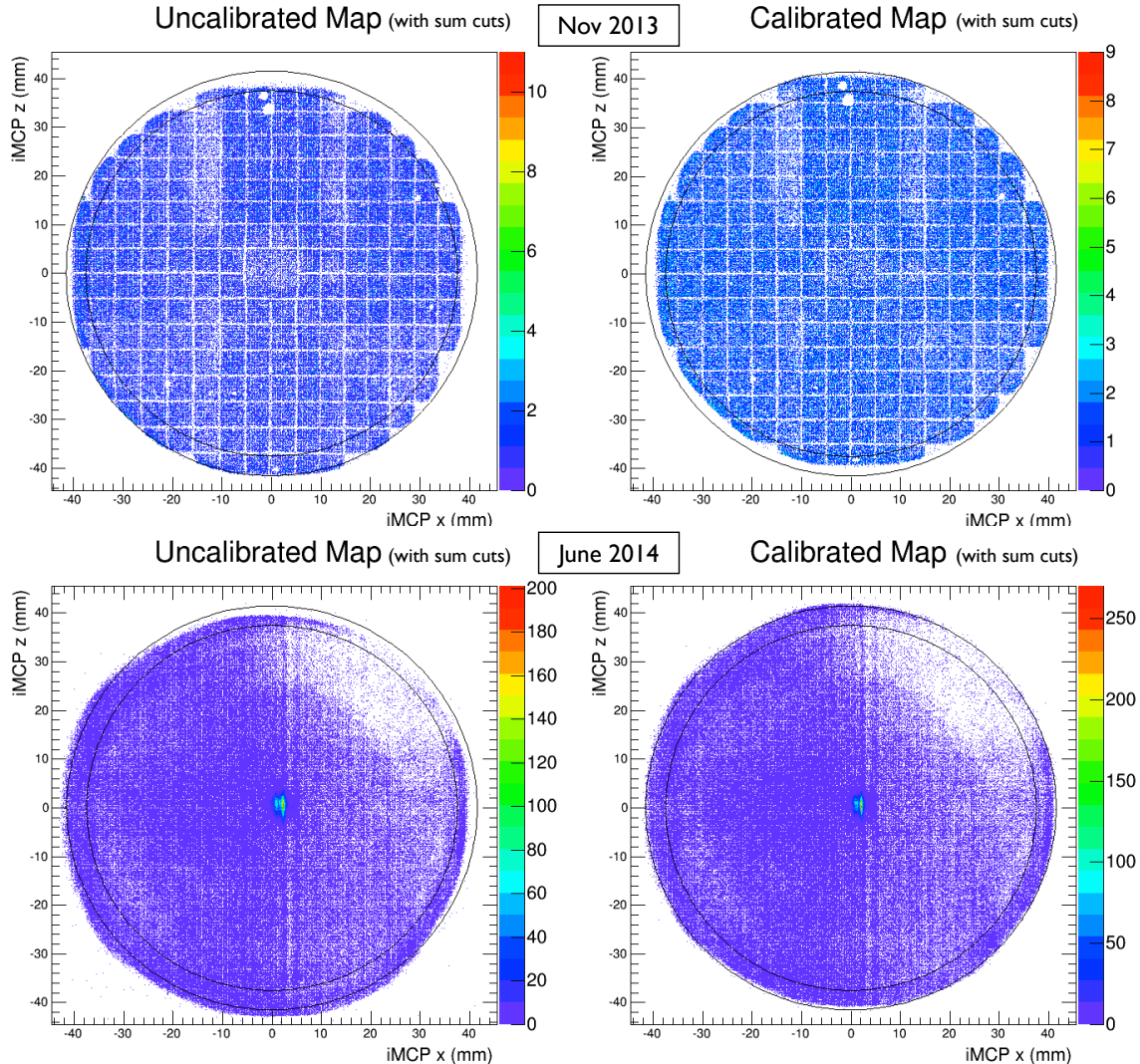


Figure 5.3: rMCP Calibration. Definitely comment about how this calibration went here, in the figure caption. (Do I definitely want a picture with the stupid line-y runs? Maybe it's better to just *not*...)

in the rMCP data taken during OP time. Can I find pictures to estimate the size of the change resulting from the magnetic field? In any case, the change is pretty small.

Chapter 6

The Experimental Signature

Possibly this can be combined with the “Background and Motivation” or “Theory” chapters? Why do I even **have** two of those chapters, if not for this? Anyway, surely I don’t need **three** of them...

6.1 General Stuff

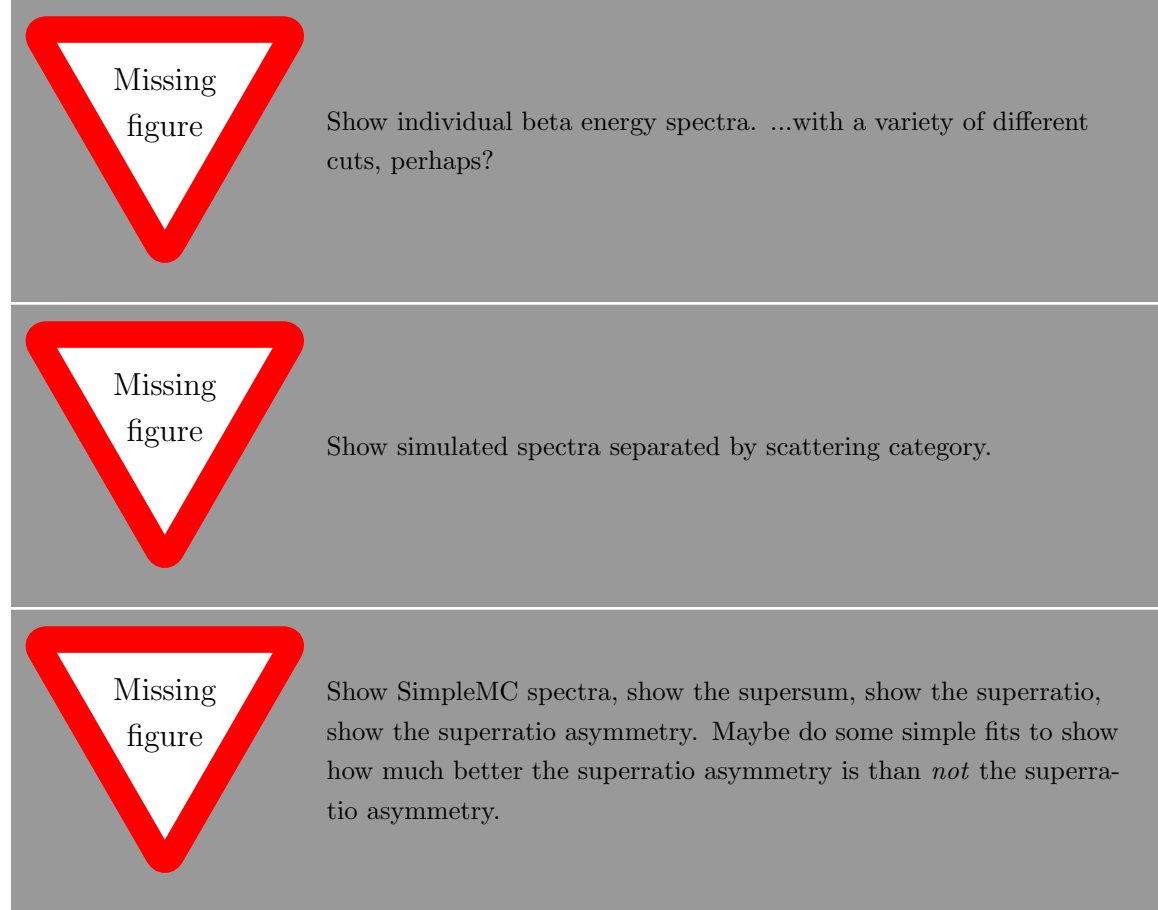
The point is, the presence of either scalar or tensor interactions will produce a b_{Fierz} term in the decay PDF. It has other effects on the PDF, but those come in at higher-order in the tiny scalar and tensor couplings. So, the Fierz term would be by far the biggest thing that changes in the PDF. The PDF describes the energy and momentum of the outgoing beta w.r.t. a variety of other things. Notably, we can write an elegant-ish description of beta momentum w.r.t. nuclear polarization direction, and ignore the neutrino completely after integrating over it. We have a PDF in beta *direction* (w.r.t. polarization), and beta *energy*. To lowest order (and lowest order is best order) the distribution w.r.t. polarization direction doesn’t change, but the distribution w.r.t. energy does change. Or ... something? The point is, it makes a change in the beta energy spectrum. This change is most pronounced at low energies, because the Fierz term is scaled by $(1/E_\beta)$. However, the asymmetry is also a function of E_β . A different function of E_β . In fact, it is scaled by (p_β/E_β) within the PDF, which is distinctly different than b_{Fierz} . So, one might ask what effect a b_{Fierz} term would produce on a constructed asymmetry spectrum.This explanation has gone way off track.

6.2 TBD

JB: You need to at some point say that the supersum is the beta energy spectrum. There are experiments trying to do this method better, but they are very difficult. UCNA published a combined energy spectrum and Abeta[Ebeta] analysis on the neutron in March 2020 [2].

I can't help but also notice the follow-up article from September 2020 [3]. Ugh.

I really need an excuse to include more pictures of data. Also, more pictures of simulations.



6.3 The Superratio and Asymmetry

The data can be combined into a superratio asymmetry. This has the benefit of causing many systematics to cancel themselves out at leading order. It also will increase the fractional size of the effects we're looking for. This can be shown by using math.

6.4 Signature of a Fierz Term in This Experiment

Not all systematics effects are eliminated. We'll want to be careful to propagate through any effects that are relevant. Using the superratio asymmetry as our physical observable makes this process a bit messier for the things that don't cancel out, but it's all just math.

6.5 Comparative Merits of the Superratio and Supersum for Measurement

Some other groups have performed similar measurements using the supersum as the physical observable. There are pros and cons to both methods. I can show, using a back-of-the-envelope calculation, that for this particular dataset, the superratio asymmetry method produces a better result.

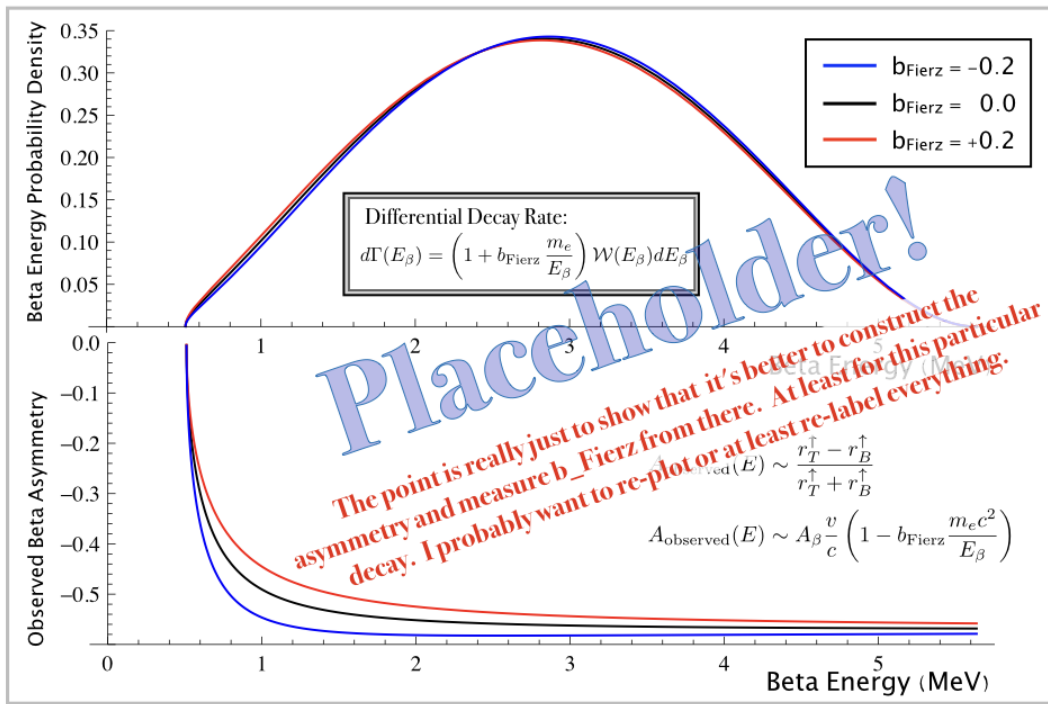


Figure 6.1: Here's why it's better to extract b_{Fierz} from an asymmetry, in this case.

Chapter 7

Analysis

Right, so. Here's how I processed the data into an answer. In bullet point form, so I don't forget stuff while I'm obsessively trying to phrase everything well.

With the Data:

- Higher-level data cleaning. Discard events during parts of the duty cycle when atoms weren't polarized. Discard events near a recorded spark time. Discard events when the photoionization laser fires. Discard events when the LED pulser used to calibrate the scintillators fires.
- Split up runs into sets, to account for changing experimental conditions. Possibly I should list what the differences between runs were somewhere. But not in this section.
- Using the “other” data set with the rMCP: Measure the trap position/size/velocity/expansion with the rMCP and with the camera. Necessitates calibrating the rMCP, which is its own whole thing. Also measure polarization.
 - rMCP calibration probably goes in another section. wev.
 - We took the mask off before the 2014 run, to give us more detector area. Use previous reference calibration *with the mask* during the test run in Nov 2013. The delay line's non-linearities should be the same, assuming we can get the centering the same. Cables have changed and stuff, so we have to re-center the pre-calibration image to where the old pre-calibration image was. ... So, center the new runs w.r.t the old run.

- We'll want to make some sum cuts for these things. We might like them to be identical, or at least identical-ish, but the peaks don't really look the same. So we'll settle for “decent sum cuts for all!”. ... So, apply sum cuts to the new runs and old run.
- Calibrate the old run, with the mask. In fact, I don't remember which order I did things in. But I have a record of it here, somewhere...
- Make some more careful cuts to clean the data.
 - Discard events without a “good” DSSD hit. Eliminates vast majority of background 511s. Necessitates having a definition of what a “good” DSSD hit is. It's subtle enough that we'll want to leave some part of this definition of “good” to be varied as a systematic effect. Notably, we consider energy agreement for each hit pixel, individual strip SNR, and overall DSSD energy threshold. Also, hit radius w.r.t. center of detector. This is a lot of stuff, all implemented by Ben – and it needs to be done fairly early on in data processing in order to keep processing times for everything else manageable.
 - Discard events where SOE-Beta TOF falls outside a certain range. Necessitates picking a “good” range. The precise definition of “good” is varied as a systematic.

With the Simulations:

- Update G4 event generator to be able to model non-zero scalar and tensor coupling. These things show up in A_β too, not just in b_{Fierz} . Though, the effects on A_β are much smaller.
- Run 3 sets of G4 simulations with a bunch of statistics (N events, for data with like $N/10$ events). Each one has the same nominal value of A_β , but with 3 different values of the scalar coupling C_S : zero, and $+/-$ (whatever). Keep $C_T = 0$. Because reasons, we're not really able to distinguish between C_S and C_T in this experiment anyway, so might as well keep the analysis simple.

- Just run one set of 0.02^*N events for the two percent branch. We can't neglect it, but it isn't going to change (much?) when we adjust BSM couplings.
- Match cuts in simulated data up to the cuts on experimental data. Obviously. DSSD cut, DSSD energy, one hit DSSD, one hit scint. TOF cut, which requires a whole extra model of background in the TOF spectrum..
 - Suppose background in the TOF spectrum is coming from decays of atoms that have gotten themselves stuck to surfaces within the chamber...
 - Run G4 to get a beta TOF spectrum (w.r.t. the decay)
 - Run COMSOL (credit to Alexandre) to track low-energy SOEs through the electric field from wherever they started, into the detectors. Energy spectra from Levinger.
 - Combine G4 and COMSOL spectra, event-by-event, while requiring that both the beta detector and the eMCP are hit according to the set of random numbers generated by each monte carlo separately. Then, the beta and SOE will each have a TOF from decay to detector, and subtracting one from the other gives a timing spectrum that can be observed experimentally. See Fig. 7.1.
 - Upper limit for the fraction of events generated this way can be estimated by assuming that all losses from the trap not due to radioactive decay emerge isotropically from the trap and then stick to whatever chamber wall is in its path. This upper limit is too big by a factor of 2.
- For each of those 3 simulations, sort the “good” data according to emission angle relative to the detector. Do each detector individually. For both polarizations.

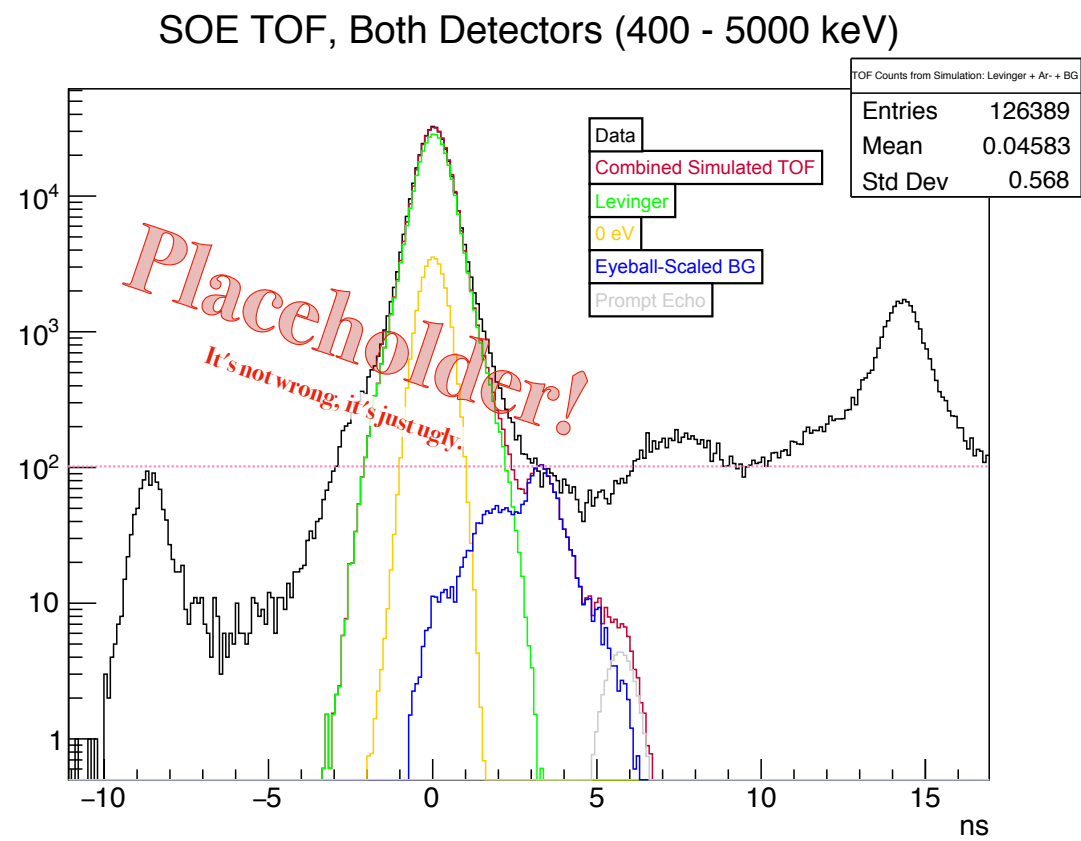


Figure 7.1: SOE TOF, model and data. In the end, I cut the data to use only events with a TOF between [A](#) and [B](#). Max. possible background is like a factor of two too big.

Chapter 8

Estimating Systematic Effects

How do I even *do* these estimations?

8.1 Low-energy Scintillator Threshold

Choice of low-energy scintillator threshold has a large systematic effect...

It's actually not nearly as big as I'd originally expected. It's huge in the line-shape thing, but pretty tiny in everything else.

8.2 BB1 Radius, Energy Threshold, Agreement

BB1 radius cut can help to eliminate scattered events. Energy threshold selection and statistical agreement between BB1 detectors' energies only makes a small effect on results. BB1 radius itself has a pretty big effect on the result, but we can at least just G4 it away. The remaining systematic effect is pretty small.

As per JB's comment in section 5.2: "statistical agreement between BB1 X and Y detectors' energies only makes a small effect on results" does not need the technical details beyond that statement."

Missing figure

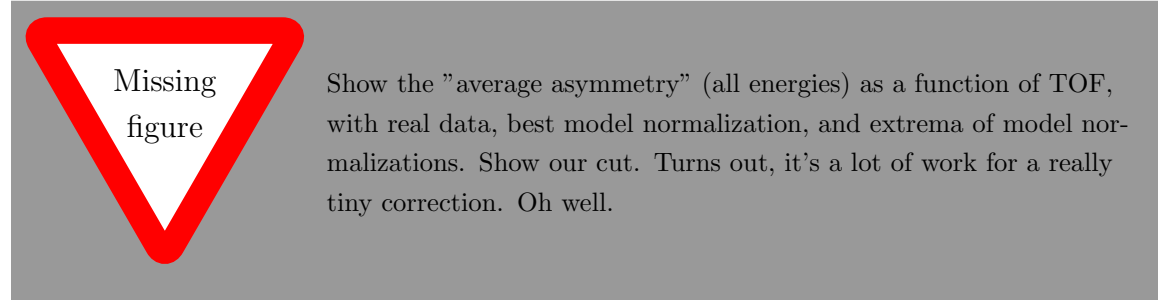
Surely this requires at **least** one image of the pixelated BB1 data. Maybe some of a few waveforms and energy distributions too.Feels like cheating to include some of that stuff, since Ben was the one who actually used it mostly.

Remember: There's noise applied to simulated BB1s, matching some spectrum.

In the end, we get our results from the scintillator energy only, without summing the BB1 energy back in. Energy absorbed in DSSDs is only used as (a) a tag for events, and (b) contributing to the total beta energy loss before the beta arrives at the scintillator.

8.3 Background Modeling – Decay from Surfaces within the Chamber

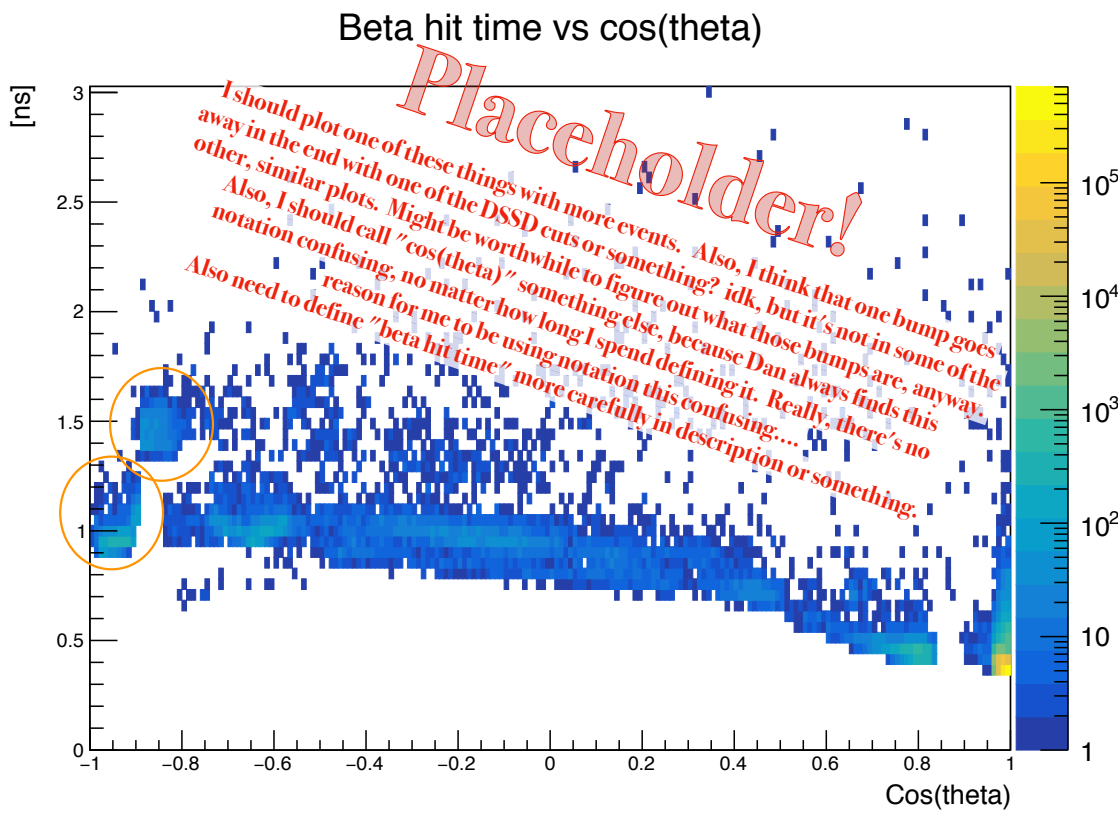
So many surfaces, all of which can get stray 37K atoms stuck to them. Then they decay from a place that isn't the actual trap center, and it contaminates our stuff.



So we model the beta TOF from the surfaces in G4, event by event. This is necessary because scattered events will have their TOF changed to account for a longer beta pathlength, and we're preferentially cutting away the events that don't have a TOF in the appropriate range.And then have COMSOL generate electron TOFs for SOEs starting from the start points picked by G4. Ran COMSOL for 0 eV SOEs, and again for Levinger spectrum SOEs. Used 9% 0eV SOEs in the end. I forget which Levinger distribution I used in the end. The point is, for each event, you've simulated a beta TOF that may or may not be scattered off of something before it hits a detector, and you have a SOE TOF for an event originating at that same point, so you subtract them to model the TOF you'd measure in an experiment. Also, because you've done the scattering with G4, you get the beta energy corrected for any scattering that happened. This way, you know precisely how much "bad stuff" you're getting rid of with the TOF cut.

8.4 Quantifying the Effects Backscatter with Geant4

Beta decay (back-)scatter from surfaces within the experimental chamber is a significant systematic, and it must be evaluated, quantified, and corrected for. This is done via a series of GEANT4 simulations. While only a small fraction of events are affected, the process results in an energy loss in the beta that can, if not understood, be misinterpreted as the exact signal we're searching for. It is therefore imperative that this be well understood.



Oh god. Have I even tried to quantify the combined systematic that comes out of the TOF cut? Do I need to, or is it double-counting? Ugh, it would be such a headache to do this. Maybe I can at least do it at the end – because I might never get my code back to the way it was.

6

Figure 8.1: Simulated Beta TOA vs emission angle w.r.t. detector orientation

8.5 Lineshape Reconstruction

This section should reference Clifford. [4].

8.5.1 Motivation

This process is used because the (back-)scatter, which it itself an important systematic, is largely independent of a wide variety of other experimental effects. These other effects must all be evaluated, but it is computationally prohibitive to re-evaluate the scattering with every other effect under consideration.

8.5.2 What is it and how does it work?

Mono-energetic beta decay events are generated in GEANT4, which outputs an energy spectrum for unscattered and forward-scattered beta events in the detector. These spectra are fit to a function to model the scintillator resolution, as well as energy loss in materials that the beta passed through before arriving at the scintillator. These spectrum fits are performed for a set of beta energies, and parameters are extrapolated to be applied to betas emitted at intermediate energies. Thus, the whole spectrum can be modeled. Pictures will make this clearer.

8.5.3 The Math-Specifics

I'll write down the specific functions I'm using, and the parameter values I'm using. (Maybe this should go in an appendix instead?) I'll describe the adjustments I make to the spectrum so that it can work even for the dataset where the scintillators' resolutions have changed.

8.5.4 The Results – Things That Got Evaluated This Way

As it turns out, only cloud parameters were evaluated this way. Trap position, size, sail velocity, temperature. But then we varied the lineshape anyhow, to account for G4 doing a bad job of modelling the bremsstrahlung (sp?).

8.5.5 The low-energy tail uncertainty, and what it does

Bremsstrahlung. It does Bremsstrahlung.

Chapter 9

Results

9.1 Measured Limits on b_{Fierz} , C_S , C_T

Results go here, with measured limits described and quantified in all formats anyone could ever care about.

9.2 Discussion of Corrections and Uncertainties

...

9.3 Relation to Other Measurements and New Overall Limits

In which I'll show exclusion plots and write down new limits, combining my result with results from the literature.

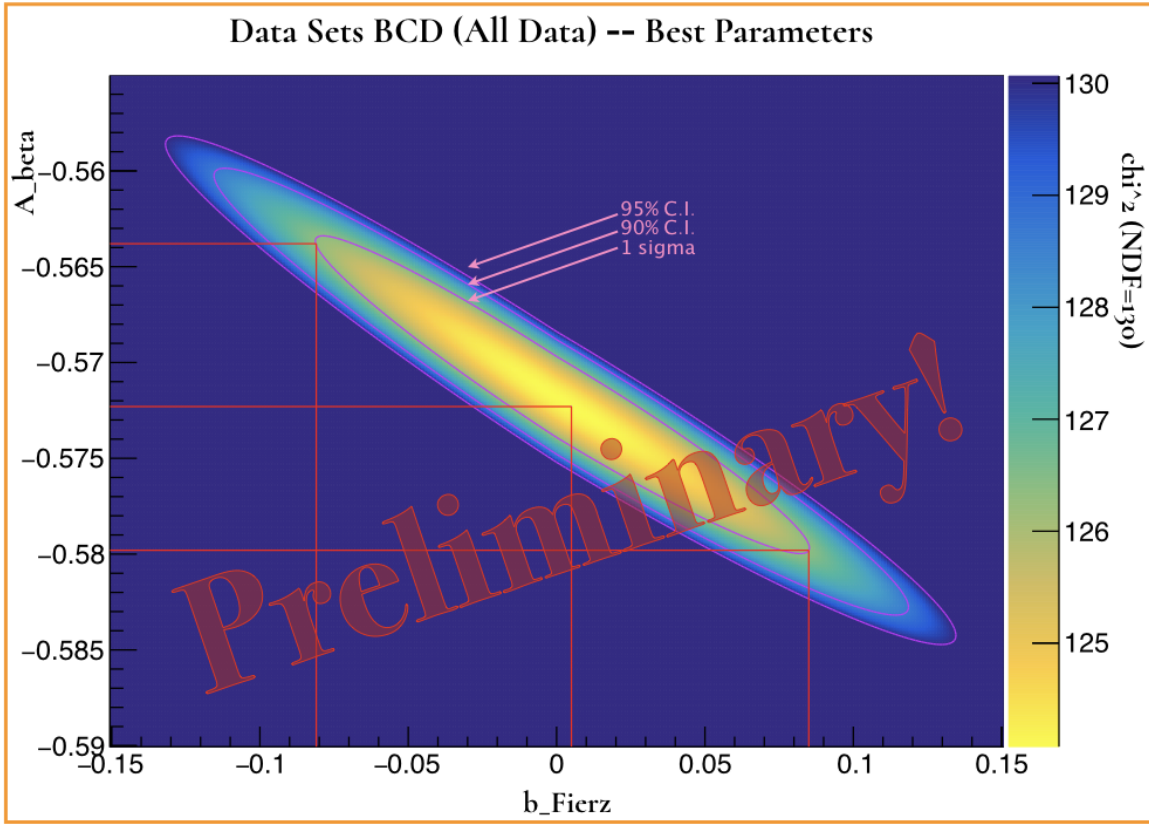


Figure 9.1: Some results. I'll want to show at least one of these things. Probably show a separate one for each runset, actually.

Bibliography

- [1] Fenker, B., Behr, J. A., Melconian, D., Anderson, R. M. A., Anholm, M., Ashery, D., Behling, R. S., Cohen, I., Craicu, I., Donohue, J. M., Farfan, C., Friesen, D., Gorelov, A., McNeil, J., Mehlman, M., Norton, H., Olchanski, K., Smale, S., Thériault, O., Vantyghem, A. N. and Warner, C. L., *Precision measurement of the nuclear polarization in laser-cooled, optically pumped ^{37}K* , New Journal of Physics, Vol. 18, No. 7, pp. 073028, 2016.
- [2] Sun, X., Adamek, E., Allgeier, B., Bagdasarova, Y., Berguno, D. B., Blatnik, M., Bowles, T. J., Broussard, L. J., Brown, M. A.-P., Carr, R., Clayton, S., Cude-Woods, C., Currie, S., Dees, E. B., Ding, X., Filippone, B. W., García, A., Geltenbort, P., Hasan, S., Hickerson, K. P., Hoagland, J., Hong, R., Holley, A. T., Ito, T. M., Knecht, A., Liu, C.-Y., Liu, J., Makela, M., Mammei, R., Martin, J. W., Melconian, D., Mendenhall, M. P., Moore, S. D., Morris, C. L., Nepal, S., Nouri, N., Pattie, R. W., Pérez Gálvan, A., Phillips, D. G., Picker, R., Pitt, M. L., Plaster, B., Salvat, D. J., Saunders, A., Sharapov, E. I., Sjue, S., Slutsky, S., Sondheim, W., Swank, C., Tatar, E., Vogelaar, R. B., VornDick, B., Wang, Z., Wei, W., Wexler, J. W., Womack, T., Wrede, C., Young, A. R. and Zeck, B. A., *Improved limits on Fierz interference using asymmetry measurements from the Ultracold Neutron Asymmetry (UCNA) experiment*, Phys. Rev. C, Vol. 101, pp. 035503, Mar 2020.
- [3] Saul, H., Roick, C., Abele, H., Mest, H., Klopf, M., Petukhov, A. K., Soldner, T., Wang, X., Werder, D. and Märkisch, B., *Limit on the Fierz Interference Term b from a Measurement of the Beta Asymmetry in Neutron Decay*, Phys. Rev. Lett., Vol. 125, pp. 112501, Sep 2020.
- [4] Clifford, E., Hagberg, E., Koslowsy, V., Hardy, J., Schmeing, H. and Azuma, R.,

Measurements of the response of a hybrid detector telescope to mono-energetic beams of positrons and electrons in the energy range 0.8–3.8 MeV, Nuclear Instruments and Methods in Physics Research, Vol. 224, No. 3, pp. 440–447, 1984.

- [5] Jelley, N. A., Fundamentals of Nuclear Physics, Cambridge University Press, 1990.
- [6] Severijns, N., Tandecki, M., Phalet, T. and Towner, I. S., *Ft values of the $T = 1/2$ mirror β transitions*, Phys. Rev. C, Vol. 78, pp. 055501, Nov 2008.
- [7] Hayen, L. and Severijns, N., *Radiative corrections to Gamow-Teller decays*, arXiv e-prints, p. arXiv:1906.09870, Jun. 2019.
- [8] Combs, D., Jones, G., Anderson, W., Calaprice, F., Hayen, L. and Young, A., *A look into mirrors: A measurement of the β -asymmetry in ^{19}Ne decay and searches for new physics*, arXiv e-prints, p. arXiv:2009.13700, Sep. 2020.
- [9] Krane, K. S., Introductory Nuclear Physics, Wiley, New York, 1988.
- [10] Severijns, N., Beck, M. and Naviliat-Cuncic, O., *Tests of the standard electroweak model in nuclear beta decay*, Rev. Mod. Phys., Vol. 78, pp. 991–1040, September 2006.
- [11] Wong, S., Introductory Nuclear Physics, Prentice Hall Advanced Reference Series Prentice Hall Labora, Prentice Hall, 1990.
- [12] Jackson, J. D., Treiman, S. B. and Wyld, H. W., *Possible Tests of Time Reversal Invariance in Beta Decay*, Phys. Rev., Vol. 106, pp. 517–521, May 1957.
- [13] Jackson, J. D., Treiman, S. B. and Wyld, H. W., *Coulomb Corrections in Allowed Beta Transitions*, Nuclear Physics, Vol. 4, pp. 206–212, Nov. 1957.
- [14] Holstein, B. R., *Recoil effects in allowed beta decay: The elementary particle approach*, Reviews of Modern Physics, Vol. 46, No. 4, pp. 789–814, Oct. 1974.
- [15] Levinger, J. S., *Effects of Radioactive Disintegrations on Inner Electrons of the Atom*, Phys. Rev., Vol. 90, pp. 11–25, Apr 1953.

- [16] Gorelov, A., Behr, J., Melconian, D., Trinczek, M., Dubé, P., Häusser, O., Giesen, U., Jackson, K., Swanson, T., D'Auria, J., Dombsky, M., Ball, G., Buchmann, L., Jennings, B., Dilling, J., Schmid, J., Ashery, D., Deutsch, J., Alford, W., Asgeirsson, D., Wong, W. and Lee, B., *Beta-neutrino correlation experiments on laser trapped ^{38m}K , ^{37}K* , Hyperfine Interactions, Vol. 127, No. 1, pp. 373–380, 2000.
- [17] Swanson, T. B., Asgeirsson, D., Behr, J. A., Gorelov, A. and Melconian, D., *Efficient transfer in a double magneto-optical trap system*, J. Opt. Soc. Am. B, Vol. 15, No. 11, pp. 2641–2645, Nov 1998.
- [18] Raab, E. L., Prentiss, M., Cable, A., Chu, S. and Pritchard, D. E., *Trapping of Neutral Sodium Atoms with Radiation Pressure*, Phys. Rev. Lett., Vol. 59, pp. 2631–2634, Dec 1987.
- [19] Harvey, M. and Murray, A. J., *Cold Atom Trap with Zero Residual Magnetic Field: The AC Magneto-Optical Trap*, Phys. Rev. Lett., Vol. 101, pp. 173201, Oct 2008.
- [20] Anholm, M., Characterizing the AC-MOT, Master's thesis, University of British Columbia, 2014.
- [21] Audi, G., Wapstra, A. and Thibault, C., *The AME2003 Atomic Mass Evaluation*, Nuclear Physics A, Vol. 729, No. 1, pp. 337 – 676, 2003.
- [22] Holstein, B. R., *Erratum: Recoil effects in allowed beta decay: The elementary particle approach*, Rev. Mod. Phys., Vol. 48, pp. 673–673, Oct 1976.
- [23] Severijns, N. and Naviliat-Cuncic, O., *Symmetry tests in nuclear beta decay*, Annual Review of Nuclear and Particle Science, Vol. 61, pp. 23–46, 2011.
- [24] Melconian, D. G., Measurement of the Neutrino Asymmetry in the Beta Decay of Laser-Cooled, Polarized ^{37}K , Ph.D. thesis, Simon Fraser University, 2005.

The citation format I'm using is really stupid. You **must** force yourself to ignore this right now,
Melissa!

Appendix A

Notable Differences in Data Selection between this and the Previous Result

A.1 Polarization Cycle Selection

Data used for our recent PRL article was slightly less polarized than we thought it was, due to an oversight in the data selection procedure.

A.2 Leading Edge / Trailing Edge and Walk Correction

Using the leading edge rather than the trailing edge to mark the timing of TDC pulses cleans up jitter, eliminates background, and changes the relative delays between different inputs. It is immediately relevant to the shape of the ‘walk correction’ on scintillator timing pulses, which give a different prediction for beta arrival time as a function of scintillator energy.

A.3 TOF Cut + Background Modelling

A SOE-beta time-of-flight cut is necessary to reduce background. The above mentioned walk correction directly results in an change in which specific events are selected in a given TOF cut. It further results in an adjustment to the expected fraction of background events in any such cut.

Appendix B

A PDF For The People

B.1 JTW

Here's a master equation from JTW to describe beta decay kinematics [12], [13]:

$$\begin{aligned} d^5\Gamma_{\text{JTW}} \equiv & \frac{F_{\mp}(Z, E_\beta)}{(2\pi)^5} p_\beta E_\beta (E_0 - E_\beta)^2 dE_\beta d^3\hat{\Omega}_\beta d^3\hat{\Omega}_\nu \\ & \times \xi \left[1 + a_{\beta\nu} \frac{\vec{p}_\beta \cdot \vec{p}_\nu}{E_\beta E_\nu} + b_{\text{Fierz}} \frac{m_e c^2}{E_\beta} + c_{\text{align}} T_{\text{align}}(\vec{J}) \left(\frac{\vec{p}_\beta \cdot \vec{p}_\nu}{3E_\beta E_\nu} - \frac{(\vec{p}_\beta \cdot \hat{\vec{j}})(\vec{p}_\nu \cdot \hat{\vec{j}})}{E_\beta E_\nu} \right) \right. \\ & \left. + \frac{\vec{J}}{J} \cdot \left(A_\beta \frac{\vec{p}_\beta}{E_\beta} + B_\nu \frac{\vec{p}_\nu}{E_\nu} + D_{\text{TR}} \frac{\vec{p}_\beta \times \vec{p}_\nu}{E_\beta E_\nu} \right) \right] \end{aligned} \quad (\text{B.1})$$

where, for convenience, we have defined a nuclear alignment term,

$$T_{\text{align}}(\vec{J}) \equiv \frac{J(J+1) - 3\langle(\vec{J} \cdot \hat{\vec{j}})^2\rangle}{J(2J-1)}. \quad (\text{B.2})$$

Note that this master equation depends on neutrino momentum, which we cannot observe directly. Furthermore, we cannot reconstruct neutrino momenta in our decay events either, because it would be necessary to account for the momentum of the recoiling daughter nucleus, treating the decay as a three-body problem. From an experimental standpoint, we failed to measure the momenta of the daughters in conjunction with the “tagged” beta decay events with which we are primarily con-

We have already specialized to β^+ decay.

cerned in this thesis. From a theoretical standpoint, JTW has intentionally neglected recoil-order terms – meaning that the daughter nucleus is treated, for the purpose of kinetic energy calculations, as being infinitely massive, and as such it must have no change in kinetic energy from the decay. This approximation makes it a bit tricky to correctly re-formulate Eq. (B.1) in terms of the momentum of the daughter instead of the momentum of the neutrino.

Fortunately, it is possible to simplify Eq. (B.1) by integrating over all possible neutrino directions, such that the result no longer depends on parameters that we do not observe. The neutrino energy itself is not a free variable in this equation, because the energy release in the decay is fixed, and given the approximation that none of that energy is allocated to the recoiling daughter, it is very straightforward to calculate the neutrino energy for a decay event in which the beta energy is known.

The result of performing this integration over neutrino direction is:

$$\begin{aligned} d^3\Gamma &= \frac{2}{(2\pi)^4} F_{\mp}(Z, E_\beta) p_\beta E_\beta (E_0 - E_\beta)^2 dE_\beta d^3\hat{\Omega}_\beta \xi \\ &\times \left[1 + b_{\text{Fierz}} \frac{m_e c^2}{E_\beta} + A_\beta \left(\frac{\vec{J}}{J} \cdot \frac{\vec{p}_\beta}{E_\beta} \right) \right], \end{aligned} \quad (\text{B.3})$$

which is a great simplification on Eq. (B.1). We still must write the remaining parameters in terms of the relevant nuclear matrix elements and fundamental coupling constants. These coupling constants are, in general, complex-valued, and JTW does not choose a phase angle for us. We write them out in Eqs. (B.4-B.6).

$$\begin{aligned} \xi &= |M_F|^2 (|C_S|^2 + |C_V|^2 + |C'_S|^2 + |C'_V|^2) \\ &+ |M_{GT}|^2 (|C_T|^2 + |C_A|^2 + |C'_T|^2 + |C'_A|^2) \end{aligned} \quad (\text{B.4})$$

$$b_{\text{Fierz}} \xi = \pm 2\gamma \text{Re}[|M_F|^2 (C_S C_V^* + C'_S C'^*_V) + |M_{GT}|^2 (C_T C_A^* + C'_T C'^*_A)] \quad (\text{B.5})$$

$$\begin{aligned} A_\beta \xi &= |M_{GT}|^2 \lambda_{J'J} \left[\pm 2\text{Re}[C_T C'^*_T - C_A C'^*_A] + 2 \frac{\alpha Z m_e}{p_\beta} \text{Im}[C_T C'^*_A + C'_T C_A^*] \right] \\ &+ \delta_{J'J} M_F M_{GT} \left(\frac{J}{J+1} \right)^{1/2} \left[2 \text{Re}[C_S C'^*_T + C'_S C_T^* - C_V C'^*_A - C'_V C_A^*] \right. \\ &\left. \pm 2 \frac{\alpha Z m_e}{p_\beta} \text{Im}[C_S C'^*_A + C'_S C_A^* - C_V C'^*_T - C'_V C_T^*] \right] \end{aligned} \quad (\text{B.6})$$

Note that JTW presents slightly different expressions for the sign convention in

components of A_β within [12] and [13]. Here, we adopt the convention from the latter publication. Furthermore, we do not require that either M_F or M_{GT} be positive (which would allow us to safely drop their absolute value indicators and make the conventions of these two papers equivalent). In order to obtain the correct, physically observed value for A_β , we require that the $M_F M_{GT}$ term in Eq. (B.6) have an overall positive value. Because we know that the scalar and tensor couplings must be small, and any imaginary contributions to the term must be small, we conclude that

$$M_F M_{GT} (C_V C_A'^* + C_V' C_A^*) < 0. \quad (\text{B.7})$$

Also, $\xi = G_v^2 \cos \theta_C f_1(E)$.

B.2 Holstein

Holstein [14] [22] generously provides explicit equations to match both Eq. (B.1) (i.e. Holstein's Eq. (51), where neutrino direction is a parameter of the probability distribution) and Eq. (B.3) (Holstein's Eq. (52), where neutrino direction has already been integrated over).

Here's Holstein's Eq. (52):

$$\begin{aligned} d^3\Gamma_{\text{Holstein}} &= 2G_v^2 \cos^2 \theta_c \frac{F_\mp(Z, E_\beta)}{(2\pi)^4} p_\beta E_\beta (E_0 - E_\beta)^2 dE_\beta d^3\hat{\Omega}_\beta \\ &\times \left\{ F_0(E_\beta) + \Lambda_1 F_1(E_\beta) \hat{\mathbf{n}} \cdot \frac{\vec{p}_\beta}{E_\beta} + \Lambda_2 F_2(E_\beta) \left[\left(\hat{\mathbf{n}} \cdot \frac{\vec{p}_\beta}{E_\beta} \right)^2 - \frac{1}{3} \frac{p_\beta^2}{E_\beta^2} \right] \right. \\ &\left. + \Lambda_3 F_3(E_\beta) \left[\left(\hat{\mathbf{n}} \cdot \frac{\vec{p}_\beta}{E_\beta} \right)^3 - \frac{3}{5} \frac{p_\beta^2}{E_\beta^2} \hat{\mathbf{n}} \cdot \frac{\vec{p}_\beta}{E_\beta} \right] \right\} \end{aligned} \quad (\text{B.8})$$

A careful reader will eventually note that Holstein's spectral functions $F_i(E_\beta)$ are not the same as the $F_i(E_\beta, u, v, s)$ in any limit, despite the notational similarities. Among other rules, Holstein's spectral functions obey these:

$$F_i(E_\beta) \neq F_i(E_\beta, u, v, s) \quad (\text{B.9})$$

$$F_i(E_\beta) = H_i(E_\beta, u, v, 0) \quad (\text{B.10})$$

$$f_i(E_\beta) = F_i(E_\beta, u, v, 0). \quad (\text{B.11})$$

For the $F_i(E_\beta)$ functions of interest to us here, we find the following relationships:

$$\begin{aligned}
F_0(E_\beta) &= H_0(E_\beta, J, J', 0) = F_1(E_\beta, J, J', 0) &= f_1(E_\beta) \\
F_1(E_\beta) &= H_1(E_\beta, J, J', 0) = F_4(E_\beta, J, J', 0) + \frac{1}{3}F_7(E_\beta, J, J', 0) &= f_4(E_\beta) + \frac{1}{3}f_7(E_\beta) \\
F_2(E_\beta) &= H_2(E_\beta, J, J', 0) = F_{10}(E_\beta, J, J', 0) + \frac{1}{2}F_{13}(E_\beta, J, J', 0) &= f_{10}(E_\beta) + \frac{1}{3}f_{13}(E_\beta) \\
F_3(E_\beta) &= H_3(E_\beta, J, J', 0) = F_{18}(E_\beta, J, J', 0) &= f_{18}(E_\beta). \quad (\text{B.12})
\end{aligned}$$

Note that the $f_i(E_\beta)$ in Eq. B.12 are the same spectral functions used to describe a polarized decay spectrum when the neutrino (ie, the recoil) is also observed – though of course such a spectrum must have other terms as well. For the spectrum of interest to us here, in which the neutrino direction has already been integrated over, we can simply look up the $H_i(E_\beta, J, J', 0) = H_i(E, u, v, s=0)$ spectral functions, and leave it at that. We find:

$$\begin{aligned}
F_0(E_\beta) &= |a_1|^2 + 2 \operatorname{Re}[a_1^* a_2] \frac{1}{3M^2} \left[m_e^2 + 4E_\beta E_0 + 2 \frac{m_e^2}{E_\beta} E_0 - 4E_\beta^2 \right] \\
&\quad + |c_1|^2 + 2 \operatorname{Re}[c_1^* c_2] \frac{1}{9M^2} \left[11m_e^2 + 20E_\beta E_0 - 2 \frac{m_e^2}{E_\beta} E_0 - 20E_\beta^2 \right] \\
&\quad - 2 \frac{E_0}{3M} \operatorname{Re}[c_1^*(c_1 + d \pm b)] + \frac{2E_\beta}{3M} (3|a_1|^2 + \operatorname{Re}[c_1^*(5c_1 \pm 2b)]) \\
&\quad - \frac{m_e^2}{3ME_\beta} \operatorname{Re} \left[-3a_1^* e + c_1^* \left(2c_1 + d \pm 2b - h \frac{E_0 - E_\beta}{2M} \right) \right] \quad (\text{B.13})
\end{aligned}$$

$$\begin{aligned}
F_1(E_\beta) &= \delta_{u,v} \left(\frac{u}{u+1} \right)^{1/2} \left\{ 2 \operatorname{Re} \left[a_1^* \left(c_1 - \frac{E_0}{3M} (c_1 + d \pm b) + \frac{E_\beta}{3M} (7c_1 \pm b + d) \right) \right] \right. \\
&\quad + 2 \operatorname{Re}[a_1^* c_2 + c_1^* a_2] \left(\frac{4E_\beta(E_0 - E_\beta) + 3m_e^2}{3M^2} \right) \Big\} \\
&\quad \mp \frac{(-1)^s \gamma_{u,v}}{u+1} \operatorname{Re} \left\{ c_1^* \left(c_1 + 2c_2 \left(\frac{8E_\beta(E_0 - E_\beta) + 3m_e^2}{3M^2} \right) - \frac{2E_0}{3M} (c_1 + d \pm b) \right. \right. \\
&\quad \left. \left. + \frac{E_\beta}{3M} (11c_1 - d \pm 5b) \right) \right\} + \frac{\lambda_{u,v}}{u+1} \operatorname{Re} \left\{ c_1^* \left[-f \left(\frac{5E_\beta}{M} \right) \right. \right. \\
&\quad \left. \left. + g \left(\frac{3}{2} \right)^{1/2} \left(\frac{E_0^2 - 11E_0E_\beta + 6m_e^2 + 4E_\beta^2}{6M^2} \right) \pm 3j_2 \left(\frac{8E_\beta^2 - 5E_0E_\beta - 3m_e^2}{6M^2} \right) \right] \right\} \quad (\text{B.14})
\end{aligned}$$

$$\begin{aligned}
F_2(E_\beta) = & \theta_{u,v} \frac{E_\beta}{2M} \operatorname{Re} \left[c_1^* \left(c_1 + c_2 \frac{8(E_0 - E_\beta)}{3M} - d \pm b \right) \right] \\
& - \delta_{u,v} \frac{E_\beta}{M} \left[\frac{u(u+1)}{(2u-1)(2u+3)} \right]^{1/2} \operatorname{Re} \left\{ a_1^* \left(\left(\frac{3}{2} \right)^{1/2} f + g \frac{E_\beta + 2E_0}{4M} \right. \right. \\
& \left. \left. \pm \left(\frac{3}{2} \right)^{1/2} j_2 \frac{E_0 - E_\beta}{2M} \right) \right\} + (-1)^s \kappa_{u,v} \frac{E_\beta}{2M} \operatorname{Re} \left[c_1^* \left(\pm 3f \pm \left(\frac{3}{2} \right)^{1/2} g \frac{E_0 - E_\beta}{M} \right. \right. \\
& \left. \left. + 3j_2 \frac{E_0 - 2E_\beta}{2M} \right) \right] + \epsilon_{u,v} \operatorname{Re} [c_1^* j_3] \left(\frac{21E_\beta^2}{8M^2} \right)
\end{aligned} \tag{B.15}$$

$$\begin{aligned}
F_3(E_\beta) = & - \delta_{u,v} (3u^2 + 3u - 1) \left[\frac{u}{(u-1)(u+1)(u+2)(2u-1)(2u+3)} \right]^{1/2} \\
& \times \operatorname{Re} [a_1^* j_3] \left(\frac{E_\beta^2 \sqrt{15}}{4M^2} \right) + \frac{\rho_{u,v}}{u+1} \operatorname{Re} \left[c_1^* (g\sqrt{3} + j_2\sqrt{2}) \left(\frac{5E_\beta^2}{4M^2} \right) \right] \\
& \pm \frac{(-1)^s \sigma_{u,v}}{u+1} \operatorname{Re} [c_1^* j_3] \left(\frac{5E_\beta^2}{2M^2} \right)
\end{aligned} \tag{B.16}$$

and we might really appreciate if these things could be simplified a bit.

In fact, we might want to add the other different-er terms in to this thing now, before we get ahead of ourselves.

Next, Holstein goes and tweaks those $F_i(E_\beta)$ terms that we've already written out, by adding in a tweak for Coulomb corrections. We'll impose the following corrections:

$$F_i(E_\beta) \rightarrow \tilde{F}_i(E_\beta) := F_\mp(Z, E_\beta) F_i(E_\beta) + F_\mp(Z, E_\beta) \Delta F_i(E_\beta) \tag{B.17}$$

Because Holstein doesn't actually write this stuff out in terms of $F_i(E_\beta)$, but rather in terms of $F_i(E_\beta, u, v, s)$, this correction presents yet another opportunity for the reader to interpret his notation incorrectly. We note that one must remember to make use of the relations in Eq. (B.12).

So clearly I'm going to need terms for $\Delta F_1(E_\beta, u, v, s)$, $\Delta F_4(E_\beta, u, v, s)$, $\Delta F_7(E_\beta, u, v, s)$, $\Delta F_{10}(E_\beta, u, v, s)$, $\Delta F_{13}(E_\beta, u, v, s)$, and $\Delta F_{18}(E_\beta, u, v, s)$. We really only have expressions for some of them in Holstein's Eq. (C4). That's annoying.

The terms $a_1, a_2, b, c_1, c_2, d, e, f, g, h, j_2, j_3$ are “structure functions”. Holstein gives some predictions for their form, assuming the impulse approximation holds, in his Eq. (67). For the most part, the values and form of these structure functions are

There was something wrong with this assumption. Something circular. I forgot. Blah.

beyond the scope of this thesis, so I will not re-write them all here. [It should be](#) Or will I?

noted that the numerical values used for these parameters came from a private communication from Ian Towner to ... someone other than me. However, it is important to note the expressions for a_i and c_i , because these will directly come into play when we try to reconcile Holstein's expression with JTW's. Therefore,

$$a(q^2) \approx \frac{g_V(q^2)}{(1 + \frac{\Delta}{2M})} \left[M_F + \frac{1}{6}(q^2 - \Delta^2)M_{r^2} + \frac{1}{3}\Delta M_{\mathbf{r} \cdot \mathbf{p}} \right] \quad (\text{B.18})$$

$$\begin{aligned} c(q^2) \approx & \frac{g_A(q^2)}{(1 + \frac{\Delta}{2M})} \left[M_{GT} + \frac{1}{6}(q^2 - \Delta^2)M_{\sigma r^2} + \frac{1}{6\sqrt{10}}(2\Delta^2 + q^2)M_{1y} \right. \\ & \left. + A \frac{\Delta}{2M} M_{\sigma L} + \frac{1}{2}\Delta M_{\sigma rp} \right] \end{aligned} \quad (\text{B.19})$$

...where the M_{xxx} 's are matrix elements of various sorts. [Also, Holstein proceeds to](#) split up $a(q^2)$ and $c(q^2)$ into their first two Taylor series terms for an expansion of q/M , maybe? Or possibly q^2/M^2 ? Anyway, that's a_1 and a_2 , and c_1 and c_2 , in Holstein notation. He doesn't do that with any of the other structure functions.

Seriously, I need to check what the taylor series is even expanding in.

Somewhere, just list out the goddamn values of things that I inherited from Ian Towner's personal communication that one time, over multiple generations of grad students.

Let's define some of that notation! Firstly,

$$\text{Holstein's } \hat{n} = \text{JTW's } \mathbf{j}, \quad (\text{B.20})$$

and the Λ_i are given by Holstein's Eq. (48):

$$\Lambda_1 := \frac{\langle M \rangle}{J} \quad (\text{B.21})$$

$$\Lambda_2 := 1 - \frac{3\langle M^2 \rangle}{J(J+1)} \quad (\text{B.22})$$

$$\Lambda_3 := \frac{\langle M \rangle}{J} - \frac{5\langle M^3 \rangle}{J(3J^2 + 3J - 1)}. \quad (\text{B.23})$$

We immediately see that Holstein's Λ_1 is closely related to JTW's $\frac{\vec{J}}{J}$, and a bit later after John points it out to us, we see that Holstein's Λ_2 is closely related to

Note: It's not the case that $|\vec{J}| == J$. It's actually super fucking infuriating notation.

JTW's T_{align} . JTW doesn't have any equivalent to Λ_3 . In particular, we find:

$$\Lambda_1 \hat{\mathbf{j}} = \frac{\langle M \rangle}{J} \hat{\mathbf{j}} = \frac{\vec{\mathbf{J}}}{J} \quad (\text{B.24})$$

$$\Lambda_2 = T_{\text{align}} \frac{(2J-1)}{(J+1)}. \quad (\text{B.25})$$

If we evaluate Holstein's Eqs. (B8), which I will absolutely not type out here, for the case $u = v = J = J' = 3/2$, we find the following values:

$$\begin{aligned} \delta_{u,v} &= 1 & \theta_{u,v} &= 1 & \rho_{u,v} &= \frac{-41}{40} \\ \gamma_{u,v} &= 1 & \kappa_{u,v} &= \frac{1}{2\sqrt{2}} & \sigma_{u,v} &= \frac{-41}{4\sqrt{35}} \\ \lambda_{u,v} &= \frac{-\sqrt{2}}{5} & \epsilon_{u,v} &= \frac{-1}{2\sqrt{5}} & \phi_{u,v} &= 0 \end{aligned} \quad (\text{B.26})$$

Furthermore, in our calculations here, we will be considering only the β^+ decay modes, and therefore we take the *lower* sign when the option arises. We also will use $s = 0$, so that $(-1)^s = +1$.

Also, pretty sure one of those never gets used. Which one was it? idk.

Appendix C

Comparing Notation between Holstein and JTW

C.1 Comparison Guide

This is a short guide to differences in notation, sign convention, and normalization. There will be many tables here, chosen to aid in conversion between the two conventions. In the mean time, here's a bunch of old handwritten notes on the topic, that I'll eventually have to typeset and process into something intelligible.

Here's a table.

Here's another table.

Here's a third table.

Here's a fourth table.

C.2 Some old handwritten notes.

One day, these will go away and be replaced by nice clean latex.

Must find a better way to smush this table with display style math font typesetting. At present, it's somehow both too smooshed and not smooshed enough.

Holstein	JTW	Thesis	Comments
k			Neutrino momentum 4-vector
	E_ν		Neutrino energy
\hat{k}	$\frac{\mathbf{p}_\nu}{E_\nu}$		3D Neutrino emission direction unit vector. Neutrinos are always treated as massless.
p			Beta momentum 4-vector, or sometimes the magnitude of the beta momentum 3-vector. Never the magnitude of the 4-vector.
E	E_e	E_β	Beta energy
\mathbf{p}	\mathbf{p}_e	\vec{p}_β	Beta momentum 3-vector
q			Recoil momentum 4-vector, or sometimes a magnitude.

Table C.1: A comparison of some kinematic terms in JTW [12] [13] and Holstein [14]. Yes, the bolding/italicization carries meaning.

Holstein	JTW	Comments
u	J	Initial state total nuclear angular momentum.
v	J'	Final state total nuclear angular momentum.
s	No equivalent?	Umm... I should check on this.

Table C.2: A comparison of some angular momenta in JTW [12] [13] and Holstein [14].

Holstein	JTW	Thesis	Comments
$G_v^2 \cos \theta_C f_1(E)$	ξ	$\xi(E_\beta)$	Normalization. Proportional to the fractional decay rate.
\hat{n}	\mathbf{j}	$\hat{\mathbf{j}}$	Nuclear polarization unit vector. Also the axis of quantization.
J	J		Total nuclear angular momentum quantum number
$\langle M \rangle$	$ \langle \mathbf{J} \rangle $		Angular momentum projection along the axis of quantization
$\Lambda^{(1)} \hat{n} = \frac{\langle M \rangle}{J} \hat{n}$	$\frac{\langle \mathbf{J} \rangle}{J}$	$\Lambda_1 \hat{\mathbf{n}}$	Dipole element vector. Proportional to nuclear polarization. <i>(Rephrase this.)</i>
$\Lambda^{(1)} = \frac{\langle M \rangle}{J}$...	Λ_1	...
$\Lambda^{(2)}$	$\frac{J(J+1)-3\langle(\vec{\mathbf{J}} \cdot \hat{\mathbf{j}})^2\rangle}{J(2J-1)} \frac{(2J-1)}{(J+1)}$	$T_{\text{align}}(\vec{\mathbf{J}}) \frac{(2J-1)}{(J+1)}$	Quadrupole element
$\Lambda^{(3)}$	No equivalent	Λ_3	Octopole element
$\Lambda^{(4)}$	No equivalent	Λ_4	Hexadecapole element

Table C.3: A comparison of the multipole elements and their normalizations (and some other stuff) in JTW [12] [13] and Holstein [14].

Term	Integral
$f_1(E_\beta)$	$\leftrightarrow \int 1 d\hat{\Omega}_k = 4\pi$
$f_2(E_\beta)$	$\leftrightarrow \int \left(\frac{\vec{p}_\beta \cdot \hat{k}}{E_\beta} \right) d\hat{\Omega}_k = 0$
$f_3(E_\beta)$	$\leftrightarrow \int \left(\left(\frac{\vec{p}_\beta \cdot \hat{k}}{E_\beta} \right)^2 - \frac{1}{3} \frac{p_\beta^2}{E_\beta^2} \right) d\hat{\Omega}_k = 0$
$f_4(E_\beta)$	$\leftrightarrow \int \left(\hat{n} \cdot \frac{\vec{p}_\beta}{E_\beta} \right) d\hat{\Omega}_k = 4\pi \left(\hat{n} \cdot \frac{\vec{p}_\beta}{E_\beta} \right)$
$f_5(E_\beta)$	$\leftrightarrow \int \left(\hat{n} \cdot \frac{\vec{p}_\beta}{E_\beta} \right) \left(\frac{\vec{p}_\beta \cdot \hat{k}}{E_\beta} \right) d\hat{\Omega}_k = 0$
$f_6(E_\beta)$	$\leftrightarrow \int \left(\hat{n} \cdot \hat{k} \right) d\hat{\Omega}_k = 0$
$f_7(E_\beta)$	$\leftrightarrow \int \left(\hat{n} \cdot \hat{k} \right) \left(\frac{\vec{p}_\beta \cdot \hat{k}}{E_\beta} \right) d\hat{\Omega}_k = \frac{1}{3} 4\pi \left(\hat{n} \cdot \frac{\vec{p}_\beta}{E_\beta} \right)$
$f_8(E_\beta)$	$\leftrightarrow \int \hat{n} \cdot \left(\frac{\vec{p}_\beta \times \hat{k}}{E_\beta} \right) d\hat{\Omega}_k = 0$
$f_9(E_\beta)$	$\leftrightarrow \int \hat{n} \cdot \left(\frac{\vec{p}_\beta \times \hat{k}}{E_\beta} \right) \left(\frac{\vec{p}_\beta \cdot \hat{k}}{E_\beta} \right) d\hat{\Omega}_k = 0$
$f_{10}(E_\beta)$	$\leftrightarrow \int T_2(\hat{n}) : \left[\frac{\vec{p}_\beta}{E}, \frac{\vec{p}_\beta}{E} \right] d\hat{\Omega}_k = 4\pi T_2(\hat{n}) : \left[\frac{\vec{p}_\beta}{E}, \frac{\vec{p}_\beta}{E} \right]$
$f_{11}(E_\beta)$	$\leftrightarrow \int T_2(\hat{n}) : \left[\frac{\vec{p}_\beta}{E}, \frac{\vec{p}_\beta}{E} \right] \left(\frac{\vec{p}_\beta \cdot \hat{k}}{E} \right) d\hat{\Omega}_k = 0$
$f_{12}(E_\beta)$	$\leftrightarrow \int T_2(\hat{n}) : \left[\frac{\vec{p}_\beta}{E}, \hat{k} \right] d\hat{\Omega}_k = 0$
$f_{13}(E_\beta)$	$\leftrightarrow \int T_2(\hat{n}) : \left[\frac{\vec{p}_\beta}{E}, \hat{k} \right] \left(\frac{\vec{p}_\beta \cdot \hat{k}}{E} \right) d\hat{\Omega}_k = \frac{1}{3} 4\pi T_2(\hat{n}) : \left[\frac{\vec{p}_\beta}{E}, \frac{\vec{p}_\beta}{E} \right]$
$f_{14}(E_\beta)$	$\leftrightarrow \int T_2(\hat{n}) : \left[\hat{k}, \hat{k} \right] d\hat{\Omega}_k = 0$
$f_{15}(E_\beta)$	$\leftrightarrow \int T_2(\hat{n}) : \left[\hat{k}, \hat{k} \right] \left(\frac{\vec{p}_\beta \cdot \hat{k}}{E} \right) d\hat{\Omega}_k = 0$
$f_{16}(E_\beta)$	$\leftrightarrow \int T_2(\hat{n}) : \left[\frac{\vec{p}_\beta}{E}, \frac{\vec{p}_\beta}{E} \times \hat{k} \right] d\hat{\Omega}_k = 0$
$f_{17}(E_\beta)$	$\leftrightarrow \int T_2(\hat{n}) : \left[\hat{k}, \frac{\vec{p}_\beta}{E} \times \hat{k} \right] d\hat{\Omega}_k = 0$
$f_{18}(E_\beta)$	$\leftrightarrow \int T_3(\hat{n}) : \left[\frac{\vec{p}_\beta}{E}, \frac{\vec{p}_\beta}{E}, \frac{\vec{p}_\beta}{E} \right] d\hat{\Omega}_k = 4\pi T_3(\hat{n}) : \left[\frac{\vec{p}_\beta}{E}, \frac{\vec{p}_\beta}{E}, \frac{\vec{p}_\beta}{E} \right]$

$C_A = C'_A$; $g = \pm \frac{1}{\sqrt{2}} M_{GT} (C_A + C'_A)$ ← prefer \oplus
 $C_V = C'_V$; $a_1 = \pm \frac{1}{\sqrt{2}} M_F (C_V + C'_V)$ ← depends on above sign.

In our code:
 $M_F = 1.0$
 $M_{GT} = -0.62376$

Also in our Code:
 $g_V = 1.00$
 $g_A = 0.91210$

* Really, the conversion above doesn't include the extra terms in a_1 and g that couple to ^{nuclear} matrix elements other than M_F and M_{GT} .

I think the point is that I should actually interpret:

$g_V = \pm \frac{1}{\sqrt{2}} (C_V + C'_V) = 1.0 \rightarrow a_1 = g_V M_F \Rightarrow C_V = C'_V = \frac{1}{\sqrt{2}}$
 $g_A = \pm \frac{1}{\sqrt{2}} (C_A + C'_A) \approx 0.91210 \rightarrow C_1 = g_A M_{GT} \Rightarrow C_A = C'_A = \frac{-0.91210}{\sqrt{2}} \approx -0.644952$

* Check: with $C_A = C'_A$ and $C = C'_V$, does JTW give the right A_β ?
 $A_\beta = 0.763683; A_\beta = 0.496903 \rightarrow A_\beta = \underline{\underline{0.375394}}$ (bad!)

$A_\beta = 0.763671 \leftarrow$ Allow M_{GT} and M_F to have opposite signs. (Bad!)
 $A_\beta = -0.568045 \leftarrow$ enforce $\oplus M_{GT}$. Or earlier JTW "convention".

* Because Holstein insists on his own sign convention, we get $M_{GT-Holstein} = -M_{GT-JTW}$

Figure C.1: "Notes 0"

In our code:

$$\boxed{\begin{array}{l} M_F = 1.0 \quad ; \quad g_v = 1.0 \quad \rightarrow \quad g_v M_F = 1.0 \\ M_{GT} = -0.62376 \quad ; \quad g_A = 0.91210 \quad \rightarrow \quad g_A M_{GT} = -0.568931 \end{array}} \Rightarrow \rho \equiv \frac{g_A M_{GT}}{g_v M_F} \approx -0.568931_{\text{Holstein}}$$

* If we require that $C_A, C_A', C_v, C_v', M_F, M_{GT}$ are all real, and enforce that these can all take values which allow for Holstein and JTW to be equivalent in some limits, we require:

$$\begin{array}{lll} \text{JTWW} & \text{Holstein} & \text{Holstein} \xrightarrow{\text{JTWW}} \\ \left\{ \begin{array}{l} f_1(E) \\ f_4(E) \end{array} \right. & \rightarrow \begin{array}{l} |a_1|^2 = |M_F|^2 (|C_v|^2 + |C_v'|^2) \\ |C_1|^2 = |M_{GT}|^2 (|C_A|^2 + |C_A'|^2) \end{array} \\ \downarrow \quad \downarrow & & \downarrow \\ \xrightarrow{\quad} & |g_1|^2 = 2|M_{GT}|^2 \cdot \text{Re}[C_A C_A'^*] \end{array}$$

$$\begin{aligned} \text{Re}[a_1^* C_1] &= -\text{Re}[M_F M_{GT} (C_v C_A'^* + C_v' C_A^*)] \leftarrow \text{later} \\ \text{Re}[a_1^* C_1] &= -\text{Re}[|M_F| |M_{GT}| (C_v C_A'^* + C_v' C_A^*)] \leftarrow \text{earlier.} \end{aligned}$$

The Results:

$$\begin{array}{ll} \text{Holstein} & \text{JTWW} \\ C_v = C_v' & a_1 = \pm \frac{1}{\sqrt{2}} M_F (C_v + C_v') = \pm M_F (\pm \sqrt{2}) (C_v) \\ C_A = C_A' & C_1 = \pm \frac{1}{\sqrt{2}} M_{GT} (C_A + C_A') = \pm M_{GT} (\pm \sqrt{2}) (C_A) \end{array}$$

$$a_1 \approx g_v M_{F,H};$$

$$C_1 \approx g_A M_{GT,H};$$

Holstein

$$\boxed{M_{GT, \text{Holstein}} = -M_{GT, \text{JTWW}}}$$

which sign?!

$$a_1 \approx g_v M_F; \quad g_v = \pm \frac{1}{\sqrt{2}} (C_v + C_v') = 1.0; \quad M_F = 1.0; \quad ; \quad C_v = C_v'$$

$$C_1 \approx g_A M_{GT}; \quad g_A = \pm \frac{1}{\sqrt{2}} (C_A + C_A') \approx 0.91210; \quad M_{GT,H} = -0.62376; \quad C_A = C_A'$$

↑ ↑
JTWW terms!

Figure C.2: "Notes 1"

$$\begin{aligned}
b \cdot \bar{z} &= \pm 2\gamma \operatorname{Re} \left[|M_F|^2 (C_S C_V^* + C'_S C_V'^*) + |M_{GT}|^2 (C_T C_A^* + C'_T C_A'^*) \right] \\
&= -2\gamma \left[|M_F|^2 (C_S C_V^* + C'_S C_V'^*) + |M_{GT}|^2 (C_T C_A^* + C'_T C_A'^*) \right] \\
&= -2\gamma |M_F|^2 (C_S + C'_S) C_V^* + -2\gamma |M_{GT}|^2 (C_T + C'_T) C_A^* \\
&= -2\gamma |M_F|^2 \cdot \frac{1}{\sqrt{2}} g_V \underbrace{(C_S + C'_S)}_{+\sqrt{2} g_S} + -2\gamma |M_{GT}|^2 \frac{(-1)}{\sqrt{2}} g_A \underbrace{(C_T + C'_T)}_{-\sqrt{2} g_T} \\
&= -2\gamma |M_F|^2 \cdot g_V \cdot g_S - 2\gamma |M_{GT}|^2 \cdot g_A \cdot g_T \\
\boxed{b \cdot \bar{z} = -2\gamma [|M_F|^2 g_V g_S + |M_{GT}|^2 g_A g_T]}
\end{aligned}$$

~~BYE~~ $\gamma = (1 - \alpha^2 z^2)^{1/2}$

Figure C.3: "Notes 2"

To Match Up Holstein and JT W:

$$g_V = \frac{1}{\sqrt{2}}(C_V + C_V') ; \quad C_V = C_V' = \frac{1}{\sqrt{2}}g_V = \frac{1}{\sqrt{2}}$$

$$a_1 \approx g_V M_F$$

$$g_A = \frac{-1}{\sqrt{2}}(C_A + C_A') ; \quad C_A = C_A' = \frac{-1}{\sqrt{2}}g_A \approx \frac{-1}{\sqrt{2}}(0.91210) \quad c_1 \approx g_A M_{GT}$$

Also define:

$$g_S \equiv \frac{1}{\sqrt{2}}(C_S + C_S') ; \quad C_S = C_S' = \frac{1}{\sqrt{2}}g_S \approx 0$$

$$g_T \equiv \frac{-1}{\sqrt{2}}(C_T + C_T') ; \quad C_T = C_T' = \frac{-1}{\sqrt{2}}g_T \approx 0$$

Then, we find:

$$\ddot{\xi} = |M_F|^2(g_V^2 + g_S^2) + |M_{GT}|^2(g_A^2 + g_T^2)$$

$$A_p \ddot{\xi} = \frac{2}{5}|M_{GT}|^2(g_A^2 + g_T^2) + 2(\frac{3}{5})^{\frac{1}{2}}M_F M_{GT}(g_V g_A - g_S g_T)$$

$$b \cdot \ddot{\xi} = -2\gamma [|M_F|^2 g_V g_S + |M_{GT}|^2 g_A g_T] ; \quad \gamma \equiv (1 - \alpha^2 \zeta^2)^{\frac{1}{2}}$$

$$F_0(E) \rightarrow F_0(E) + |M_F|^2 g_S^2 + |M_{GT}|^2 g_T^2$$

$$F_i(E) \rightarrow F_i(E) + \delta_{uv} \left(\frac{u}{u+v} \right) (-2) \cdot M_F M_{GT} \cdot g_S g_T + \alpha_{uv} \left(\frac{1}{u+v} \right) |M_{GT}|^2 g_T^2$$

Figure C.4: "Notes 3"

- * In some limits, Holstein and JT_W are equivalent. For simplicity, we will require that JT_W's terms $C_A, C_A', C_V, C_V', M_F$, and M_{GT} are entirely real.
- * The physical interpretation of this is that we ~~do not~~ require time-reversal symmetry to be obeyed.
- * We use the following relationships:

$$\begin{aligned} \vec{z} &= f(E) \rightarrow |C_V|^2 = |M_F|^2 \cdot (|C_V|^2 + |C_V'|^2) \\ A_B \cdot \vec{z} &= f'(E) \rightarrow |C_V'|^2 = |M_{GT}|^2 \cdot (|C_A|^2 + |C_A'|^2) \\ &\quad \text{use the later JT}_W \text{ sign convention.} \end{aligned}$$

$$\begin{aligned} |C_V|^2 &= 2 \cdot |M_{GT}|^2 \cdot \operatorname{Re}[C_A C_A'^*] \\ \operatorname{Re}[a_i^* C_V] &= -M_F M_{GT} \cdot \operatorname{Re}[C_V C_A'^* + C_V' C_A] \end{aligned}$$

- * Then, via trial and error, we find that the following set of relationships gives consistent results:

$$\left. \begin{array}{l} C_V = C_V'; \\ C_A = C_A'; \end{array} \right. \begin{array}{l} a_i = \pm \frac{1}{\sqrt{2}} M_F (C_V + C_V') \\ g_i = \pm \frac{1}{\sqrt{2}} M_{GT} (C_A + C_A') \end{array} \} \text{ Thus far, either set of signs is consistent. But they must be opposite.}$$

- * In our code, which evaluates Holstein, we use these:

$$\left. \begin{array}{l} a_i \approx g_V M_F; \\ g_i \approx g_A M_{GT}; \end{array} \right. \begin{array}{l} M_F = 1.0 \\ M_{GT} = -0.62376 \end{array} \} \begin{array}{l} g_V = 1.0 \\ g_A \approx 0.91210 \end{array} \quad \begin{array}{l} \text{Note that we believe we know } M_F \text{ better than we know } g_A. \text{ So, to measure "A}_B\text{" we vary } g_A \text{ and leave } M_{GT} \text{ fixed.} \end{array}$$

- * We'll define some quantities, ρ :

$$\rho_{JT_W} = \frac{C_A \cdot M_{GT}}{C_V \cdot M_F}; \quad \rho_{\text{Holstein}} = \frac{g_A \cdot M_{GT}}{g_V \cdot M_F} \approx -0.568931$$

* This ρ_{JT_W} uses our own definition from PRL.

* Note that A_B comes out physically wrong unless ρ_{JT_W} is \oplus , ie, in A_B , there's a term $\sim [C_V C_A'^* + C_V' C_A]$ and we need the whole thing to come out \oplus . $\therefore C_V$'s and C_A 's must have opposite signs.

- * We'll take the convention that every body has the same matrix elements:

$$\begin{array}{l} M_{GT, JT_W} = M_{GT, \text{Holstein}} \\ M_{F, JT_W} = M_{F, \text{Holstein}} \end{array}$$

- * Then:

$$\left. \begin{array}{l} C_V = C_V' \Rightarrow \oplus \\ C_A = C_A' \Rightarrow \ominus \end{array} \right\} \text{ This because at the end of the day, we want Holstein's } a_i \text{ to be } \oplus, \text{ and } g_i \text{ to be } \ominus, \text{ or else we don't produce the right physics.}$$

$$\left. \begin{array}{l} g_V = \frac{1}{\sqrt{2}} (C_V + C_V') = 1.0 \\ g_A = \frac{1}{\sqrt{2}} (C_A + C_A') \approx +0.91210 \end{array} \right\} \quad \begin{array}{l} C_V = C_V' = \frac{+1}{\sqrt{2}} g_V = \frac{1}{\sqrt{2}} \\ C_A = C_A' = \frac{-1}{\sqrt{2}} g_A \approx \frac{-1}{\sqrt{2}} (0.91210) \end{array}$$

Figure C.5: "Notes 4"

- * In some limits, Holstein and JTW are equivalent. We require that JTW's terms $C_A, C_A', C_V, C_V', M_F$, and M_{GT} must all be entirely real. We can probably do this WLOG. (Or without very much loss of generality, at least.)
- * Use the following relationships:

$$\xi = f_v(E) \rightarrow |q_v|^2 = |M_F|^2 (|C_V|^2 + |C_V'|^2)$$

$$|q_A|^2 = |M_{GT}|^2 (|C_A|^2 + |C_A'|^2)$$

$$A \cdot \xi = f_A(E) \rightarrow |C_V|^2 = 2 \cdot |M_{GT}|^2 \cdot \text{Re}[C_V C_A'^*]$$

$$\text{Re}[q_A] = -\text{Re}[M_F M_{GT} (C_V C_A'^* + C_V' C_A)] \leftarrow \text{later JTW convention.}$$

we'll only use this.

- * Then, the following relationships give us internally consistent results:

$$\begin{aligned} C_V &= C_V' ; & q_v &= \pm \frac{1}{\sqrt{2}} M_F (C_V + C_V') \\ C_A &= C_A' ; & q_A &= \pm \frac{1}{\sqrt{2}} M_{GT} (C_A + C_A') \end{aligned} \quad \begin{array}{l} \text{either set of signs is consistent.} \\ \text{But they must be opposite.} \end{array}$$

Code has these signs for q_v and q_A .
Do I know why?

- * In our code (which evaluates Holstein), we use these values:

\oplus	$q_v \approx g_v M_F$	$M_F = 1.0$	$g_v = 1.0$
\ominus	$q_A \approx g_A M_{GT}$	$M_{GT} = -0.62376$	$g_A = 0.91210$

- * We can also define:

$\rho_{\text{Holstein}} \equiv \frac{g_A M_{GT}}{g_v M_F} \approx -0.568931$	$\rho_{\text{JTW}} \equiv \frac{C_A M_{GT}}{C_V M_F} \leftarrow \text{we use } \rho_{\text{JTW}} \text{ def. in PRL.}$
--	--

- * We do not get the correct JTW A_B unless we require that ρ_{JTW} is \oplus . Equivalently, we require that $\text{Re}[M_F M_{GT} (C_V C_A'^* + C_V' C_A)]$ must be \oplus . But M_{GT} is \ominus ! \rightarrow Option 1: Take $M_{GT, \text{JTW}} = -M_{GT, \text{Holstein}}$. \rightarrow Option 2: Take $C_A = C_A'$ to be \ominus , and $C_V = C_V'$ to be \oplus .

(really, there are other options.
But let's leave M_F and C_V alone.)

- * For Holstein to come out right, we need C_A to be \ominus , and q_A to be \oplus . I think.

* When we require q_A to be \oplus , or M_{GT} ? They're not quite equivalent.

$$\begin{aligned} g_v &= \frac{1}{\sqrt{2}} (C_V + C_V') = 1.0 \\ g_A &= \frac{-1}{\sqrt{2}} (C_A + C_A') = 0.91210 \Rightarrow C_A \text{ must be } \ominus \text{ then, bc } g_A \text{ is } \oplus \text{ and} \\ &\quad M_{GT, \text{Holstein}} \text{ is } \ominus, \text{ and we need } C_A \text{ to be } \ominus. \end{aligned}$$

- * OK. Now what do I do with C_A and C_V ? \rightarrow can't just stick them into M_F and M_{GT} . even in JTW it doesn't come out consistent.
- * Have to write JTW in Holstein notation so I can figure out where to put C_A, C_V in.

Figure C.6: "Notes 5"

Appendix D

Holstein/JTW Comparison Confusion

Ben at pg 17(30) claims the relation between JTW and Holstein for A_β is:

$$A_\beta = \frac{f_4(E) + \frac{1}{3}f_7(E)}{f_1(E)} \quad (\text{D.1})$$

See, it's counterintuitive, because I would have guessed that it would be just

$$A_\beta = \frac{f_4(E)}{f_1(E)} \quad (\text{D.2})$$

...But it's not. That extra f_7 term is there, being weird. In Holstein (51), it's all like,

$$d^5\Gamma = (\dots) + (\dots) * \Lambda_1(\hat{n} \cdot \hat{k})(\frac{\vec{p}}{E} \cdot \hat{k}) f_7(E), \quad (\text{D.3})$$

and that just doesn't look like A_β .

So, maybe there's some magic that happens when you integrate it and it turns into (52). From (52), I would (naively??) think that:

$$A_\beta = \frac{F_1(E)}{F_0(E)} \quad (\text{D.4})$$

Is it even true?!? Let's see what Holstein has to say...

In general,

$$f_i(E) = F_i(E, J, J', 0) \quad (\text{D.5})$$

$$F_i(E) = H_i(E, J, J', 0) \quad (\text{D.6})$$

So here specifically, we have:

$$F_0(E) = H_0(E, u, v, s) = F_1(E, u, v, s) \quad (\text{D.7})$$

$$F_1(E) = H_1(E, u, v, s) = F_4(E, u, v, s) + \frac{1}{3}F_7(E, u, v, s) \quad (\text{D.8})$$

$$= f_4(E) + \frac{1}{3}f_7(E) \quad (\text{D.9})$$

So I guess whatever the fuck Ben did to get his result checks out, and my naive supposition was correct. But now how do I translate that into JTW for anything else?!

JTW just straight-up has *nothing* that corresponds to the f_7 term in Holstein. The integral that puts f_7 into A_β has simply *not been done* at the point where JTW writes down their equation.

So, okay, let's take a look at how the dominant terms in f_4 , f_1 , and f_7 scale. From Holstein (pg 807):

$$f_1(E) \approx a_1^2 + c_1^2 \quad (\text{D.10})$$

$$f_4(E) \approx (\text{const}) * 2a_1c_1 + (\text{const})c_1^2 \quad (\text{D.11})$$

$$f_7(E) \approx (\text{const}) * a_1c_1 \frac{E_0}{M} + (\text{const})a_1c_1 \frac{E}{M} + (\text{const})c_1^2 \frac{E_0}{2M} + (\text{const})c_1^2 \frac{E}{2M} \quad (\text{D.12})$$

OK, so I think f_7 wouldn't be included in JTW anyway, because it's too high order in E/M . (Is there really nothing in f_7 that's not multiplied by at least one factor of $1/M$?? yep, nothing.)

So here's what Coulomb-JTW says (set $C_S = C'_S = C_T = C'_T = 0$, and require that $C_A = C'_A$ and $C_V = C'_V$ are real):

$$\xi = |M_F|^2(2C_V^2) + |M_{GT}|^2(2C_A^2) \quad (\text{D.13})$$

$$A_\beta \xi = |M_{GT}|^2 \frac{1}{J+1} \left[+2C_A^2 + M_F M_{GT} \left(\frac{J}{J+1} \right)^{1/2} * (-2C_V C_A) \right] \quad (\text{D.14})$$

Indeed, there are no E/M terms. So we agree with ourselves here. That's nice. But actually, we need to figure out how to convert **all** of the JTW letters into Holstein notation. Not just A_β . Of particular importance is anything with a **linear** dependence on C_T (or C_S). That includes $bFierz$, for which there is no Holstein equivalent, but also:

- Real parts of b_{Fierz}
- Imaginary parts of $a_{\beta\nu}$
- Imaginary parts of c_{align}
- Imaginary parts of A_β
- Real parts of B_ν
- Real parts of D_{TR}

...which is actually all of the things. All of them. So, I claim these are the relationships:

$$\xi = f_1(E) \quad (?) \quad (\text{D.15})$$

$$a_{\beta\nu} = f_2(E) / f_1(E) \quad (\text{D.16})$$

$$\frac{\langle \vec{J} \rangle}{J} \cdot \frac{\vec{p}}{E} A_\beta = \Lambda_1 \hat{n} \cdot \frac{\vec{p}}{E} f_4(E) / f_1(E) \quad (\text{D.17})$$

$$\frac{\langle \vec{J} \rangle}{J} \cdot \frac{\vec{p}_\nu}{E E_\nu} B_\nu = \Lambda_1 \hat{n} \cdot \vec{k} f_6(E) / f_1(E) \quad (\text{D.18})$$

$$\frac{\langle \vec{J} \rangle}{J} \cdot \frac{(\vec{p} \times \vec{p}_\nu)}{E E_\nu} D_{\text{TR}} = \Lambda_1 \hat{n} \cdot \left(\frac{\vec{p}}{E} \times \hat{k} \right) f_8(E) / f_1(E) \quad (\text{D.19})$$

$$\left[\frac{J(J+1) - 3\langle (\vec{J} \cdot \hat{j})^2 \rangle}{J(2J-1)} \right] \left[\frac{1}{3} \frac{\vec{p} \cdot \vec{p}_\nu}{E E_\nu} - \frac{(\vec{p} \cdot \hat{j})(\vec{p}_\nu \cdot \hat{j})}{E E_\nu} \right] c_{\text{align}} = \Lambda_2 \left[(\hat{n} \cdot \frac{\vec{p}}{E})(\hat{n} \cdot \hat{k}) - \frac{1}{3} (\frac{\vec{p}}{E} \cdot \hat{k}) \right] f_{12}(E) / (\text{D.20})$$

Other Holstein terms in (51) have no JTW equivalent, either because JTW didn't include recoil-order corrections, or because JTW didn't bother with higher multipole moments. These Holstein-specific spectral functions are not used in JTW:

- $f_3(E)$ (dipole)
- $f_5(E)$ (dipole)
- $f_7(E)$ (dipole)
- $f_9(E)$ (dipole)
- $f_{10}(E)$ (quadrupole)
- $f_{11}(E)$ (quadrupole)
- $f_{13}(E)$ (quadrupole)
- $f_1(E)$ (quadrupole, used elsewhere)
- $f_{16}(E)$ (quadrupole)
- $f_{17}(E)$ (quadrupole)
- Octopoles: $f_{18}, f_{19}, f_{20}, f_{21}, f_{22}, f_{23}, f_{24}$
- 16-poles: f_{25}, f_{26}, f_{27} .

OK, so what needs to happen now is for me to convert the JTW alphabet into *other* Holstein notation. Since I know how they scale with the $f_i(E)$'s, let's see if we can convert those specific $f_i(E)$'s into any of the Holstein notation that is going into my code – ie, the $F_i(E)$'s. In particular, we'll want $f_1(E), f_2(E), f_4(E), f_6(E), f_8(E), f_{12}(E)$. This will actually have the pleasant side-effect of telling us how to fucking do that goddamn neutrino momentum integral in JTW. I think. So, from Holstein:

- $f_1(E) = F_1(E, u, v, s) = H_0(E, u, v, s) = F_0(E)$
- $f_2(E) = F_2(E, u, v, s) = ?$
- $f_4(E) = F_4(E, u, v, s) = ?$

- $f_6(E) = F_6(E, u, v, s) = ?$
- $f_8(E) = F_8(E, u, v, s) = ?$
- $f_{12}(E) = F_{12}(E, u, v, s) = ?$

...which, let's be honest, doesn't really help. Let's go the other direction, then.

- $F_0(E) = H_0(E, u, v, s) = F_1(E, u, v, s) = f_1(E)$ as before, but also:
- $F_1(E) = H_1(E, u, v, s) = F_4(E, u, v, s) + \frac{1}{3}F_7(E, u, v, s) = f_4(E) + \frac{1}{3}f_7(E)$
- $F_2(E) = H_2(E, u, v, s) = F_{10}(E, u, v, s) + \frac{1}{3}F_{13}(E, u, v, s) = f_{10}(E) + \frac{1}{3}f_{13}(E)$
- $F_3(E) = H_3(E, u, v, s) = F_{18}(E, u, v, s) = f_{18}(E)$

So, okay, I can write *my* PDF in terms of only Holstein's $f_1(E)$, $f_4(E)$, $f_7(E)$, $f_{10}(E)$, $f_{13}(E)$, $f_{18}(E)$. I can write JTW's PDF in terms of only Holstein's $f_1(E)$, $f_2(E)$, $f_4(E)$, $f_6(E)$, $f_8(E)$, $f_{12}(E)$. Those ... aren't the same thing. Like, at all. If I integrate those, do they come out to be the same things? Somehow?

OK. I can separate some terms out into what they *should* correspond to based on their multipole dependence... Roughly speaking,

$$F_0(E) \leftrightarrow f_1(E) \quad (\text{obviously}) \quad (\text{D.21})$$

$$F_1(E) \leftrightarrow f_4(E), f_5(E), f_6(E), f_7(E), f_8(E), f_9(E) \quad (\text{D.22})$$

$$F_2(E) \leftrightarrow f_{10}(E), f_{11}(E), f_{12}(E), f_{13}(E), f_1(E), f_{16}(E) \quad (\text{D.23})$$

$$F_3(E) \leftrightarrow \dots \text{who even cares?} \quad (\text{D.24})$$

- * Check: in Holstein, are there simple relationships between those things?
- * Check: if I do the integrals of the momentum-thingies multiplying those specific $f_i(E)$'s in Eq. (51) do they turn out the way I expect? ie, do I recover the corresponding terms in Eq. (52)?

Appendix E

Compare by Multipoles!

My code uses Holstein's Eq. (52), rather than Eq. (51). In his notation, I'm using $F_i(E)$'s rather than $f_i(E)$'s. I need to convert between them. This is because:

- (a): Coulomb/Radiative corrections (some terms, up to $f_{15}(E)$):
 $f_1, f_2, f_4, f_6, f_7, f_{12}, f_{14}, f_{15}$
- (b): C_S/C_T inclusion (JTW has equivalents for only some terms, up to $f_{12}(E)$):
 $f_1, f_2, f_4, f_6, f_8, f_{12}$.

Holstein and JTW terms have *this* relationship:

$$\xi = f_1(E) \quad (? \text{ times some constant? doesn't matter.}) \quad (\text{E.1})$$

In fact,

$$\xi = G_v^2 \cos \theta_C f_1(E) \quad (\text{E.2})$$

$$a_{\beta\nu} = f_2(E) / f_1(E) \quad (\text{E.3})$$

$$\frac{\langle \vec{J} \rangle}{J} \cdot \frac{\vec{p}}{E} A_\beta = \Lambda_1 \hat{n} \cdot \frac{\vec{p}}{E} f_4(E) / f_1(E) \quad (\text{E.4})$$

$$\frac{\langle \vec{J} \rangle}{J} \cdot \frac{\vec{p}_\nu}{E_\nu} B_\nu = \Lambda_1 \hat{n} \cdot \vec{k} f_6(E) / f_1(E) \quad (\text{E.5})$$

$$\frac{\langle \vec{J} \rangle}{J} \cdot \frac{(\vec{p} \times \vec{p}_\nu)}{EE_\nu} D_{\text{TR}} = \Lambda_1 \hat{n} \cdot (\frac{\vec{p}}{E} \times \hat{k}) f_8(E) / f_1(E) \quad (\text{E.6})$$

$$\begin{aligned}
& \left[\frac{J(J+1) - 3\langle(\vec{J} \cdot \hat{j})^2\rangle}{J(2J-1)} \right] \left[\frac{1}{3} \frac{\vec{p} \cdot \vec{p}_\nu}{EE_\nu} - \frac{(\vec{p} \cdot \hat{j})(\vec{p}_\nu \cdot \hat{j})}{EE_\nu} \right] c_{\text{align}} \\
& = \Lambda_2 \left[(\hat{n} \cdot \frac{\vec{p}}{E})(\hat{n} \cdot \hat{k}) - \frac{1}{3} (\frac{\vec{p}}{E} \cdot \hat{k}) \right] f_{12}(E) / f_1(E)
\end{aligned} \tag{E.7}$$

- JTW Monopole Terms: $\xi, \quad \xi \frac{m}{E} * b_{\text{Fierz}}, \quad \xi \frac{\vec{p} \cdot \vec{p}_\nu}{EE_\nu} * a_{\beta\nu}$
- JTW Dipole Terms: $\xi \frac{\langle \vec{J} \rangle}{J} \cdot \frac{\vec{p}}{E} * A_\beta, \quad \xi \frac{\langle \vec{J} \rangle}{J} \cdot \frac{\vec{p}_\nu}{E_\nu} * B_\nu, \quad \xi \frac{\langle \vec{J} \rangle}{J} \cdot \frac{\vec{p} \times \vec{p}_\nu}{EE_\nu} * D_{\text{TR}}$
- JTW Quadrupole Terms: $\xi \left(\frac{J(J+1)-3\langle(\vec{J} \cdot \hat{j})^2\rangle}{J(2J-1)} \right) \left(\frac{1}{3} \frac{\vec{p} \cdot \vec{p}_\nu}{EE_\nu} - \frac{(\vec{p} \cdot \hat{j})(\vec{p}_\nu \cdot \hat{j})}{EE_\nu} \right) * c_{\text{align}}$

...

- Holstein (52) Monopole Term:

$$F_0(E) = f_1(E)$$

- Holstein (52) Dipole Term:

$$\begin{aligned}
& \Lambda_1 (\hat{n} \cdot \frac{\vec{p}}{E}) * F_1(E) \\
& = \Lambda_1 (\hat{n} \cdot \frac{\vec{p}}{E}) * (f_4(E) + \frac{1}{3} f_7(E))
\end{aligned}$$

- Holstein (52) Quadrupole Term:

$$\begin{aligned}
& \Lambda_2 \left((\hat{n} \cdot \frac{\vec{p}}{E})^2 - \frac{1}{3} \frac{p^2}{E^2} \right) * F_2(E) \\
& = \Lambda_2 \left((\hat{n} \cdot \frac{\vec{p}}{E})^2 - \frac{1}{3} \frac{p^2}{E^2} \right) * (f_{10}(E) + \frac{1}{3} f_{13}(E)) \\
& = \Lambda_2 T_2(\hat{n}) : [\frac{\vec{p}}{E}, \frac{\vec{p}}{E}] * (f_{10}(E) + \frac{1}{3} f_{13}(E))
\end{aligned}$$

- Holstein (52) Octopole Term:

$$\begin{aligned}
& \Lambda_3 \left((\hat{n} \cdot \frac{\vec{p}}{E})^3 - \frac{3}{5} \frac{p^2}{E^2} (\hat{n} \cdot \frac{\vec{p}}{E}) \right) * F_3(E) \\
& = \Lambda_3 \left((\hat{n} \cdot \frac{\vec{p}}{E})^3 - \frac{3}{5} \frac{p^2}{E^2} (\hat{n} \cdot \frac{\vec{p}}{E}) \right) * f_{18}(E) \\
& = \Lambda_3 T_3(\hat{n}) : [\frac{\vec{p}}{E}, \frac{\vec{p}}{E}, \frac{\vec{p}}{E}] * f_{18}(E)
\end{aligned}$$

- Holstein (52) Hexadecapole Term:

(none)

...

- Holstein (51) Monopole Terms:

$$f_1(E), \quad \frac{\vec{p} \cdot \hat{k}}{E} * f_2(E), \quad \left(\frac{(\vec{p} \cdot \hat{k})^2}{E^2} - \frac{1}{3} \frac{p^2}{E^2} \right) * f_3(E)$$

- Holstein (51) Dipole Terms:

$$\begin{aligned}\Lambda_1(\hat{n} \cdot \frac{\vec{p}}{E}) * f_4(E), & \quad \Lambda_1(\hat{n} \cdot \frac{\vec{p}}{E}) \frac{\vec{p} \cdot \hat{k}}{E} * f_5(E), \\ \Lambda_1(\hat{n} \cdot \hat{k}) * f_6(E), & \quad \Lambda_1(\hat{n} \cdot \hat{k}) \frac{\vec{p} \cdot \hat{k}}{E} * f_7(E), \\ \Lambda_1 \hat{n} \cdot \left(\frac{\vec{p}}{E} \times \hat{k} \right) * f_8(E) & \quad \Lambda_1 \hat{n} \cdot \left(\frac{\vec{p}}{E} \times \hat{k} \right) \frac{\vec{p} \cdot \hat{k}}{E} * f_9(E)\end{aligned}$$

- Holstein (51) Quadrupole Terms:

$$\begin{aligned}\Lambda_2 T_2(\hat{n}) : [\frac{\vec{p}}{E}, \frac{\vec{p}}{E}] * f_{10}(E), & \quad \Lambda_2 T_2(\hat{n}) : [\frac{\vec{p}}{E}, \frac{\vec{p}}{E}] (\frac{\vec{p} \cdot \hat{k}}{E}) * f_{11}(E), \\ \Lambda_2 T_2(\hat{n}) : [\frac{\vec{p}}{E}, \hat{k}] * f_{12}(E), & \quad \Lambda_2 T_2(\hat{n}) : [\frac{\vec{p}}{E}, \hat{k}] (\frac{\vec{p} \cdot \hat{k}}{E}) * f_{13}(E), \\ \Lambda_2 T_2(\hat{n}) : [\hat{k}, \hat{k}] * f_{14}(E), & \quad \Lambda_2 T_2(\hat{n}) : [\hat{k}, \hat{k}] (\frac{\vec{p} \cdot \hat{k}}{E}) * f_{15}(E) \quad (?) \\ \Lambda_2 T_2(\hat{n}) : [\frac{\vec{p}}{E}, \frac{\vec{p}}{E} \times \hat{k}] * f_{16}(E), & \\ \Lambda_2 T_2(\hat{n}) : [\hat{k}, \frac{\vec{p}}{E} \times \hat{k}] * f_{17}(E) &\end{aligned}$$

- Holstein (51) Octopole Terms:

$$\Lambda_3 T_3(\hat{n}) : [\frac{\vec{p}}{E}, \frac{\vec{p}}{E}, \frac{\vec{p}}{E}] * f_{18}(E)$$

(also some other stuff, but this is the only term that doesn't integrate to zero.)

- Holstein (51) Hexadecapole Terms:

(some stuff. don't care.)

Holstein's tensor notation definitions:

$$T_2(\hat{n}) : [\vec{a}, \vec{b}] = \left((\hat{n} \cdot \vec{a})(\hat{n} \cdot \vec{b}) - \frac{1}{3} \vec{a} \cdot \vec{b} \right) \quad (\text{E.8})$$

$$T_3(\hat{n}) : [\vec{a}, \vec{b}, \vec{c}] = \left((\hat{n} \cdot \vec{a})(\hat{n} \cdot \vec{b})(\hat{n} \cdot \vec{c}) - \frac{1}{5} \left((\hat{n} \cdot \vec{a})(\vec{b} \cdot \vec{c}) + (\hat{n} \cdot \vec{b})(\vec{a} \cdot \vec{c}) + (\hat{n} \cdot \vec{c})(\vec{a} \cdot \vec{b}) \right) \right) \quad (\text{E.9})$$

$$T_4(\hat{n}) : [\vec{a}, \vec{b}, \vec{c}, \vec{d}] = (\text{some stuff}) \quad (\text{E.10})$$

Integrals by inspection: [***** REINSPECT THEM TOMORROW MELISSA, FOR THE LOVE OF GOD.] ... Actually, I'm'a just reference Table C.4.

Appendix F

Proposed Notation

F.1 Things.2

Actually though, I'm back up. Let's talk about dot products in spherical coordinates. Of course, in Cartesian coordinates,

$$\vec{p}_\beta = p_\beta \begin{bmatrix} \sin \theta_\beta \cos \phi_\beta \\ \sin \theta_\beta \sin \phi_\beta \\ \cos \theta_\beta \end{bmatrix}; \quad \vec{p}_r = p_r \begin{bmatrix} \sin \theta_r \cos \phi_r \\ \sin \theta_r \sin \phi_r \\ \cos \theta_r \end{bmatrix}; \quad \vec{p}_\nu = p_\nu \begin{bmatrix} \sin \theta_\nu \cos \phi_\nu \\ \sin \theta_\nu \sin \phi_\nu \\ \cos \theta_\nu \end{bmatrix} \quad (\text{F.1})$$

According to insight that Alexandre thought was very obvious, because it was, JTW-style notation only happened in the first place because the lab frame matters. It's measured w.r.t. polarization or alignment or something. The integration over the two leptons is really an integration over the lab frame + one lepton.

F.2 Things.3

Suppose I integrate jtw over everything but electron energy. What's left?

$$\omega d(\text{stuff}) = \left(\frac{1}{2\pi}\right)^5 (4\pi)^2 p_\beta E_\beta E_\nu^2 dE_\beta \xi \left[1 + b_{\text{Fierz}} \left(\frac{m_e}{E_\beta}\right)\right]. \quad (\text{F.2})$$

...Or, in units that don't suck, with terminology that's useful to us (and assuming massless neutrinos, which is fine, 'cause the uncertainty in Q is like 200 eV or

something (check value)),

$$\omega d(\text{stuff}) = 4 \left(\frac{1}{2\pi} \right)^3 \frac{(E_\beta^2 - m_e^2 c^4)^{1/2}}{c} E_\beta (Q - E_\beta - E_{r\text{kin}})^2 dE_\beta \xi \left[1 + b_{\text{Fierz}} \left(\frac{m_e c^2}{E_\beta} \right) \right] \quad (\text{F.3})$$

Integrate over the beta energy (**NOT** between $E_\beta = m_e c^2$ and $E_\beta = m_e c^2 + Q$; fix this in the code!) and we find:

$$\omega = 4 \left(\frac{1}{2\pi} \right)^3 (...) \quad (\text{F.4})$$

This is *probably* interpreted as the overall decay rate, somehow.

F.3 Beta End-point Energy

Note that nuclear physics notational convention, which is fucking retarded, apparently defines kinetic energy T s.t.

$$E = T + mc^2, \quad (\text{F.5})$$

but of course, it's still the case that

$$E = (p^2 c^2 + m_e^2 c^4)^{1/2}. \quad (\text{F.6})$$

But since $Q = T_{\text{final}} - T_{\text{initial}}$, we're sort-of stuck, if we want to describe the beta end-point energy in terms of Q , we find that

$$E_{\text{end}} = Q + m_e c^2 \quad (\text{F.7})$$

$$Q = (p_{\text{max}}^2 c^2 + m_e^2 c^4)^{1/2} - m_e c^2 \quad (\text{F.8})$$

... actually, pretty sure that's all wrong. Actually-actually, it's fine. See “jtw_integration_scratch3.nb” for more-other details. That version, I believe, finally got all the thingies right.

F.4 Beta End-point Energy.2

Firstly, some Q-values for ^{37}K (via bnl).

$$Q_{\text{EC}} = 6.14745(23) \text{ MeV} \quad (\text{F.9})$$

$$Q_{\beta+} = 5.12545(23) \text{ MeV} \quad (\text{F.10})$$

It would be better if I knew the branching ratio for EC/ $\beta+$ though.

Anyway, in the jtw notation,

$$E_0 := Q + m_e c^2. \quad (\text{F.11})$$

Is that \uparrow even true?? Because I'm really not sure it is. Via Kofoedhansen, $(E_0 - E_e) = E_\nu$. So there.

What does that mean in terms of the individual particles' energies? Well, if that's the beta end-point energy, it just means that that's the total (kinetic + rest) energy for the beta. So, we can distribute Q of kinetic energy around to the other particles.

$$Q = T_\beta + T_\nu + T_r \quad (\text{F.12})$$

$$= (E_\beta - m_\beta c^2) + (E_\nu - m_\nu c^2) + (E_r - M_r c^2) \quad (\text{F.13})$$

$$\approx E_\beta - m_\beta c^2 + E_\nu + T_r \quad (\text{F.14})$$

$$E_0 \approx E_\beta + E_\nu + T_r \quad (\text{F.15})$$

$$T_\beta = (p_\beta^2 c^2 + m_e^2 c^4)^{1/2} - m_e c^2 \quad (\text{F.16})$$

$$T_\nu = (p_\nu^2 c^2 + m_\nu^2 c^4)^{1/2} - m_\nu c^2 \quad (\text{F.17})$$

$$T_r = (p_r^2 c^2 + M_r^2 c^4)^{1/2} - M_r c^2 \quad (\text{F.18})$$

A thing that's worth noting is that (I think!) recoil-order corrections have been implicitly excluded at some point here. ...Is this even true??

Appendix G

Derivation of the b_{Fierz} Dependence of the Superratio Asymmetry

Consider, from JTW, the probability distribution for outgoing beta particles in terms of only the electron energy and direction w.r.t. parent nuclear polarization (other parameters have been integrated over). We have

$$P(E_\beta) = W(E_\beta) \left[1 + b_{\text{Fierz}} \frac{mc^2}{E_\beta} + A_\beta \frac{v}{c} |\vec{P}| \cos \theta \right]. \quad (\text{G.1})$$

In the TRINAT geometry with two polarization states (+/-) and two detectors (T/B), we are able to describe four different count rates, with different combinations of polarization states and detectors. Thus, we have:

$$r_{T+}(E_\beta) = \varepsilon_T(E_\beta) \Omega_T N_+ \left[1 + b_{\text{Fierz}} \frac{mc^2}{E_\beta} + A_\beta \frac{v}{c} |\vec{P}_+| \langle \cos \theta \rangle_{T+} \right] \quad (\text{G.2})$$

$$r_{B+}(E_\beta) = \varepsilon_B(E_\beta) \Omega_B N_+ \left[1 + b_{\text{Fierz}} \frac{mc^2}{E_\beta} + A_\beta \frac{v}{c} |\vec{P}_+| \langle \cos \theta \rangle_{B+} \right] \quad (\text{G.3})$$

$$r_{T-}(E_\beta) = \varepsilon_T(E_\beta) \Omega_T N_- \left[1 + b_{\text{Fierz}} \frac{mc^2}{E_\beta} + A_\beta \frac{v}{c} |\vec{P}_-| \langle \cos \theta \rangle_{T-} \right] \quad (\text{G.4})$$

$$r_{B-}(E_\beta) = \varepsilon_B(E_\beta) \Omega_B N_- \left[1 + b_{\text{Fierz}} \frac{mc^2}{E_\beta} + A_\beta \frac{v}{c} |\vec{P}_-| \langle \cos \theta \rangle_{B-} \right], \quad (\text{G.5})$$

where $\varepsilon_{T/B}(E_\beta)$ are the (top/bottom) detector efficiencies, $\Omega_{T/B}$ are the fractional solid angles for the (top/bottom) detector from the trap position, $N_{+/-}$ are the number of atoms trapped in each (+/-) polarization state, and $|\vec{P}_{+/-}|$ are the magnitudes

of the polarization along the detector axis for each polarization state. $\langle \cos \theta \rangle_{T/B,+/-}$ is the average of $\cos \theta$ for *observed* outgoing betas, for each detector and polarization state combination. This latter term is approximately ± 1 , and contains important sign information. For a pointlike trap in the center of the chamber, 103.484 mm from either (DSSSD) detector, each of which is taken to be circular with a radius of 15.5 mm, we find that $\langle |\cos \theta| \rangle_{T/B,+/-} \approx 0.994484$, and is the same for all four cases (or for $r = 15.0$ mm, we find that $\langle |\cos \theta| \rangle_{T/B,+/-} \approx 0.994829$). Note that a horizontally displaced trap will decrease the magnitude of $\langle |\cos \theta| \rangle$, but all four values will remain equal to one another. In the case of a vertically displaced trap, these four values will no longer all be equal, however it will still be the case that $\langle |\cos \theta| \rangle_{T+} = \langle |\cos \theta| \rangle_{T-}$, and $\langle |\cos \theta| \rangle_{B+} = \langle |\cos \theta| \rangle_{B-}$.

For simplicity, we will henceforth assume that the trap is vertically centered, and take $|\vec{P}_+| = |\vec{P}_-|$. We also define the following:

$$A' = A'(E_\beta) \equiv A_\beta \frac{v}{c} |\vec{P}| \langle |\cos \theta| \rangle \quad (G.6)$$

$$b' = b'(E_\beta) \equiv b_{\text{Fierz}} \frac{mc^2}{E_\beta}, \quad (G.7)$$

and choose a coordinate system in which the + polarization state is, in some sense, ‘pointing up’ toward the top detector, such that

$$\langle \cos \theta \rangle_{T+} \approx +1 \quad (G.8)$$

$$\langle \cos \theta \rangle_{B+} \approx -1 \quad (G.9)$$

$$\langle \cos \theta \rangle_{T-} \approx -1 \quad (G.10)$$

$$\langle \cos \theta \rangle_{B-} \approx +1. \quad (G.11)$$

This allows us to rewrite the four count rates in simplified notation, as:

$$r_{T+} = \varepsilon_T N_+ (1 + b' + A') \quad (G.12)$$

$$r_{B+} = \varepsilon_B N_+ (1 + b' - A') \quad (G.13)$$

$$r_{T-} = \varepsilon_T N_- (1 + b' - A') \quad (G.14)$$

$$r_{B-} = \varepsilon_B N_- (1 + b' + A'). \quad (G.15)$$

We further define the ‘superratio’, s , to be:

$$s = \frac{r_{T-} r_{B+}}{r_{T+} r_{B-}}. \quad (\text{G.16})$$

We are now in a position to define the ‘superratio asymmetry’, A_{super} , as

$$A_{\text{super}} = A_{\text{super}}(E_\beta) \equiv \frac{1 - \sqrt{s}}{1 + \sqrt{s}}. \quad (\text{G.17})$$

This is explicitly an experimental quantity that is measured directly by the above combination of count rates.

Writing the superratio out explicitly in terms of A' and b' , factors of $\varepsilon_{T/B}$ and $N_{+/-}$ cancel out entirely, and we find that

$$s = \frac{(1 + b' - A')^2}{(1 + b' + A')^2}. \quad (\text{G.18})$$

From here it is immediately clear that in absence of other corrections (*e.g.* backscattering, unpolarized background, ...), if $b' = 0$ it follows that $A_{\text{super}} = A'$. In the case where $b' \neq 0$, we find that

$$A_{\text{super}} = \frac{A'}{1 + b'} \quad (\text{G.19})$$

$$\approx A' (1 - b' + b'^2), \quad (\text{G.20})$$

where we have utilized the assumption that $b' \ll 1$. Thus,

$$A_{\text{super}} \approx A_\beta \frac{v}{c} |\vec{P}| \langle |\cos \theta| \rangle - A_\beta \frac{v}{c} |\vec{P}| \langle |\cos \theta| \rangle \left(b_{\text{Fierz}} \frac{mc^2}{E_\beta} \right) + A_\beta \frac{v}{c} |\vec{P}| \langle |\cos \theta| \rangle \left(b_{\text{Fierz}} \frac{mc^2}{E_\beta} \right)^2. \quad (\text{G.21})$$

Appendix H

Some Corrections to the Superratio Stuff

We consider further modifications to the rates described in Eqs. (G.2-G.5). In particular, we consider the effect of non-identical polarization magnitudes for the two polarization states and a trap displaced from the center.

We define for the polarization states:

$$P \equiv \frac{1}{2} (|\vec{P}_+| + |\vec{P}_-|) \quad (\text{H.1})$$

$$\Delta P \equiv \frac{1}{2} (|\vec{P}_+| - |\vec{P}_-|) \quad (\text{H.2})$$

and immediately find that

$$|\vec{P}_+| = P + \Delta P \quad (\text{H.3})$$

$$|\vec{P}_-| = P - \Delta P. \quad (\text{H.4})$$

Further, we also define:

$$\langle |\cos \theta| \rangle_T \equiv \langle |\cos \theta| \rangle_{T+} = \langle |\cos \theta| \rangle_{T-} \quad (\text{H.5})$$

$$\langle |\cos \theta| \rangle_B \equiv \langle |\cos \theta| \rangle_{B+} = \langle |\cos \theta| \rangle_{B-}, \quad (\text{H.6})$$

and

$$\langle |\cos \theta| \rangle \equiv \frac{1}{2} (\langle |\cos \theta| \rangle_T + \langle |\cos \theta| \rangle_B) \quad (\text{H.7})$$

$$\Delta \langle |\cos \theta| \rangle \equiv \frac{1}{2} (\langle |\cos \theta| \rangle_T - \langle |\cos \theta| \rangle_B). \quad (\text{H.8})$$

It immediately follows that

$$\langle |\cos \theta| \rangle_T = \langle |\cos \theta| \rangle + \Delta \langle |\cos \theta| \rangle \quad (\text{H.9})$$

$$\langle |\cos \theta| \rangle_B = \langle |\cos \theta| \rangle - \Delta \langle |\cos \theta| \rangle. \quad (\text{H.10})$$

With this new set of variables defined, we can re-write Eqs. (G.2-G.5) as

$$r_{T+}(E_\beta) = \varepsilon_T(E_\beta) N_+ \left[1 + b' + (A_\beta \frac{v}{c})(P + \Delta P) (\langle |\cos \theta| \rangle + \Delta \langle |\cos \theta| \rangle) \right] \quad (\text{H.11})$$

$$r_{B+}(E_\beta) = \varepsilon_B(E_\beta) N_+ \left[1 + b' - (A_\beta \frac{v}{c})(P + \Delta P) (\langle |\cos \theta| \rangle - \Delta \langle |\cos \theta| \rangle) \right] \quad (\text{H.12})$$

$$r_{T-}(E_\beta) = \varepsilon_T(E_\beta) N_- \left[1 + b' - (A_\beta \frac{v}{c})(P - \Delta P) (\langle |\cos \theta| \rangle + \Delta \langle |\cos \theta| \rangle) \right] \quad (\text{H.13})$$

$$r_{B-}(E_\beta) = \varepsilon_B(E_\beta) N_- \left[1 + b' + (A_\beta \frac{v}{c})(P - \Delta P) (\langle |\cos \theta| \rangle - \Delta \langle |\cos \theta| \rangle) \right] \quad (\text{H.14})$$

and the superratio becomes

$$s = \frac{(1 + b' - (A_\beta \frac{v}{c})(P - \Delta P) (\langle |\cos \theta| \rangle + \Delta \langle |\cos \theta| \rangle)) (1 + b' - (A_\beta \frac{v}{c})(P + \Delta P) (\langle |\cos \theta| \rangle - \Delta \langle |\cos \theta| \rangle))}{(1 + b' + (A_\beta \frac{v}{c})(P + \Delta P) (\langle |\cos \theta| \rangle + \Delta \langle |\cos \theta| \rangle)) (1 + b' + (A_\beta \frac{v}{c})(P - \Delta P) (\langle |\cos \theta| \rangle - \Delta \langle |\cos \theta| \rangle))} \quad (\text{H.15})$$

where $\varepsilon_{T/B}$ and $N_{+/-}$ still completely cancel out. After a bit of algebra, this simplifies to:

$$s = \frac{(1 + b' - A' + A_\beta \frac{v}{c} \Delta P \Delta \langle |\cos \theta| \rangle)^2 - (A_\beta \frac{v}{c})^2 (\Delta P \langle |\cos \theta| \rangle - P \Delta \langle |\cos \theta| \rangle)^2}{(1 + b' + A' + A_\beta \frac{v}{c} \Delta P \Delta \langle |\cos \theta| \rangle)^2 - (A_\beta \frac{v}{c})^2 (\Delta P \langle |\cos \theta| \rangle + P \Delta \langle |\cos \theta| \rangle)^2} \quad (\text{H.16})$$

Note that in the superratio ΔP and $\Delta \langle |\cos \theta| \rangle$ have cancelled out to first order, and the remaining dependencies are quadratic only. Eq. (H.16) is exact, but still a huge enough expression to be pretty unwieldy to work with. Let's introduce some

shorthand notation to make this less painful:

$$A'' := A_\beta \frac{v}{c} \quad (\text{H.17})$$

$$c := \langle |\cos \theta| \rangle \quad (\text{H.18})$$

$$\Delta c := \Delta \langle |\cos \theta| \rangle \quad (\text{H.19})$$

$$r' := 1 + b' + A_\beta \frac{v}{c} \Delta P \Delta \langle |\cos \theta| \rangle \quad (\text{H.20})$$

In this notation, we find that

$$s = \frac{(r' - A')^2 - (A'')^2 (\Delta P c - P \Delta c)^2}{(r' + A')^2 - (A'')^2 (\Delta P c + P \Delta c)^2}, \quad (\text{H.21})$$

which hurts a lot less to look at. Then, the superratio asymmetry is

$$A_{\text{super}} = \frac{1 - \sqrt{\frac{(r' - A')^2 - (A'')^2 (\Delta P c - P \Delta c)^2}{(r' + A')^2 - (A'')^2 (\Delta P c + P \Delta c)^2}}}{1 + \sqrt{\frac{(r' - A')^2 - (A'')^2 (\Delta P c - P \Delta c)^2}{(r' + A')^2 - (A'')^2 (\Delta P c + P \Delta c)^2}}} \quad (\text{H.22})$$

$$= \frac{\left[\sqrt{(r' + A')^2 - (A'')^2 (\Delta P c + P \Delta c)^2} - \sqrt{(r' - A')^2 - (A'')^2 (\Delta P c - P \Delta c)^2} \right]^2}{\left[(r' + A')^2 - (A'')^2 (\Delta P c + P \Delta c)^2 \right] - \left[(r' - A')^2 - (A'')^2 (\Delta P c - P \Delta c)^2 \right]} \quad (\text{H.23})$$

$$= \frac{\left(\begin{array}{l} 2 \left[(r')^2 + (A')^2 - (A'')^2 ((P \Delta c)^2 + (\Delta P c)^2) \right] \\ -2 \left[(r' + A')^2 - (A'')^2 (\Delta P c + P \Delta c)^2 \right]^{1/2} \left[(r' - A')^2 - (A'')^2 (\Delta P c - P \Delta c)^2 \right]^{1/2} \end{array} \right)}{4 \left[(r' A') - (A'')^2 (P c \Delta P \Delta c) \right]} \quad (\text{H.24})$$

Appendix I

The Parity Operator: Vectors and Axial Vectors and Pseudoscalars, oh my!

via Samuel Wong, 1990. pg 212.

I.1 Scalars

A scalar does not change sign under the parity operation, because why even would it?

I.2 Vectors

Vectors, or “polar vectors” (V) are exactly what I think they are. Position \vec{r} and (linear) momentum \vec{p} are examples. The thing about these vectors is that they change sign (or, really, direction) under a parity transformation.

I.3 Axial Vectors

Axial vectors (A) *don’t* change sign under a parity transformation. An example is angular momentum, $\vec{L} = \vec{r} \times \vec{p}$. This is where the ”mirror” thing breaks down. A mirror only is only a one-dimensional parity operator, so if you think of a thing

with angular momentum and its reflection in a mirror, you imagine the mirror image with reversed angular momentum too. But in reality, if you change the sign of *all components* of \vec{r} and simultaneously all components of \vec{p} , it's clear that the quantity $(\vec{r} \times \vec{p})$ remains unchanged. Pauli spin matrices, $\vec{\sigma}$, are axial vectors.

I.4 Pseudoscalars

Pseudoscalars, (P). You'd think they were scalars, because they're just a number, but have to remember that you got them by taking the scalar product of a (polar) vector and an axial vector. If you apply the parity operator to the quantity $P = (\vec{V} \cdot \vec{A})$, \vec{V} changes sign (for all components) while \vec{A} does not. So the resultant "scalar" P has to change sign too. That's how you know that P is really a pseudoscalar.

I.5 Tensors

...Yeah, Wong doesn't really get into that. At least not here.

I.6 Comments on Parity Conservation

An interaction made from a mixture of scalars and pseudoscalars, or a mixture of vectors and axial vectors, does *not* conserve parity.

For the strong and electromagnetic forces, parity *is* strictly conserved. Not so for the weak force!

I.7 Q-Values

The Q -value for a particular interaction is defined as the difference between the kinetic energies of the final and initial systems.

$$Q = T_f - T_i \quad (\text{I.1})$$

In particular, for β^+ decay, we're including which things? ... as part of the mass of the various systems?

I.8 Helicity

Helicity, h , is a pseudoscalar.

$$h = \frac{\vec{\sigma} \cdot \vec{p}}{|\vec{p}|} \quad (\text{I.2})$$

I.9 Conserved Vector Current Hypothesis

The CVC hypothesis asserts that the Fermi interactions of nucleons within a nucleus are *not* changed by all the surrounding mesons. (What?)

JB: You're describing a consequence of CVC, and are not stating the actual hypothesis.

JB: I think you don't have time to explain the CVC hypothesis. You'll just have to assume it. I personally found that the technical derivation was the only way to see what was going on.

JB: A good sketch of CVC is done in Commins' notes and his book with Bucksbaum [?]. Ian townner did it in his notes. I reproduce this in my own course notes for Phys 505 (p.21-28 of the thing John attached to that email). First you show in Dirac notation that the E&M current for pointlike particles is conserved—this just needs one use of the Dirac Equation and conservation of electric charge. Then look what happens for finite nucleons. Then construct the analogous weak interaction current for the nucleon, including three possible current terms that transform like Lorentz vectors, and note the consequences if that current is still conserved.

Figure out how to cite somebody's unpublished/semi-unpublished notes.

JB: Jelley [5] describes the qualitative background on his text page 110 (attached). Feynman and Gell-Mann proposed that the isovector weak vector current and the isovector E&M vector current are members of an isotriplet of currents all of which are conserved. [This idea eventually went straight into the SM electroweak interaction, with the addition of nonabelian and massive operators for the weak part, though figuring out how to make a consistent theory with the massive bosons took the combination of Yang-Mills gauge theories and then Weinberg and Salam's approaches.]

JB: What you say is one consequence, that meson exchange currents don't change the vector part of the weak interaction– this is consistent with conservation of electric charge and its analog in the weak interaction. This particular consequence is a very powerful tool in electromagnetic effects in nuclei, e.g. if you take the isovector combination of magnetic moments (^{37}Ar - ^{37}K e.g.) you get something without meson exchange corrections and therefore precisely sensitive to other higher-order physics effects. Arima and Towner separately studied this for significant parts of their careers. The axial vector interaction is changed by meson exchange currents. The recent calculation of Gysbeg et al. accounting for most of the Gamow-Teller strength is including meson exchange currents in what they call 2-body currents, natural higher-order corrections in their chiral EFT expansion of the strong interaction between nucleons when you consider electroweak interactions.

JB: But there are lots of other things that also don't change the Fermi interaction... so picking out meson exchange currents for discussion is maybe not fully motivated. Lots of people state one consequence or another of CVC to motivate what they are doing, without explaining.

Paraphrased JB: Don't try to derive CVC in this thesis. Just cite the hypothesis and say that our Abeta stuff provides a test of it.

JB: Something else beyond the thesis scope, sorry: a nonzero b_{Fierz} does not necessarily break CVC, as the vector part of the SM weak interaction could still be conserved whether or not there are other quark-lepton currents with different Lorentz structure. You could make a nonzero b_{Fierz} from a 2nd-class scalar in the nucleon-electron weak current which would break CVC, but that could not be distinguished from a quark-electron extra scalar current.

Appendix J

Constraining the Analysis with Lifetime Measurements

J.1 Background/Introduction

The goal here is to understand what physical interpretation to give to (linear combinations of) G4 simulations with sets of coupling constants that may or may not be physically possible, given previous lifetime measurements that were not taken into account. The results aren't broken forever or anything, but some care must be given to the interpretation.

John and Dan say this paper is widely accepted to be wrong about some of the things. (Some assumption was wrong, I guess?) So then presumably what I've written here can't be trusted either.

JB: The paper that fixes the known mistakes in Severijns et al. [6] is L. Hayen and N. Severijns, 2019 [7]. It's conveniently located on the arXiv, and I should definitely go read it. The known mistake was using the ratio of integrals of the lepton momentum f_A/f_V more than once—there is a more subtle radiative correction for the Gamow-Teller piece. A paper using the formalism is D. Combs et al [8] (which is *also* conveniently located on the arXiv) with ^{19}Ne and ^{37}K results—their extraction is so close to Ben and Dan's that we conclude we are doing the formalism well. i.e. we used the f_A/f_V ratio correctly.

We'll loosely follow Severijns et. al.'s procedure [6]. In this paper, (which conveniently sets b_{Fierz} to zero as soon as the math starts getting messy), we see that the authors will eventually need to split their treatment into "Fermi" and "Gamow-Teller" parts to arrive at their final result. This becomes clear upon examining their

1D decay rate element:

$$d\Gamma = (\text{constants}) \xi \left(1 + \frac{m}{W} b\right) F(\pm Z, W) S(\pm Z, W) (W - W_0)^2 pW dW \quad (\text{J.1})$$

where we find that the nuclear shape correction function, $S(\pm Z, W)$, is slightly different in the case of Fermi and Gamow-Teller decays. Though they note that $S(\pm Z, W) = 1$ for both types of decay under the allowed approximation, and it changes only slightly under a more complete treatment, it is this term which gives rise to the statistical rate functions f_V and f_A . Note that the overall value of the ratio f_A/f_V directly changes any estimate of the mixing ratio ρ , so we will need at least an estimate of its value in order to do anything useful.

In particular,

$$f_{V/A} = \int F(\pm Z, W) S_{V/A}(\pm Z, W) (W - W_0)^2 pW dW \quad (\text{J.2})$$

No matter the form of $S(\pm Z, W)$ — and I definitely *do not* know its form — this is clearly a very challenging integral. Luckily, a calculation result is provided (with no associated uncertainty given):

$$\frac{f_A}{f_V} \Big|_{37K} = 1.00456. \quad (\text{J.3})$$

So, we follow their calculation through, and at the end it yields this result:

$$Ft^{\text{mirror}} = \frac{2Ft^{0^+ \rightarrow 0^+}}{1 + \frac{f_A}{f_V}\rho^2}, \quad (\text{J.4})$$

with

$$\rho \approx \frac{C_A M_{GT}^0}{C_V M_F^0}. \quad (\text{J.5})$$

But of course, there's no reason why we can't do a similar calculation while including non-zero values of C_S and C_T . Probably.

J.2 Now What?

In the case where $b_{\text{Fierz}} = 0$, this treatment gets us to the sort of results we might want. However, if we start introducing non-zero scalar or tensor coupling constants, it's unclear (to me) how we should treat the associated shape correction function(s). Eg, do we think the shape correction function $S_V(\pm Z, W)$ is associated with a *Fermi* decay, or with a *vector* coupling? In the case of zero scalar or tensor couplings, the question is irrelevant because the calculation must be the same either way – M_F and C_V go together every time.

With $b_{\text{Fierz}} \neq 0$, the distinction changes the calculation though, since its terms have factors of (eg) $M_F^2 C_V$. Perhaps there are a whole different set of shape correction functions associated specifically with C_S and C_T .

I *might* be able to find a treatment in the literature somewhere where they do one thing or the other. For my own mental clarity, I would really like to know the answer. However, I recognize that for the purpose of evaluating scalar and tensor coupling constants, the distinction is largely academic, and won't really affect the answer. I have to just pick something and go with it.

J.3 After Picking Something...

I declare (and so it has to be true, regardless of reality) that the shape correction function $S_{V/A}(\pm Z, W)$ is associated with the matrix element $M_{F/GT}$ rather than the coupling constant $C_{V/A}$. So, given this, we'll switch our notation a bit and write down a new decay rate:

$$d\Gamma = \left(\vec{\xi} + \frac{m}{W} (b\vec{\xi}) \right) \cdot d\vec{\Gamma}_0, \quad (\text{J.6})$$

where the vector components are the Fermi and Gamow-Teller components of the decay:

$$\vec{\xi} = \begin{bmatrix} 2M_F^2 (C_V^2 + C_S^2) \\ 2M_{GT}^2 (C_A^2 + C_T^2) \end{bmatrix} \quad (\text{J.7})$$

$$(\vec{b}\vec{\xi}) = \begin{bmatrix} \pm 2\gamma \operatorname{Re}[C_S C_V^* + C'_S C_V'^*] \\ \pm 2\gamma \operatorname{Re}[C_T C_A^* + C'_T C_A'^*] \end{bmatrix} \quad (\text{J.8})$$

$$d\vec{\Gamma}_0 = (\text{constants}) \begin{bmatrix} F_F(\pm Z, W) S_F(\pm Z, W) (W - W_0)^2 pW dW \\ F_{GT}(\pm Z, W) S_{GT}(\pm Z, W) (W - W_0)^2 pW dW \end{bmatrix}. \quad (\text{J.9})$$

We find that the integrals involved here are still hard. I will need to make some simplifying assumptions to get anywhere.

Appendix K

An R_{slow} Thesis Proposal

K.1 An Old R_{slow} Abstract

The nuclear weak force is known to be a predominantly left-handed vector and axial-vector (V-A) interaction. An experiment is proposed to further test that observation, constraining the strength of right-handed (V+A) currents by exploiting the principle of conservation of angular momentum within a spin-polarized beta decay process. Here, we focus on the decay $^{37}\text{K} \rightarrow ^{37}\text{Ar} + \beta^+ + \nu_e$. The angular correlations between the emerging daughter particles provide a rich source of information about the type of interaction that produced the decay.

We obtain a sample of neutral, cold, nuclear spin-polarized ^{37}K atoms with a known spatial position, via the TRIUMF accelerator facility, by intermittently running a magneto-optical trap (MOT) to confine and cool the atoms, then cycling the trap off to polarize the atoms. With β detectors placed opposite each other along the axis of polarization, we are able to directly observe the momenta of β^+ particles emitted into 1.4% of the total solid angle nearest this axis. We also are able to extract a great deal of information about the momentum of the recoiling ^{37}Ar daughters by measuring their times of flight and hit positions on a microchannel plate detector with a delay line. Because the nuclear polarization is known to within < 0.1% [1], and we are able to account for many systematic effects by periodically reversing the polarization and by collecting unpolarized decay data while the atoms are trapped within the MOT, we expect to be well equipped to implement a test of ‘handedness’ within the nuclear weak force.

K.2 Motivation

The nuclear weak force has long been known to be a predominantly left-handed chiral interaction, meaning that immediately following an interaction (such as a beta decay) with a weak force carrying boson (W^+ , W^- , Z), normal-matter leptons (such as the electron and electron neutrino) emerge with left-handed chirality while the anti-leptons (e.g. the positron and electron anti-neutrino) emerge with right-handed chirality. In the limit of massless particles, the particle’s chirality is the same as its helicity. Thus, in a left-handed model, the direction of an (ultrarelativistic) normal lepton’s spin is antiparallel direction of its motion, and the direction of spin for an anti-lepton is parallel to its direction of motion. For a non-relativistic particle the property of chirality is fairly abstract, and describes the appropriate group representation and projection operators to be used in calculations. It should be noted that a fully chiral model is also one which is maximally parity violating.

This odd quirk of the nuclear weak force is not only *predominantly* true, but it is, to the best of our current scientific knowledge, *always* true – that is, attempts to measure any right-handed chiral components of the weak force have produced results consistent with zero [10][23]. This project proposes a further measurement to constrain the strength of the right-handed component of the weak interaction.

K.3 The Principle of the Measurement

Of particular interest is the decay process: $^{37}\text{K} \rightarrow ^{37}\text{Ar} + \beta^+ + \nu_e$. Among other useful properties, this is a ‘mirror’ decay, meaning that the nuclear wavefunctions of the parent and daughter are identical up to their isospin quantum number. This property allows us to place strong constraints on the size of the theoretical uncertainties for this decay process within the Standard Model. We further exploit this property by noting that both the ^{37}K parent and the ^{37}Ar daughter have nuclear spin $I = 3/2$, a fact which is key to this experiment.

K.4 The Decay Process

The kinematics of nuclear β^+ decay are described by the following probability density function:

$$W(\langle I \rangle | E_\beta \hat{\Omega}_\beta \hat{\Omega}_\nu) = \left(\frac{1}{2\pi} \right)^5 F(-Z, E_\beta) p_\beta E_\beta (E_0 - E_\beta)^2 dE_\beta d\hat{\Omega}_\beta d\hat{\Omega}_\nu \xi \left[1 + a_{\beta\nu} \frac{\vec{p}_\beta \cdot \vec{p}_\nu}{E_\beta E_\nu} + b_{\text{Fierz}} \frac{m_e}{E_\beta} \right. \\ + c_{\text{align}} \left(\frac{\frac{1}{3} \vec{p}_\beta \cdot \vec{p}_\nu - (\vec{p}_\beta \cdot \hat{j})(\vec{p}_\nu \cdot \hat{j})}{E_\beta E_\nu} \right) \left(\frac{I(I+1) - 3\langle (\vec{I} \cdot \hat{i})^2 \rangle}{I(2I-1)} \right) \\ \left. + \frac{\langle \vec{I} \rangle}{I} \left(A_\beta \frac{\vec{p}_\beta}{E_\beta} + B_\nu \frac{\vec{p}_\nu}{E_\nu} + D_{\text{TR}} \frac{\vec{p}_\beta \times \vec{p}_\nu}{E_\beta E_\nu} \right) \right], \quad (\text{K.1})$$

where \vec{I} is the nuclear spin-polarization, $F(-Z, E_\beta)$ is the Fermi function, and parameters ξ , $a_{\beta\nu}$, b_{Fierz} , c_{align} , A_β , B_ν , and D_{TR} are functions that vary with the strengths of the vector, axial, scalar, and tensor couplings (constant throughout nature), as well as the Fermi and Gamow-Teller nuclear matrix elements (specific to the individual decay) [12][13].

The decay may be treated as a three-body problem in which the available kinetic energy is divided up between the beta, the neutrino, and the recoiling ^{37}Ar nucleus, and (of course) the total linear and angular momentum are conserved. While the neutrino cannot be detected directly, its kinematics may be reconstructed from observations of the beta and the recoiling daughter nucleus. By placing detectors above and below the decaying atom along the axis of its polarization, we are able to obtain information about the outgoing beta's energy and momentum, in the cases of interest to us, where it is emitted along (or close to) the axis of polarization.

The recoiling ^{37}Ar nucleus is a bit trickier to work with, but the task is not impossible. One useful feature of the $^{37}\text{K} \rightarrow {}^{37}\text{Ar}$ transition is that, in addition to the β^+ emitted in the decay itself, one or more *orbital* electrons from the parent atom are typically lost. In the majority of decay events only one orbital electron is ‘shaken off’ and so the daughter ^{37}Ar atom is electrically neutral [16][24]. In the remaining cases, two or more orbital electrons are lost this way, and the daughter atom is positively charged. If we apply an electric field perpendicular to the direction of polarization, these positively charged $^{37}\text{Ar}^{(+n)}$ ions may be collected into a detector, from which hit position and time of flight information may be extracted. These shake-off electrons

are emitted with an average energy of only $\sim 2\text{ eV}$ so to a very good approximation the other decay products are not perturbed by the presence of shake-off electrons.

It should be noted that for the class of decays of greatest interest, where the beta and the neutrino emerge back-to-back along the polarization axis, the recoiling daughter nucleus will have zero momentum along the directions perpendicular to this axis, and on average less total energy than if the beta and neutrino were emitted in a parallel direction. Henceforth, daughter nuclei from a back-to-back decay as shown in Figure ?? will be described as ‘slow’ recoils. In terms of observables, this means that if the electric field is configured to point along one of the axes perpendicular to the polarization direction, then when the recoiling ion is swept away into a detector, the slow recoil’s hit position should be exactly along the projection of the polarization axis. Furthermore, the slow recoil’s time of flight should be in the middle of the time of flight spectrum, since other recoils will be emitted with momentum towards or away from the detector.

K.5 Current Status

In June 2014, after several years of preparatory work beforehand (the author has been continuously involved with this project since 2010), approximately 7 days of beam time at TRIUMF was dedicated to the TRINAT ^{37}K beta decay experiment. Approximately half of this data is suitable for use in this project. During this period, approximately 10,000 atoms were held within the trap at any given time. The cleaned spectra show around 50,000 polarized beta-recoil coincidence events in total, divided among measurements at three different electric field strengths (535 V/cm, 415 V/cm, 395 V/cm).

At the present time, analysis is underway. The recoil MCP hit position data has been calibrated, and systematic effects in the trap position and size measurements are being considered. The largest two remaining hurdles for the analysis both lie in improvements to the Monte Carlo.

The first challenge is to implement particle tracking within a *non-uniform* electric field. Using the true non-uniform electric field will shift the time-of-flight spectra overall by around 1%, and is expected to change the *shape* of spectra as well, since the deviation from uniformity changes significantly as a function of flight trajectory,

and is greater the farther a particle ventures from the central axis. This would affect the measured hit positions as well. Taken together, the shape of the time-of-flight spectra (as in Figure ??) and the recoil hit position are critical to our reconstruction of the decay process, it is critical that we model them correctly.

The second challenge will be to allow our simulation to vary vector, axial, scalar, and tensor coupling constants separately while holding other physical parameters (such as the half-life and Fermi/Gamow-Teller ratio) constant. This, too, will be absolutely critical to the analysis, and its implementation is likely to be non-trivial.

A fit to simulation has shown that the data that has already been collected has sufficient statistical power to measure the *fractional* contribution of any polarized ‘new physics’ beta decay parameter (ie right-handed, scalar, and tensor currents within the weak interaction) to a sensitivity of $\sim 2\%$ of its true value. Systematic limitations are still being assessed. Quantifying this observable’s sensitivity to physics beyond the Standard Model in comparison to previously measured constraints [10][23] is work in progress.

Appendix L

Things that Should Be Very Fucking Obvious

JB: “You don’t need anything about the atomic hyperfine structure in this thesis.”

...

Me: yeah, that’s fair. I probably should cut this whole section actually.

L.1 Lifetimes and Half-Lives

Since different people use different notation to describe exponential decay of a physical quantity, it is useful to be able to relate two of the most common methods for describing the decay. We begin with the rate equation,

$$\frac{dN}{dt} = -\gamma N, \quad (\text{L.1})$$

where it is clear that the “rate” of decay must be γN . If we initially have N_0 of the quantity in question, then Eq. L.1 has as its solution

$$N(t) = N_0 e^{-\gamma t}. \quad (\text{L.2})$$

Note that the physical interpretation of γ is the “linewidth”.

We’ll wish to convert γ into other quantities of interest. In particular, we can

re-write the solution L.2 as

$$N(t) = N_0 e^{-t/\tau}, \quad (\text{L.3})$$

where $\tau = 1/\gamma$ is referred to as the “lifetime”. Then, we find the half-life $t_{1/2}$ by enforcing the fact that it is the time at which the number of remaining atoms is equal to half of what was originally present. Therefore,

$$N(t_{1/2}) = N_0 e^{-t_{1/2}/\tau} = \frac{1}{2} N_0 \quad (\text{L.4})$$

$$e^{-t_{1/2}/\tau} = 1/2 \quad (\text{L.5})$$

$$t_{1/2}/\tau = \ln(2). \quad (\text{L.6})$$

Thus, we see that

$$t_{1/2} = \ln(2) \tau, \quad (\text{L.7})$$

where τ is the “lifetime” of the state, and $t_{1/2}$ is its “half-life”.